TRANSPORTATION RESEARCH
RECORD

No. 1425

Soils, Geology, and Foundations

Field Performance of Subsurface Drainage

A peer-reviewed publication of the Transportation Research Board

TRANSPORTATION RESEARCH BOARD
NATIONAL RESEARCH COUNCIL

NATIONAL ACADEMY PRESS
WASHINGTON, D.C. 1993

Transportation Research Record 1425
ISSN 0361-1981
ISBN 0-309-05572-5
Price: $24.00

Subscriber Category
IIIA soils, geology, and foundations

Printed in the United States of America

Transportation Research Record 1425

Contents

Foreword v

Field and Laboratory Comparison of Pavement Edge Drains in Kentucky 1
L. John Fleckenstein and David L. Allen

Performance Evaluation of Retrofit Edge Drain Projects 11
Gordon K. Wells and William A. Nokes

Comparison of Compaction Methods in Narrow Subsurface Drainage Trenches 18
Graham R. Ford and Barbara E. Eliason

Hydraulic Requirements of Permeable Bases 28
James A. Crovetti and Barry J. Dempsey

Methodology for Inspection of Collector Systems 37
Zubair Ahmed and Thomas D. White

Drainage and Backfill Provisions for Approaches to Bridges 45
S. Abdol Chini, Amde M. Wolde-Tinsae, and M. Sherif Aggour

Determination of Free-Draining Base Materials Properties 54
Haiping Zhou, Lucinda Moore, Jim Huddleston, and Jeffrey Gower

Foreword

One of the major concerns in construction of new or rehabilitation of an existing pavement is how to effectively remove water from under the pavement to ensure improved performance and extend service life. Currently, there are numerous designs of pavement drainage systems. These systems include open-graded subbase material, prefabricated edge drains, trenches wrapped with a geotextile and backfilled with a permeable material, or trenches simply filled with a permeable material. One of the concerns regarding these systems is how effective they are in performing their expected function. As a result, there have been, and continue to be, numerous studies on the effectiveness of providing for drainage in pavement design. There have been new techniques, both field and laboratory, developed for investigating performance of drainage systems. The seven papers in this Record are on the recent developments in the area of pavement drainage systems. These papers stress the need for careful design, construction, and continual monitoring of pavement drainage systems to ensure acceptable performance no matter what system is used.

Fleckenstein and Allen discuss Kentucky's prefabricated edge drain installation procedure and its effects on performance of the drainage system. They also discuss a test chamber that was constructed to test the prefabricated panels in the vertical position, which simulates the field conditions.

Wells and Nokes describe the system used in California to evaluate the performance of retrofitted edge drains. The system includes what is called "a ride score" and a statistical test in the evaluation technique.

Ford and Eliason investigated four different compaction methods for narrow subsurface drainage trenches to determine which method would minimize shoulder settlement above the pavement edge drain trenches. This study conducted in Minnesota included a vibratory "ski," a vibratory Vermeer wheel, a front end loader tire, and a water flooding technique.

Crovetti and Dempsey discuss design requirements, such as effects of pavement geometry, infiltration rates, and required permeabilities for various conditions, for open-graded permeable materials (OGPM). They focus on the requirements of OGPM to handle surface water infiltration into the pavement systems.

Ahmed and White present a methodology for inspecting the performance of two types of collector systems, both older and newer installations, in Indiana. The systems were the perforated pipe underdrains and the geotextile fin drains.

Chini et al. present a summary of a literature review and survey of state transportation agencies on the current state of the art and practice in the design and construction of bridge approaches. The critical items in the design and construction, along with recommendations on drainage systems, are presented.

Zhou et al. discuss a laboratory study conducted in Oregon to determine the desirable material properties of an asphalt treated permeable material and an open-graded aggregate material. Recommendations include selection of layer and drainage coefficients for pavement design, and use of a proposed open-graded aggregate gradation in pavement construction.

Field and Laboratory Comparison of Pavement Edge Drains in Kentucky

L. JOHN FLECKENSTEIN AND DAVID L. ALLEN

A new test procedure developed by Kentucky Transportation Center investigators for testing highway panel drains is introduced. Because of installation problems and possible siltation problems, the Kentucky Department of Highways, since 1989, has been installing panel drains on the back side of the trench with the more open side of the panel facing a sand backfill. A test procedure was developed to simulate field installation conditions.

Kentucky Transportation Center investigators have been evaluating panel-type edge drains since 1985. Several edge drain failures occurred in earlier installations. The majority of the earlier panel drains were placed next to the concrete pavement and backfilled with the excavated trench material, which was dynamically compacted. The dynamic compaction (vibrating tamping skid or shoe) tended to collapse the core of the edge drains. In response to this problem, Kentucky Department of Highways officials reevaluated the installation procedure. Since 1989, the edge drains have been installed on the shoulder side of the trench and backfilled with a sand slurry. The sand is flushed into the trench using approximately one gallon of water per linear foot of edge drain. The sand slurry minimizes construction problems (if the sand is properly densified), and the sand provides an extra filter medium. In the past 6 years, hundreds of sites have been examined with a borescope. In almost all cases, the edge drains installed with the sand slurry are performing much better than installations installed under the old procedure. It is apparent that even under current installation procedures distress occurs in some of the weaker and less-rigid edge drains and some cores perform better than others. It was evident that laboratory testing should be performed to compare with field data. Current laboratory test methods were reviewed and it was the opinion of the authors that the flat parallel plate test (ASTM D1621) is not a suitable test procedure. Work done by Frobel (*1*) on eccentric (angle) loading of panel drains simulates shear-type forces that are placed on panels during and after installation, but does not model the full vertical component. It appears that most of the distress in the panels is occurring because of vertical compression and eccentric loading. In response to this, a vertical edge drain compression chamber that closely simulates in-situ conditions was constructed. This paper discusses the test chamber, test method, test results using the chamber, and compares the results with field performance data and other laboratory test methods.

Kentucky Transportation Center, University of Kentucky, Transportation Research Building, Lexington, Ky. 40506-0043.

LABORATORY EVALUATION

Vertical Edge Drain Compression Chamber

In 1991 a vertical edge drain compression chamber was constructed to test edge drains under conditions similar to field conditions. The chamber is 311.14 mm (12.25 in.) long (I.D.), 106.68 mm (4.20 in.) wide (I.D.), and 501.65 mm (19.75 in.) tall. The front and back of the chamber are made of ½-in. tempered glass for viewing the specimen. The remainder of the chamber is constructed of stainless steel and high grade aluminum alloy. The bottom of the chamber is perforated to allow water to escape. A 101.6-mm (4-in) × 279.4-mm (11-in.) aluminum plate 25.4 mm (1 in.) thick is used as a loading plate. The chamber is shown in Figures 1 and 2.

Method of Testing

The vertical dimension of the cores was not modified, except for the Type F panel. Initially Type F was a 457.20-mm (18-in.) panel that was modified to a 304.8-mm (12-in.) panel for testing. Six different brands of edge drain panels were tested in this study. Their core profiles are shown in Figure 3. Four series of tests were conducted on each panel. The edge drain samples were cut into 298.45-mm (11.75-in.) lengths. The cores of the samples were cut so that the filter fabric was approximately 6.35 mm (0.25 in.) longer than the ends of the core. The sample was placed in the chamber against the wall parallel with the long dimension of the chamber. Plexiglass inserts 6.35 mm (0.25 in.) thick were placed between the sample and viewing windows. The specimen was then backfilled with a coarse clean sand. The sand was placed to a height of 101.6 mm (4 in.) above the top of the panel. The loading plate was placed on top of the sand. The chamber was then placed into an MTS load frame. The initial height of the sample was measured. A fluorescent light was secured to the back glass window. The illuminated core of the drain was traced onto 215.9-mm (8.5-in.) × 355.6-mm (14-in.) graph paper (The area of the traced cores was later calculated using a planimeter.) The load was applied at a rate of 45.39 kg (100 lb) or 15.65 kP (2.27 psi)/minute. The vertical deflection of the panel was recorded at 45.39-kg (100-lb) increments and the core was traced every 113.39 kg (250 lb) or 156.51-kP (5.68-psi) increment. The load was held constant for approximately 2 min while the core was traced. The test was discontinued at a load of 453.59 kg (1,000 lb) or 156.51 kP (22.7 psi). The resulting horizontal stresses developed from the 453.59-kg (1,000-lb) vertical load were derived from finite

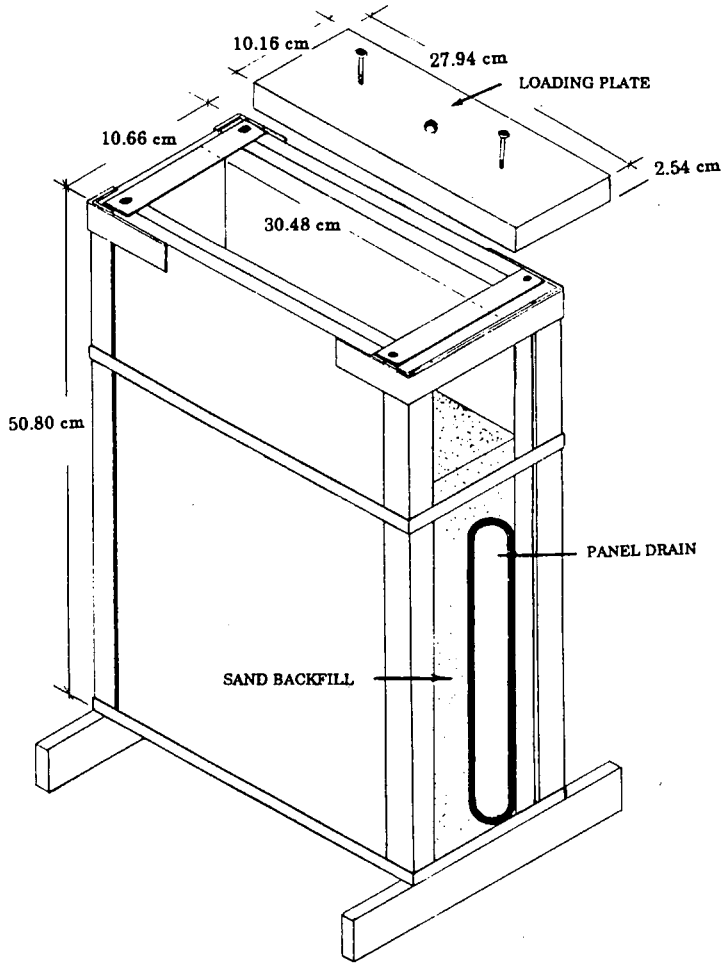

FIGURE 1 Edge drain compression chamber.

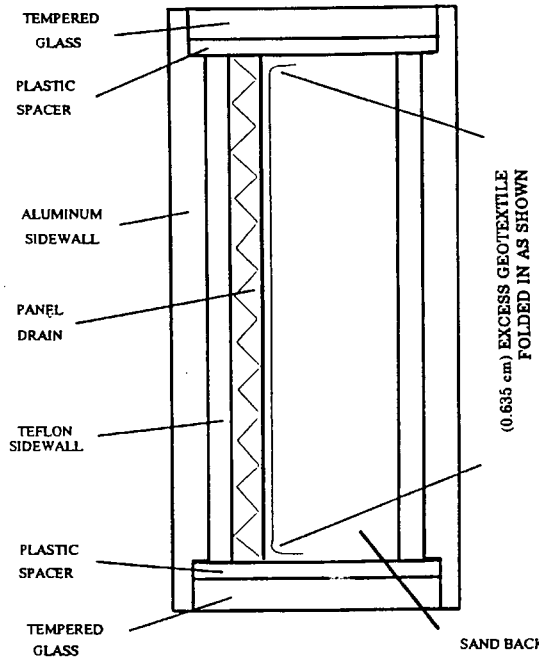

FIGURE 2 Top view of compression chamber.

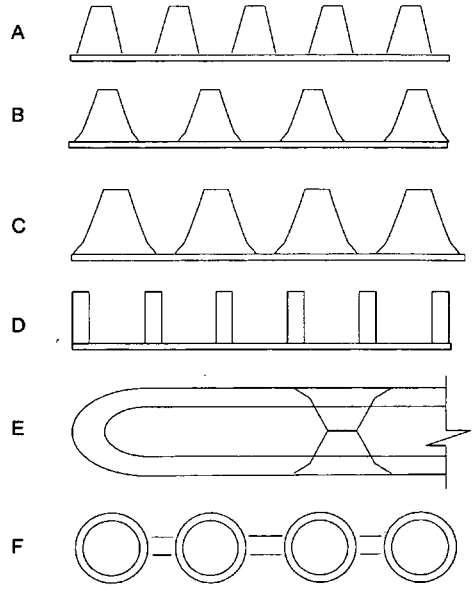

FIGURE 3 Profile of edge drains tested.

element modeling and directly measured using an earth pressure meter. The derived and measured horizontal stresses are discussed in later sections.

Series of Vertical Compression Tests

In Series 1, the tests were conducted with the sand dry (approximate moisture content of 4.0 percent) and loose [approximately 1329.53 kg/m^3 (83 lb/ft^3)], with the open side of the drain facing the sand backfill. In Series 2, the tests were conducted with the sand wet and dense, with the more open side of the drain facing the backfill. The sand was densified to approximately 1601.84 kg/m^3 (100 lb/ft^3) by pouring 3.78 L (1 gal) of water on top of the sand (the amount of water per linear foot of drain used to densify the sand during actual field installations). In Series 3, the tests were conducted with the more open side of the panel facing the wall of the chamber and the sand was not densified. In Series 4, the panels were tested in the same manner as in Series 3, except the sand was densified.

Results of Series 1

The vertical deflection measurements are given in Figure 4 and Table 1. Core Type E deflected the least of the panels tested. At 156.51 kPa (22.7 psi) of pressure, Type E deflected 6.09 mm (0.24 in.), which is 1.9 percent of the vertical height. Type D panel deflected the most. At 156.51 kPa (22.7 psi) of vertical pressure, Type D deflected 52.83 mm (2.08 in.), which is 16.8 percent of the vertical height.

The changes in core capacity of each panel drain at 156.51 kPa (22.7 psi) are shown in Figure 5 and Table 2. The two enclosed cores performed the best (Type E and F). The core capacity of Type E increased by 2.1 percent and Type F decreased by 2.46 percent. The capacity of Type D core reduced the most at 57.6 percent. The capacity for each core type for a given load is shown in Figure 6 and Table 3.

Results of Series 2

The tests in Series 2 (dense sand) were performed at the same rate, and data were recorded at the same frequency as in Series 1. In most cases, increasing the density of the sand increased the performance of the panel drain.

At 156.51 kPa (22.7 psi), Type E deflected the least. Type E core deflected 4.57 mm (0.18 in.), which is 1.4 percent of the vertical height. Type B deflected the most at 23.36 mm (0.92 in.) or 8.1 percent of the vertical height. The deflection of each panel is shown in Figure 4 and Table 1. Type A drain was the only edge drain that increased in vertical deflection when the sand was densified. The most significant change in vertical deflection occurred in the Type D and Type F drains. Vertical deflection of Type D decreased by 62 percent, and Type F decreased by 68 percent.

The change in core capacity at 156.51 kPa (22.7 psi) is shown in Figure 5 and Table 2. The core capacity of Type E increased by 1.1 percent, and Type B core decreased by 33.80 percent. The most significant change in core capacity when the sand was densified was the Type D drain, which increased 32 percent. The capacity of each core type for a given load is shown in Figure 6 and Table 3.

Comparison of the results from these tests makes it apparent that Type E performed better than the other panels. The core capacity of the two enclosed cores (Type E and the Type F) deflected less than the other four more open cores. The more open cores (Type A, B, C, and D) had core losses equal to or greater than 25 percent. It appears that fabric intrusion between the support columns and rolling over of the top and bottom rows of support columns were causing the reduction in core area.

Results of Series 3

To help eliminate fabric intrusion, a third and fourth set of tests were conducted on the open type cores. In these series, the panels were turned backwards in the compression box.

It is also possible to turn these panels backwards in the field because they have a high percentage of open area on the backside. The backside of the Type B core was 15.3 percent open; Type C was 13.5 percent open; Type A was 11.3 percent open; and Type D was 47.6 percent open. The open area of Type E was 3.9 percent on one side and 5.8 percent on the other. Type F core was 0.80 percent open.

The panels were tested with the more open side of the panel facing the wall of the chamber and the sand in a loose state. Type A drain had the least vertical deflection (1.6 percent) at 156.51 kPa (22.7 psi), and Type D drain deflected the most at 12 percent. In all cases, the more open panels deflected less in Series 3 than in Series 1 (Figure 4 and Table 1).

In most cases, the reduction in core capacity was less in Series 3 than in Series 1 and 2. Panel Types A, B, and C had less core reduction in Series 3 at 156.51 kPa (22.7 psi). Type D had greater core loss in Series 3 than in Series 2 (Figure 5 and Table 4). The capacities of each core type for a given load are given in Figure 6 and Table 3.

Results of Series 4

The performance of the open-type cores in most cases increased when the panels were turned backwards and the sand densified. Type A core deflected the least in the vertical direction. Type A deflected 3.1 percent at 156.51 kPa (22.7 psi) and Type B deflected the most at 5.0 percent (Figure 4 and Table 1).

The percent change in the core capacities for a given load are shown in Figure 5 and Table 4. At 151.68 kPa (22 psi), Type A core had less capacity loss and the Type C had the greatest capacity loss of 15.2 percent. The capacities of each core type for a given load are given in Figure 6 and listed in Table 3.

Summary of Vertical Compression Tests

Information obtained from the four series of tests performed indicates that Type E panel performed the best of the six panels. Type E panel had the least amount of vertical de-

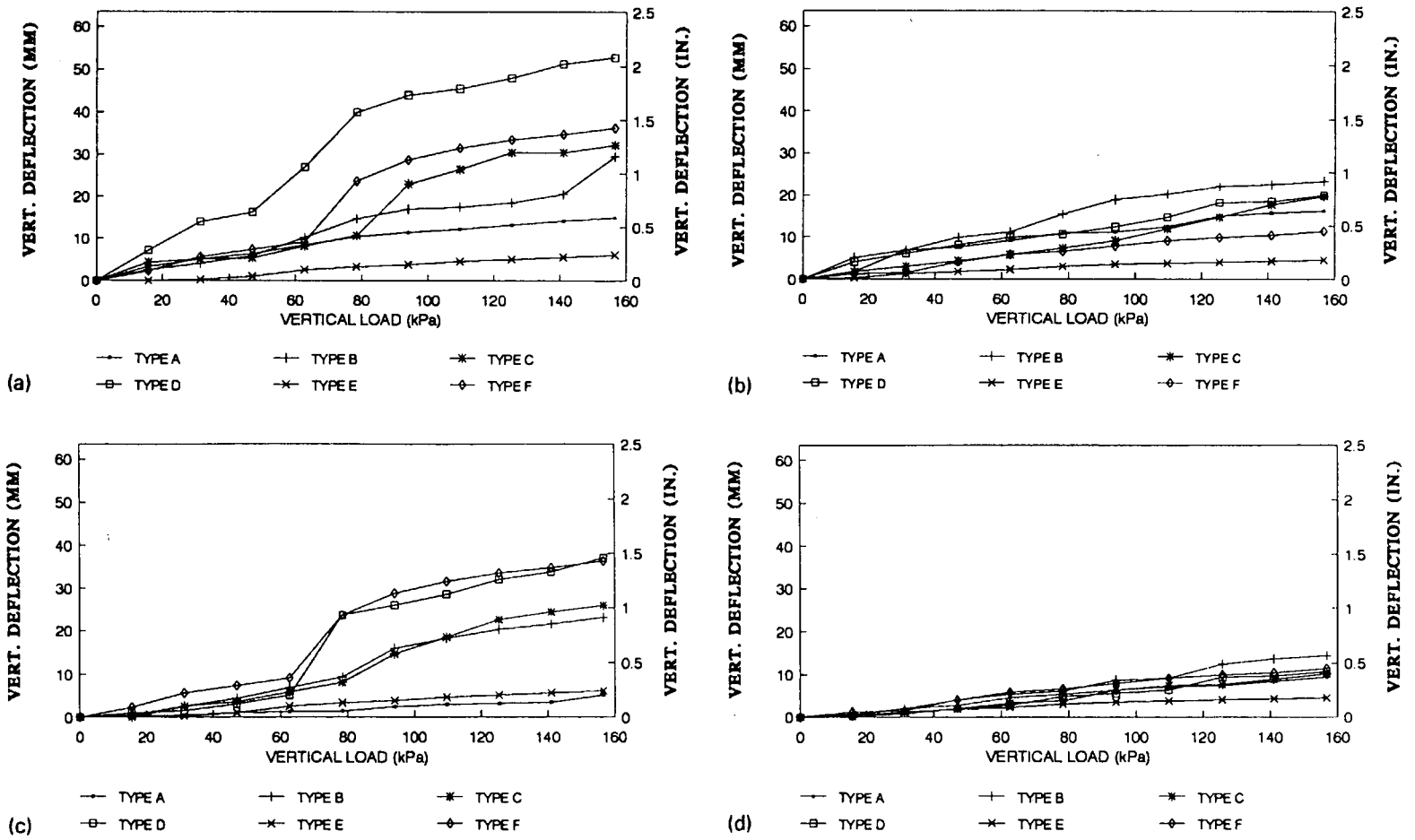

FIGURE 4 Vertical compression: (*a*) Series 1, vertical compression (sand backfill, loose); (*b*) Series 2, vertical compression (sand backfill, dense); (*c*) Series 3, vertical compression (sand loose, panels backwards); (*d*) Series 4, vertical compression (sand dense, panels backwards).

TABLE 1 Percentage Vertical Compression at 156.51 kPa

Panel Type	Open Side of Panel Facing Sand Backfill		Rigid Back Side of Panel Facing Sand Backfill	
	Series 1. Backfill Loose	Series 2. Backfill Dense	Series 3. Backfill Loose	Series 4. Backfill Dense
Type A	4.9%	5.3%	1.6%	3.1%
Type B	10.2%	8.1%	8.0%	5.0%
Type C	10.0%	6.5%	8.5%	3.3%
Type D	16.8%	6.5%	12.0%	3.5%
Type E	1.92%	1.4%	1.92%	1.4%
Type F	11.7%	3.7%	11.7%	3.7%

*Type E and Type F are solid cores and are identical on both sides of the panel. The data are contained in series 3 and 4 comparison.

flection and the least amount of core reduction in most of the four series of tests. Type E core also had the largest amount of core flow area. The test data indicate that solid type cores (Types E and F) had the least amount of core reduction in all the tests. Type E core area actually increased by 1 to 2 percent in all the tests. The Type F core decreased 2 to 4 percent. Although the Type F core showed little core reduction in all the tests, compression occurred in the webs linking the round flow tubes when the sand was loose. The more open cores (Type A, B, C, and D) are prone to loss of core flow area because of the top rows of support columns rolling over and the rigid backing folding and compressing. In all cases, the more open cores performed substantially better when the more open side was placed against the wall of the chamber. Type A core showed the least amount of distress of the open-type cores. The Type A core is of similar design to Types B and C, but is more rigid because of its chemical composition. The Type A core is PVC, and the other cores are high-density polyethylene.

Flat Parallel Plate Test

Flat parallel plate tests were conducted according to ASTM D1621. The load was recorded at 10 percent strain except for the Type A core. The Type A core exceeded the limits of the testing equipment, and the test was aborted at 8 percent strain. At 8 percent strain, Type A core was 574.33 kPa (83.3 psi). The full results are given in Figure 7.

HORIZONTAL STRESS

Measured in Laboratory

Horizontal stress on the side wall of the chamber was measured using a round 228.6-mm (9-in.) diameter earth pressure meter. The measured horizontal force was approximately 19 kPa (2.76 psi) at 156.51 kPa (22.7 psi) vertical load.

Finite Element Modeling

Finite element modeling was conducted to evaluate horizontal forces produced during loading of a panel drain system. A modulus of elasticity [E = 68 947.6 kPa (10,000 psi)] and Poisson's ratio (u = 0.35) was assumed for the sand backfill, and a modulus of elasticity [E = 3 447.38 kPa (500 psi)] and Poisson's ratio (u = 0.45) was assumed for the edge drain panel. As shown in Figure 8, at a depth of 152.4 mm (6 in.), which is the center of the panel, the resulting horizontal force at 156.51 kPa (22.7 psi) vertical load is approximately 16.54 kPa (2.4 psi). The finite element plot indicates that higher horizontal stresses occur at the top and the bottom of the panel. A horizontal stress of approximately 96.52 kPa (14 psi) occurs near the top and approximately 48.26 kPa (7 psi) at the bottom of the panel. These points are probably higher than actual field values because the panel was modeled as a rigid structure and the node points (nodes between the sand and the panel) were attached not allowing the sand to migrate around the panel.

Field Measurements

Horizontal and vertical stresses were measured in the field during construction using a round earth pressure meter 228.6 mm (9 in.) in diameter and two 50.5-mm × 254 mm (2-in. × 10-in.) rectangular earth pressure meters. One of the rectangular earth pressure meters was placed close to the surface of the backfill to measure vertical load, and the other rectangular meter and the round meter were used to measure side wall pressures. One was placed against the trench wall and the other against the panel. Actual installation pressures were not attainable because of the nature of the contractor's schedule. Loads were applied to the top of the sand backfill using a crew cab pickup truck and a loaded Class 7 Dump Truck, with the third drop axle raised. At the first test site, using the crew cab pickup truck for loading, a vertical pressure of 194.77 kPa (28.25 psi) was measured. A horizontal pressure

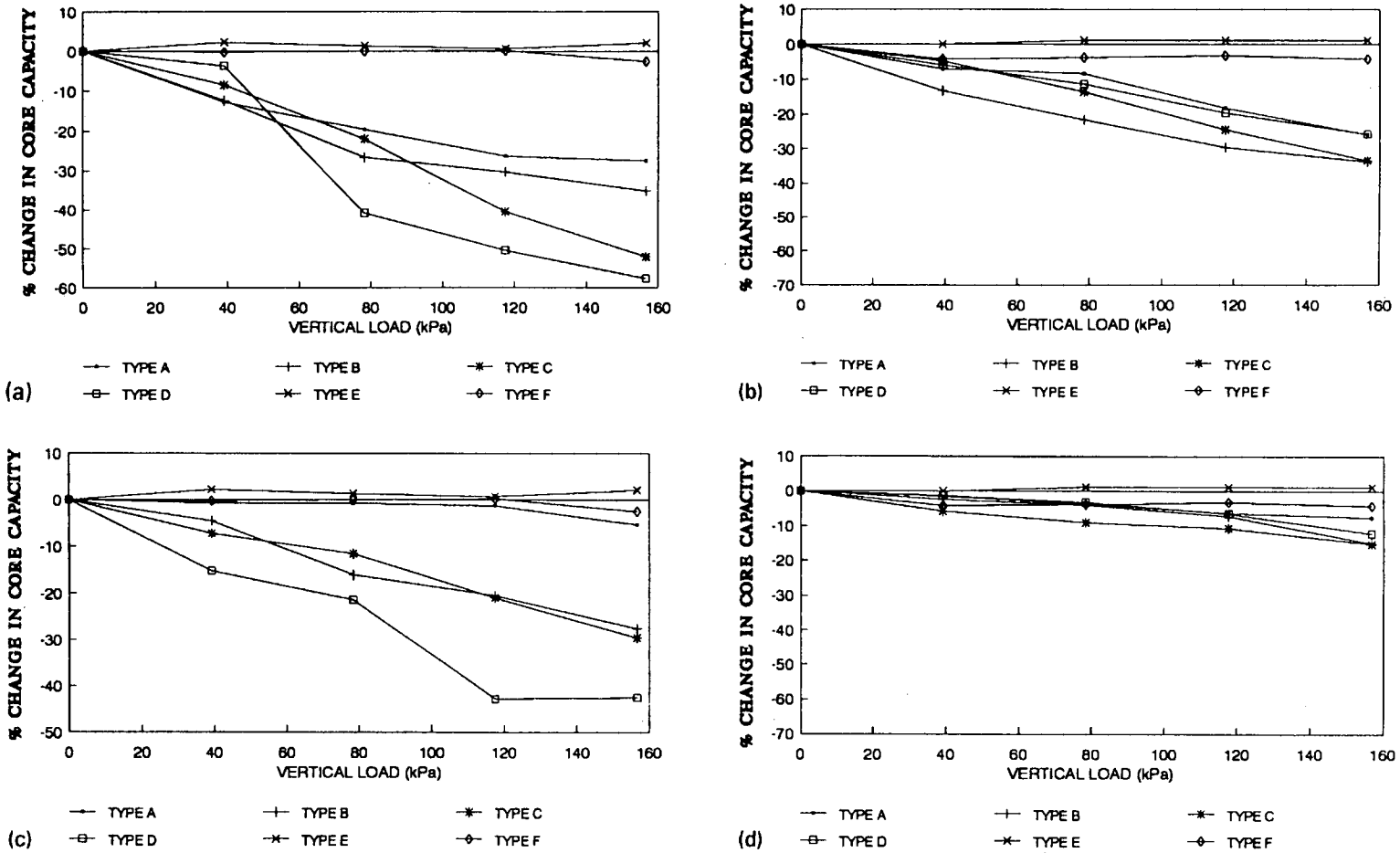

FIGURE 5 Change in core capacity: (*a*) Series 1, change in core capacity (sand backfill, loose); (*b*) Series 2, change in core capacity (sand backfill, dense); (*c*) Series 3, change in core capacity (sand loose, panels backwards); (*d*) Series 4, change in core capacity (sand dense, panels backwards).

TABLE 2 Change in Core Capacity: Open Side of Panel Facing Sand

		Series 1. Sand Backfill Loose					Series 2. Sand Backfill Dense				
Panel Type	Vertical Load kPa>>	0	39.2	78.3	117.2	156.5	0	39.2	78.3	117.2	156.5
Type A	Percent Change in Core Capacity>>	0	-12.7	-19.5	-26.2	-27.4	0	-7.0	-8.4	-18.3	-25.9
Type B		0	-12.3	-26.5	-30.2	-35.0	0	-13.3	-21.6	-29.6	-33.7
Type C		0	-8.4	-21.9	-40.4	-52.0	0	-4.7	-13.6	-24.5	-33.4
Type D		0	-3.6	-40.7	-50.4	-57.6	0	-5.9	-11.4	-19.6	-25.7
Type E		0	+2.2	+1.3	+0.6	+2.1	0	0	+1.1	+1.1	+1.1
Type F		0	-0.2	0	+0.2	-2.46	0	-4.1	-3.7	-3.1	-4.1

of 15.16 kPa (2.2 psi) was measured with the round gauge, and 41.36 kPa (6 psi) was measured with the rectangular gauge. At the second test site, using the loaded dump truck, a horizontal pressure of 61.02 kPa (8.85 psi) reading was recorded. The full vertical pressure reading was not obtained because of the slow reaction time of the earth pressure meter and a tight construction schedule; however, a vertical pressure of 468.84 kPa (68 psi) (plus) was recorded before the test was aborted.

FIELD PERFORMANCE OF PANELS

To date, only four of the six cores tested have been monitored in the field (Types B, C, D, and E). Before 1989, edge drains were installed on the pavement side of the trench and backfilled with existing excavated trench material. The material was compacted with a vibratory compactor. Many miles of an earlier design of Type D core were installed in this manner. All five sites that were borescoped and excavated showed similar signs of core collapse (column collapse) as indicated by Frobels eccentric loading testing. Slight to moderate core compression was noticed in field inspections of the earlier Type E core.

Since 1989, numerous miles of edge drains have been installed on the backside of the trench and backfilled with a sand slurry. Two miles of a core similar to Type B core and several miles of Type E core were installed on the Mountain Parkway and on Interstate 75 in Kentucky. At both sites, the core similar to Type B was installed with the fabric facing the sand backfill. In both cases, the top row of support columns was rolled over and slight fabric intrusion had occurred in areas. Series 1 and 2 laboratory tests showed similar signs of this type of roll over starting in the very early stages of the tests. Failure of the filter fabric on the similar edge drain to Type B core was observed on Interstate 75. The support columns had pushed through the filter fabric and slight to moderate post compression had occurred. This failure was very localized and occurred in the first 25 to 50 ft of the installation. The remaining mile of installation appears to be in satisfactory condition. The Type E drain installed at both sites appears to be in excellent condition. There were no signs of vertical or horizontal compression.

Several miles of the new Type D core were installed on Interstate 64 in 1990 and 1991. Type D core was installed with the more open side facing the shoulder. Rolling over of the top row of support columns occurred during installation. It was apparent during installation that the sand was not being properly densified. Substantial trench settlement resulted. The resulting settlement caused the bottom four rows of support columns to "J," forcing the bottom of the edge drain toward the center of the trench. Cracking of the rigid backing occurred at the start of the "J." The top two rows of support columns were partially rolled over.

Type C and E drains were installed on the Bluegrass Parkway in 1991. Type C drain was installed with the more open side facing the sand backfill. The top row of support columns had partially rolled over during installation. Slight fabric intrusion was occurring in some areas. The Type E core appeared to be in excellent condition.

CONCLUSIONS

It is apparent that the panels are distressed more under the old method of installation using excavated trench material and dynamic type compaction. Furthermore, it is apparent that using the sand slurry reduces the chances of installation damage. Proper density needs to be achieved during installation of the sand backfill or damage will occur from trench settlement. In most cases, increasing the density of the sand increased the performance of the panel drain.

Information obtained from the four series of tests performed indicates that Type E panel performed best of the six panels tested. The more solid type cores (Types E and F) had the least amount of core reduction. Type D and Type F were the most susceptible to vertical compression when the sand was loose. Type D core was also the most susceptible to reduction in core capacity when the sand was loose. The open cores (Types A, B, C, and D) are prone to loss of core capacity because of the top rows of support columns rolling over and the rigid backing folding and compressing. In all cases, the open cores performed substantially better when the more open side was placed against the wall of the chamber. The Type A core showed the least amount of distress of these types, probably because of its chemical composition (PVC).

To date, the maximum horizontal pressure measured in the field was 61.02 kPa (8.85 psi). It is the opinion of the authors that this was measured under extreme conditions and that actual installation pressures are probably less.

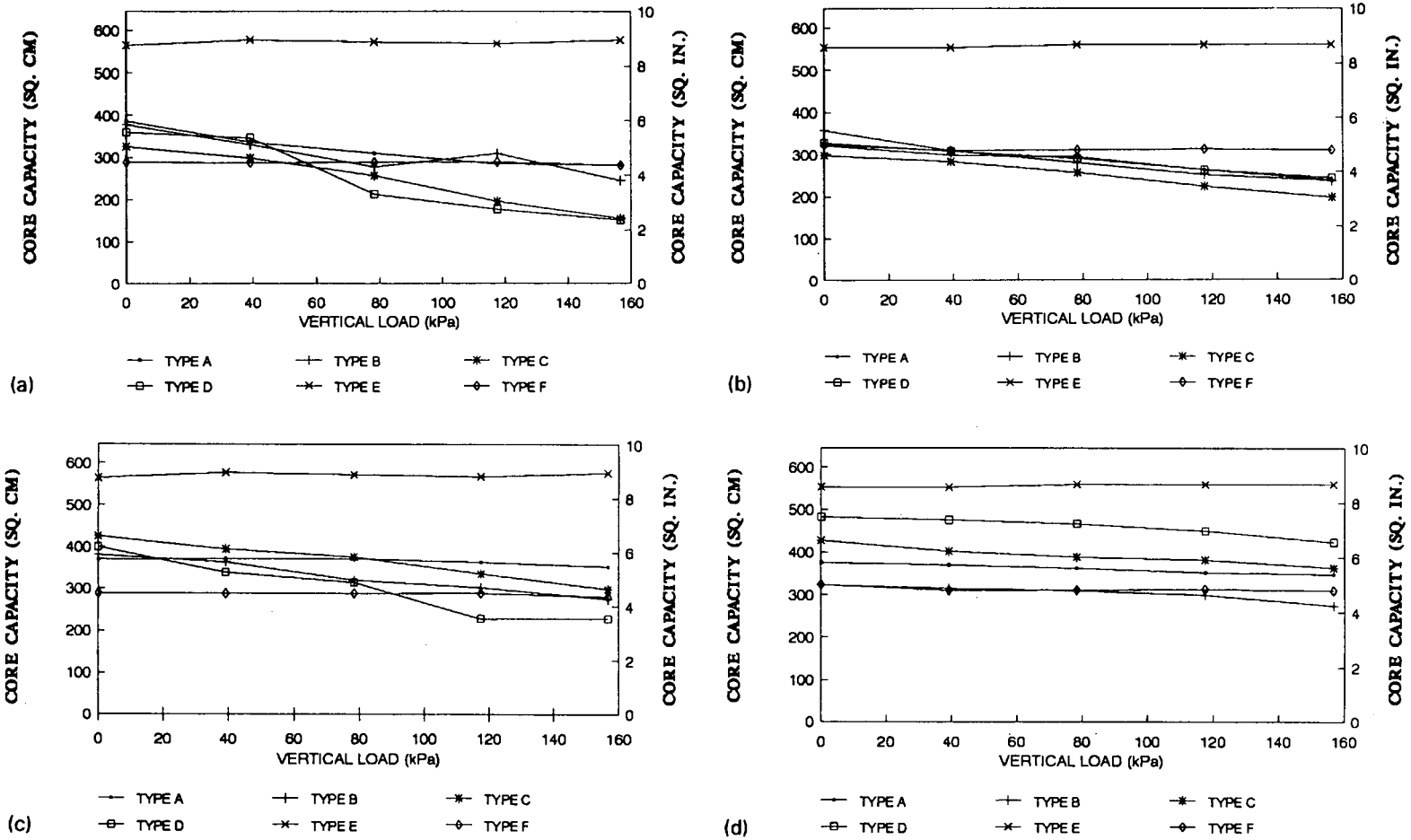

FIGURE 6 Core capacity: (*a*) Series 1, core capacity (sand backfill, loose); (*b*) Series 2, core capacity (sand backfill, dense); (*c*) Series 3, core capacity (sand loose, panels backwards); (*d*) Series 4, core capacity (sand dense, panels backwards).

TABLE 3 Core Capacity at 0 and 156.5 kPa (in.^{2})

Panel Type	Open Side of Panel Facing Sand Backfill				Rigid Back Side of Panel Facing Sand Backfill			
	Series 1. Backfill Loose		Series 2. Backfill Dense		Series 3. Backfill Loose		Series 4. Backfill Dense	
	0 kPa	156.5 kPa	0 kPa	156.5 kPa	0 kPa	156.5k Pa	0 kPa	156.5 kPa
Type A	385.8	279.9	321.2	238.1	369.0	349.0	375.5	347.1
Type B	377.4	245.2	357.4	236.7	380.6	275.5	322.6	274.2
Type C	325.8	156.1	297.4	198.1	425.2	298.7	427.7	362.6
Type D	359.3	152.2	327.7	243.2	399.3	229.0	482.6	423.8
Type E	564.5	576.7	570.9	560.0	564.5	576.7	553.5	560.0
Type F	288.4	281.3	323.2	309.6	288.4	281.3	323.2	309.7

TABLE 4 Change in Core Capacity: Rigid Back Side of Panel Facing Sand

Panel Type	Vertical Load kPa>>	Series 3. Sand Backfill Loose					Series 4. Sand Backfill Dense				
		0	5.68	11.36	17.0	22.7	0	5.68	11.36	17.0	22.7
Type A	Percent Change in Core Capacity>>	0	+0.7	+0.7	-1.3	-5.3	0	-1.5	-3.6	-6.3	-7.5
Type B		0	-4.5	-16.1	-20.5	-27.6	0	-2.4	-4.0	-7.2	-15.0
Type C		0	-7.2	-11.6	-21.0	-29.6	0	-5.8	-9.0	-10.7	-15.2
Type D		0	-15.3	-21.4	-42.8	-42.6	0	-1.3	-3.2	-6.5	-12.1
Type E		0	+2.2	+1.3	+0.6	+2.1	0	0	+1.1	+1.1	+1.1
Type F		0	-0.2	0	+0.2	-2.46	0	-4.1	-3.7	-3.1	-4.1

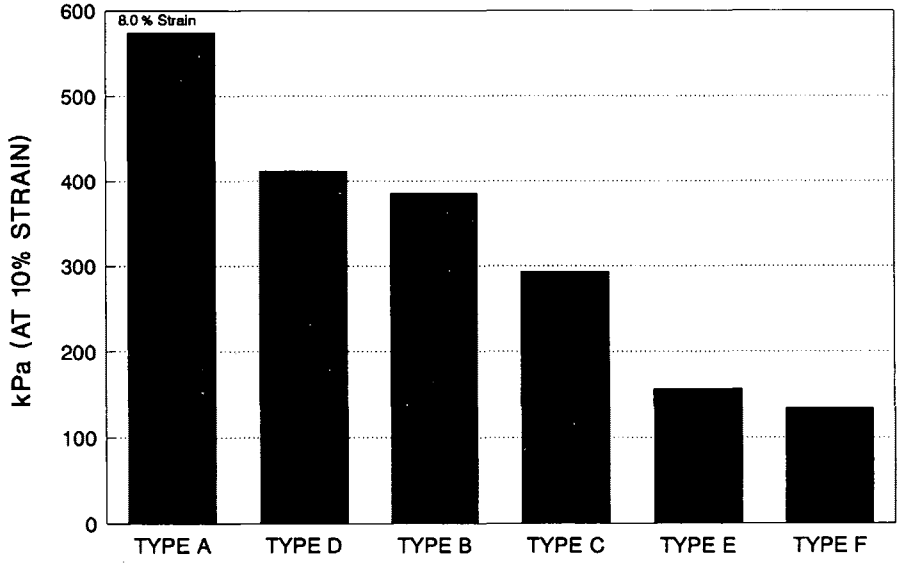

FIGURE 7 Flat parallel plate test (10 percent strain).

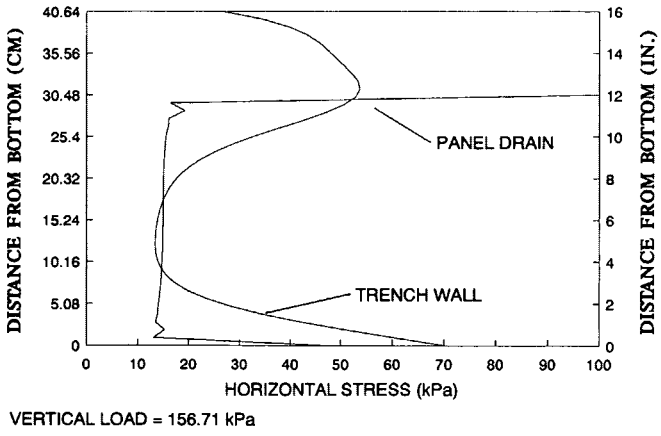

FIGURE 8 Finite element modeling (stressed introduced at panel).

The distress observed in the panels at 156.51 kPa (22.7 psi) vertical pressure from the laboratory testing exceeds most distresses that have been observed in the field since 1989 (using sand slurry for backfill). Further field monitoring is necessary to confirm the maximum load needed for laboratory testing and edge drain design.

The flat parallel plate test does not correlate with field performance. The Type E panel is one of the weaker panels in the flat parallel plate test, but its performance appears to be the best of all the panels installed in Kentucky. However, the flat parallel plate is a relatively simple test that may be used for monitoring quality control.

It is the opinion of the authors that the vertical edge drain compression test does an excellent job of modeling in situ conditions in Kentucky.

ACKNOWLEDGMENTS

The study reported herein was funded by FHWA and the Kentucky Transportation Cabinet through the University of Kentucky Research Foundation.

REFERENCE

1. Frobel, R. K. Eccentric (Angled) Loading of Prefabricated Highway Edge Drains, In *Transportation Research Record 1329*, TRB, National Research Council, Washington, D.C., 1991.

Publication of this paper sponsored by Committee on Subsurface Drainage.

Performance Evaluation of Retrofit Edge Drain Projects

GORDON K. WELLS AND WILLIAM A. NOKES

Accelerated slab breakup was noted on many retrofit-edge-drain-only and rehabilitated concrete pavements in California. Concern about the earlier-than-anticipated need for further rehabilitation led to an evaluation of 26 projects that incorporated retrofit edge drains. Results of this study show that before retrofit edge drain installation, the amount of slab breakup and environmental factors significantly affect subsequent pavement performance. More important, it is also suggested that environmental factors strongly influence the undrained performance of concrete pavement. Therefore, the future use of current and alternative concrete pavement designs should address environmental factors that can contribute to poor pavement performance in California.

In January 1986, the California Department of Transportation (Caltrans) Pavement Management System (PMS) coordinator sent New Technology, Materials and Research (NTMR), a list of recently retrofitted-edge-drain-only projects where substantial cracking occurred. These portland cement concrete pavement (PCCP) projects were sufficiently cracked to warrant unplanned rehabilitation. In May 1986, FHWA Region 9 independently sent Caltrans a list including the same projects along with additional major rehabilitation projects where FHWA reviews noted accelerated cracking. Despite differences in repair strategies, these two programs (retrofit edge drain only versus PCCP major rehabilitation) were both experiencing cracking faster than expected. In short, Caltrans' PCPP strategies to extend the service life for these projects using retrofit edge drains did not appear to be entirely successful. As a result, NTMR evaluated the effectiveness of retrofit edge drains to determine the actual success of retrofit edge drains and identify causes of accelerated cracking. At that time potential implications for alternative PCCP design criteria in California were unknown.

BACKGROUND

The original methods of selecting candidate retrofit-edge-drain-only projects that were programmed into the PMS system are

1. Ride Score <30—Ride score (a dimensionless number) equals the sum of the 3.2 mm (⅛ in.) displacements between an automobile chassis and its rear axle as determined by a Portland Cement Association type of road meter device.

California Department of Transportation, Division of New Technology, Materials and Research, Office of Pavement, 5900 Folsom Boulevard, Sacramento, Calif. 95819.

$$\text{Ride score} = \frac{\text{sum of 3.2-mm displacements}}{(\text{distance, km}) * 31}$$

$$= \frac{\text{sum of ⅛-in. displacements}}{(\text{distance, mi}) * 50} \quad (1)$$

2. Third-Stage slab cracking <10 percent—Third-stage cracking is defined as a fragmented slab, as shown in Figure 1.

Starting in March 1982, retrofit-edge-drain-only projects were selected on the basis of a ride score criteria of <45 instead of <30. In addition, guidelines were recommended for ranking retrofit edge drain projects that applied factors for truck traffic using the estimated accumulated 80 kN (18 kip) equivalent single-axle load (ESAL) converted to a traffic index (TI)

$$TI = 9.0\left(\frac{ESAL}{10^6}\right)^{0.119} \quad (2)$$

The TI, pavement age, and annual rainfall (*I*) were subsequently revised for implementation, as given in the following tables:

Age (years)	*Factor*
1–4.9	2
5–9.9	4
10–14.9	6
≥15	8

Annual Rainfall [cm (in.)]	*Factor*
<25.4 (<10)	1.5
25.4–50.5 (10–19.9)	1.2
50.6–101.3 (20–39.9)	0.8
101.4–152.1 (40–59.9)	0.6
≥152.2 (≥60)	0.5

TI	*Factor*
≤12	1.0
>12	0.8

The product of these three factors resulted in ranking (the lowest number representing the highest rank) for proposed retrofit-edge-drain-only projects. The intent was to obtain a desired 10-year service life extension for pavements with a ride score of less than 45.

Further NTMR evaluation resulted in revised retrofit-edge-drain-only project selection guidelines in October 1986 (*2*). The recommended criteria were (a) first-stage cracking (non-intersecting cracks; see Figure 1) ≤10 percent, (b) third-stage cracking ≤1 percent, (c) service life ≤10 years, and (d) ac-

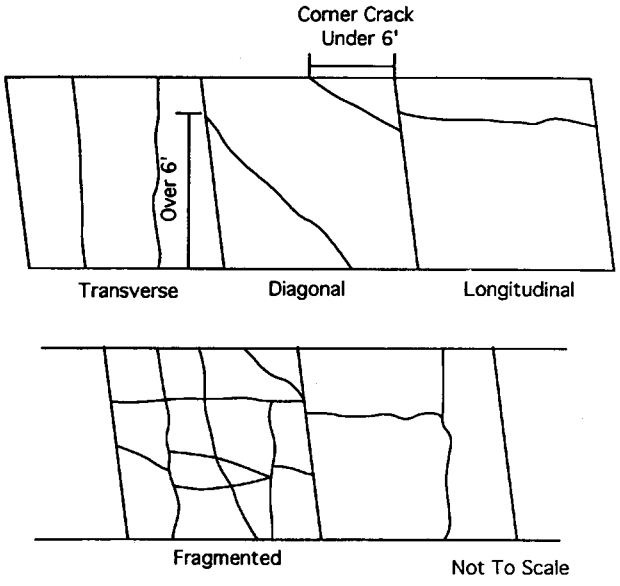

FIGURE 1 Diagram of (*top*) first- and (*bottom*) third-stage JPCP cracking.

cumulated ESAL ≤13 million. The ride score was still required to be <45.

Unfortunately, these guidelines were not adopted for Caltrans' PCCP major rehabilitation program. Different project priority criteria were established for PCCP major rehabilitation (see Table 1). For Priority 1 and 2 projects [bad ride (rough) and major structural damage], the following criteria were used: (a) ride score >45 and (b) third-stage cracking (fragmented slabs) >10 percent. The rehabilitation strategy for these projects is to crack and seat the PCCP, then place a 30.5-mm (0.10-ft) asphalt concrete pavement (ACP) leveling course, pavement reinforcing fabric, a 30.5-mm (0.10-ft) ACP lift, and then a 45.7-mm (0.15-ft) ACP surface course. Retrofit edge drains are also installed.

The subject of this study is the performance of Priority 5 and 6 major rehabilitation projects (see Table 1), where the ride score >45. The rehabilitation strategies were as follows:

1. Subseal slabs using a cement/fly-ash grout,
2. Diamond-grind the surface,
3. Install retrofit edge drains,
4. Rout and seal random cracks, and
5. Replace fragmented slabs (in rare cases where necessary).

Table 1 presents the PMS Priority Guide for PCCP Major Rehabilitation as discussed. The state highway system has been divided into three classes for rehabilitation purposed on the basis of their functional classification as follows:

- Class 1—Rural principal arterials and their extensions into urban areas;
- Class 2—Roads that are not defined as Class 1 or 3, primarily minor arterials; and
- Class 3—Collectors, low-volume roads, and other logical segments added for continuity.

METHODOLOGY

The study of retrofit edge drain effectiveness was based mostly on retrofit-edge-drain-only projects described in the work by Wells, *Evaluation of Edge Drain Performance* (*1*), as well as additional rehabilitation projects that included retrofit edge drains constructed in the same and other geographic locations not described in the work by Wells. The PCCP projects investigated in this study are 203- or 229-mm (8- or 9-in.) thick, nonreinforced, nondowelled, jointed plain concrete pavement (JPCP) with random joint spacings of 4.0, 5.8, 5.5, and 3.7 m (13, 19, 18, and 12 ft), with weakened plain joints skewed counter clockwise 2 in 12. All these JPCP projects were constructed on cement treated bases 101.6 to 152.4 mm (4 to 6 in.) thick.

Data bases were developed using the biennial PMS Rigid Pavement Survey before and after installing retrofit edge drains. The mean percentages of first- and third-stage cracking (for each project) were calculated to establish the JPCP structural condition at the time of edge drain construction for all 26 projects incorporating retrofit edge drains (15 retrofit-edge-drain-only and 11 major rehabilitation projects). These data were used as the baseline for comparison and evaluation of subsequent performance. The data base included

1. Project location;
2. Service life (years) before edge drain installation or rehabilitation;

TABLE 1 PMS Priority Guide For PCCP Rehabilitation Projects (1986)

Class of Highway	1	2	3
1. Major Structural Problem and Bad Ride (Ride Score >45, Third Stage Cracking >10 Percent).	1	2	11
2. Bad Ride Only (Ride Score >45.	5	6	*

*Maintenance only work.

3. Mean percent first- and third-stage cracking (as mentioned);
4. Average grout subsealing quantity, in kilograms (or pounds) per hole,
5. Accumulated ESAL between construction and rehabilitation (*3*);
6. Average annual rainfall, in centimeters (*4*);
7. Average annual heating and cooling degree days, in degree-days Celsius (*4*); and
8. When applicable, the year when the project with retrofit edge drains was triggered again for rehabilitation.

Review of the 26 projects resulted in quantitative conclusions about factors that affect JPCP performance where retrofit edge drains were installed and provided insight about incorporating environmental criteria explicitly in new PCCP design.

EVALUATION OF PERFORMANCE

An analysis of all 26 projects was performed to identify causes of failure. Performance data are given in Table 2. For purposes of this study, a retrofit edge drain project failure is defined as (a) >10 percent third-stage cracking on a PMS survey before the 10-year design service life extension or (b) when NTMR and Office of Highway Construction project reviews indicated that premature distress, in the form of new third-stage or corner cracking, was occurring or that cracking had occurred in the repaired or replaced slabs.

Seven failed and 10 nonfailed retrofit edge drain projects where grout subsealing was done in conjunction with installation of retrofit edge drains were compared by analyzing the average grout quantity. These projects were analyzed using the two-sample Students' *t*-test and nonparametric Mann-Whitney (*5*) statistical test comparing the failed and nonfailed projects to determine whether the grout subsealing quantity significantly influenced pavement performance. A 95 percent confidence level was used for the two-tail tests. The results showed that grout subsealing quantity is not significantly different for the failed and nonfailed projects, thus showing that subsealing was not a significant factor in pavement performance for this study.

The 26 projects were stratified into failed or nonfailed projects and were analyzed using the following variables (Descriptive statistics of these variables are shown in Table 3.):

1. Mean percent first- (percent Stage 1) and third-stage (percent Stage 3) cracking before installation of retrofit edge drains,
2. Undrained service life accumulated ESAL,
3. Undrained service life in years (Life),
4. Average annual rainfall (Rain), and
5. Average annual heating (Heat) and cooling (Cool) degree-days.

An annual heating degree-day is used as an indication of fuel consumption. In the United States, one heating degree is given for each degree that the average daily mean temperature goes below a baseline of 18.3°C (65°F). Temperatures over 18.3°C (65°F) are not counted for heating degree-days. Average heating degree-days are totaled for each month and then for the year.

One cooling degree is given for each degree the average daily temperature rises above the baseline of 18.3°C (65°F). Temperatures under 18.3°C (65°F) are not counted for cooling degree-days. The annual cooling degree-days are calculated in the same manner as previously defined for annual heating degree-days.

The variables given in Table 3 were analyzed by using the two-sample *t*-test and the Mann-Whitney test to determine whether there were significant differences between the failed and nonfailed sites. Two-tail tests at a 95 percent confidence

TABLE 2 Performance of 26 Retrofit Edge Drain Projects

Cracking Stage	%	Total Projects	Failed Projects	% Failed	Average Years To Failure*
First	≤5	11	3	27	3.0
	>5	15	8	53	4.3
	≤10	18	6	33	3.8
	>10	8	5	63	4.0
Third	≤1	13	1	8	3.0
	>1	13	10	77	4.0
Undrained Service Life (Years)					
≤10		6	1	17	8.0
>10		20	10	50	3.5

*Of 11 failed projects.

TABLE 3 Variable Descriptive Statistics

Variable-11 Failed Sites	Mean	Std Dev
%Stage 1	13.36	9.95
%Stage 3	4.09	3.62
Life	15.27	4.43
ESAL	10.86	4.23
Rain (cm)	53.80 (21.18 in)	29.41 (11.58 in)
Heat (°C-Days)	1671.61 (3040.9 °F-Days)	522.92 (973.26 °F)
Cool (°C-Days)	724.33 (1335.8 °F-Days)	270.41 (518.74 °F)
Rain*Cool (°C-Days)[a]	15574.3 (28065.8 °F-Days)	12748.0 (22978.4 °F)
Variable-15 Nonfailed Sites		
%Stage 1	7.67	8.16
%Stage 3	1.13	1.24
Life	14.93	6.31
ESAL	13.10	7.57
Rain (cm)	38.61 (15.20 in)	22.50 (8.86 in)
Heat (°C-Days)	1343.1 (2449.5 °F-Days)	238.86 (461.95 °F-Days)
Cool (°C-Days	733.5 (1352.3 °F-Days)	272.17 (521.90 °F-Days)
Rain*Cool (°C-Days)[a]	10094.1 (18201.3 °F-Days)	4310.9 (7791.7 °F-Days)

[a] Interaction variable.

level (p = .05) were used. Table 4 gives the probability of the variables being different due to chance alone.

The test results in Table 4 show a strong significant difference (<99 percent confidence) in the percentage of Stage 3 cracking between the failed and nonfailed sites; also, test results suggest a significant difference in the percentage of Stage 1 cracking and Heat between failed and nonfailed sites. These results will be discussed later in the analysis.

Correlation of third-stage to first-stage cracking before installing edge drains was studied using linear regression. Correlation of postinstallation cracking was not possible because of the rapid failures and subsequent Priority 1 and 2 rehabilitation. All 26 projects were studied to see whether third-stage cracking is readily predictable from early, less-critical first-stage cracking. A statistically significant regression equation resulted for the 11 failed projects when third-stage cracking was modeled as a function of first-stage cracking (Figure 2). No significant correlation was found for either the 15 nonfailed or the combined 26 project data set.

Cumulative frequency distributions were plotted to examine and further evaluate differences between failed and nonfailed projects. Figure 3 shows that retrofit edge drain projects

TABLE 4 Two-Sample *t*-Test and Mann-Whitney Test Probabilities

Variable	t-test Probability	Mann-Whitney Probability
%Stage 1	0.122	0.046[a]
%Stage 3	0.007[a]	0.001[a]
Life	0.880	0.959
ESAL	0.386	0.452
Rain	0.148	0.204
Heat	0.050[a]	0.055
Cool	0.937	0.917
Rain*Cool	0.133	0.421[b]

[a] Significant difference.
[b] Interaction variable)

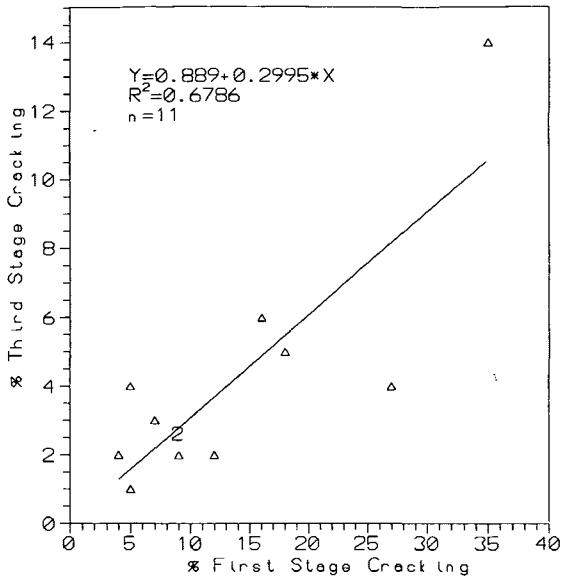

FIGURE 2 Percentage first- and third-stage cracking.

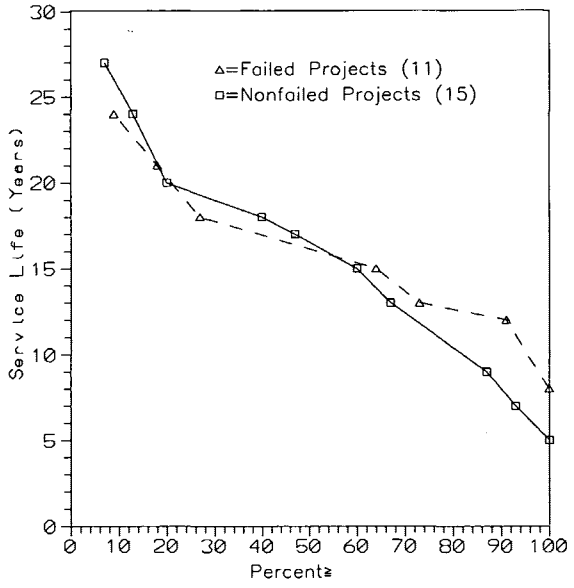

FIGURE 4 Cumulative frequency distribution, service life (years).

that ultimately failed had a higher amount of both first- and third-stage cracking before installation of edge drains. Although this may explain why 11 retrofit edge drain projects failed, it does not explain why these projects had cracked so badly to begin with or how cracking would have progressed if edge drains had not been installed. Service life and accumulated ESAL were studied to investigate further the causes of preretrofit cracking. Additional cumulative frequency plots, shown in Figures 4 and 5, indicate no significant difference between failed and nonfailed projects in terms of service life and accumulated ESAL.

Ultimately, environmental conditions were found to significantly affect the performance of the JPCP. Figure 6 shows a trend toward higher annual rainfall at projects that failed (however probabilities were not significant at 95 percent confidence, as shown in Table 4). Figure 7 shows that annual heating degree-days are higher at failed projects (differences are significant at 95 percent confidence in Table 4) but annual cooling degree-days are generally similar. These plots were influential in showing how the environment affects the JPCP as well as suggesting the need for explicit consideration of environmental variables in PCCP design. The points plotted

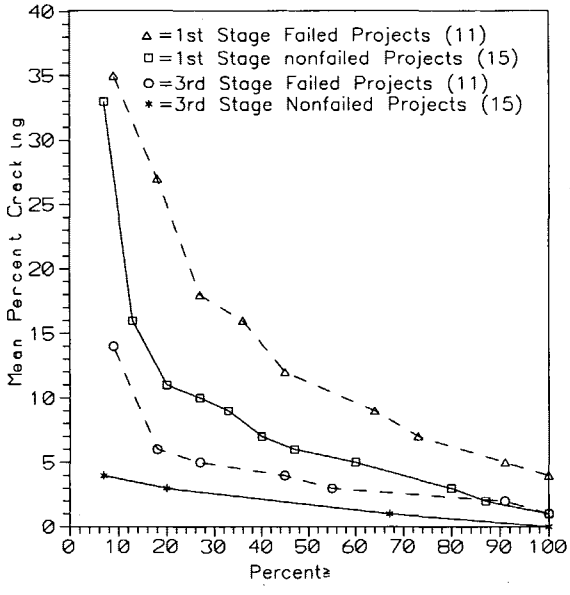

FIGURE 3 Cumulative frequency distribution, first- and third-stage cracking.

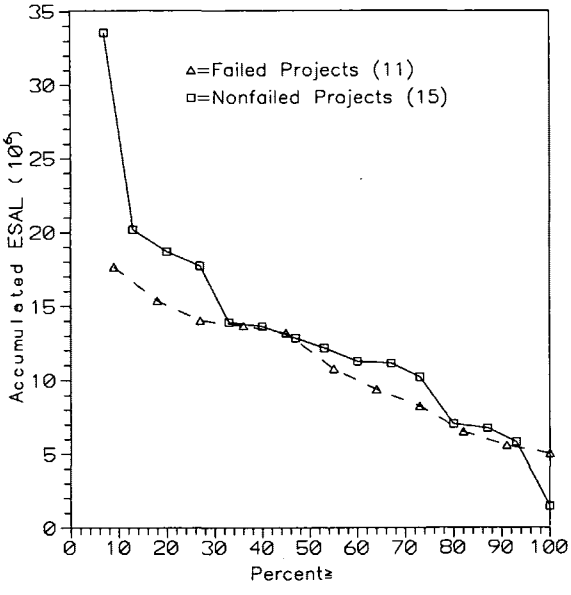

FIGURE 5 Cumulative frequency distribution, ESAL.

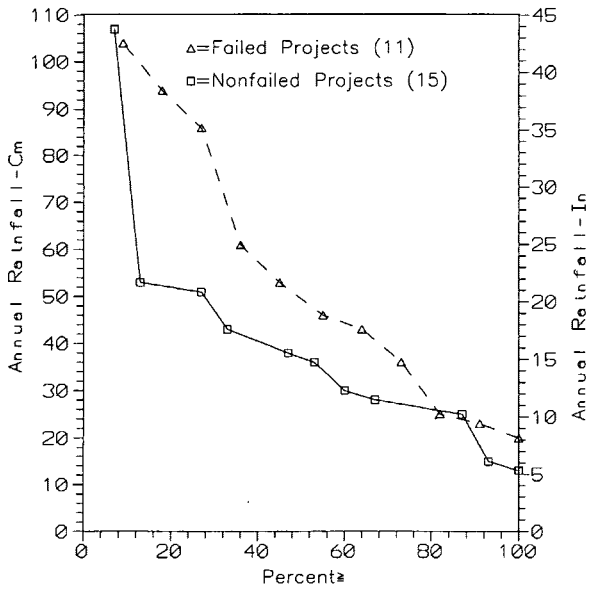

FIGURE 6 Cumulative frequency distribution, annual rainfall.

in Figures 3 through 7 represent the maximum values within each interval. These results showed the need to incorporate environmental variables into regression studies.

Subsequent linear regression studies of the 11 failed projects suggest that susceptibility of slabs to third-stage cracking is more predictable using environmental parameters instead of first-stage cracking only, as discussed earlier. This is evident from multiple linear regression analyses that investigated environmental factors, traffic load (ESAL), and service life, which are known to cause cracking via the faulting process (*1*,*6*).

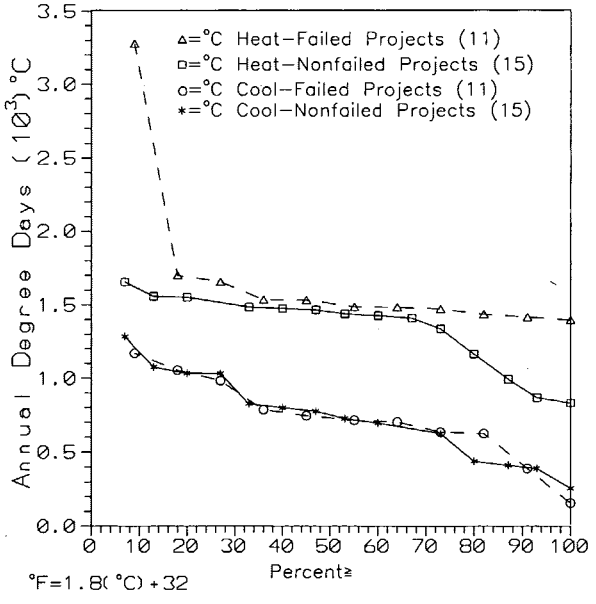

FIGURE 7 Cumulative frequency distribution, annual heating and cooling degree-days.

Environmental parameters that were investigated included annual heating degree days and an interaction variable of the product of annual rainfall and annual cooling degree days. All the variables were statistically significant at a 99 percent confidence level, as shown in Table 5.

Note that the regression equation in Table 5 has an adjusted $r^2 = .96$, showing much stronger correlation than that based only on first-stage cracking where $r^2 = .68$. The multiple regression equation appears well suited for potential use in design for rehabilitation and new construction for California PCCP.

First-stage cracking was subsequently modeled as a function of the environmental parameters annual rainfall, annual heating and cooling degree-days, and the interaction variable of the product of annual rain and annual heating degree-days to further evaluate nontraffic influences. First-stage cracking has a much weaker correlation with environmental factors than does third-stage cracking.

CONCLUSIONS

Analysis of the data from the 26 retrofit edge drain projects revealed that the amount of third-stage cracking before retrofit edge drain installation is a critical factor in subsequent JPCP performance (Table 2). Only 1 project out of 13 with third-stage cracking ≤1 percent failed prematurely, but 10 projects out of 13 failed with third-stage cracking >1 percent.

The data suggest that preretrofit edge drain cracking on the 11 projects that ultimately failed is correlated with environmental factors, service life, and ESAL. Other research suggests that the rate and variation of heating may be even more important than thermal gradients within the pavement (*7*). This research may explain why previous research (*1*,*6*) attempting to relate only rainfall to the rate of JPCP faulting (and eventual cracking) was inconclusive.

Despite limitations in the data base, these results show that third-stage cracking is significantly related to environmental conditions, service life, and accumulated ESAL on those projects where premature failure of the JPCP occurred after retrofit edge drains were installed. Limitations include (a) small data base (11 failure projects), (b) measurements of cracking are subjective judgments, (c) values for environmental parameters were estimated using data from the closest meteorological station, and (d) ESAL estimates are samples of partial-day, 24-hr and 7-day counts (*3*), which can be subject to error.

Related reports support the results of the study. A PMS study (*8*) indicated, for JPCP exhibiting between 1 and 10 percent third-stage cracking, that third-stage cracking can be expected to double every 2 years. An FHWA research paper presented at the 1988 Annual Meeting of TRB (*9*) included the statement

> . . . when 5% or more of the right lane required full depth replacement, the project was probably not a suitable CPR candidate, projects requiring between 2 and 5 percent full depth replacement of the right lane were marginal CPR candidates.

These findings show a need for careful consideration of the amount of third-stage cracking and environmental factors before placement of retrofit edge drains on JPCP. More im-

TABLE 5 Multiple Regression Analysis

Dependent Variable: %3rd Stage Cracking

Ind Var	B Coef	Std Err(B)	t-value	Prob
Heat	.002784	.000283	9.8225	<.0001
Rain*Cool	.000213	.000015	14.6358	<.0001
Life	-.543476	.058189	-9.3399	<.0001
ESAL	.483927	.077947	6.2084	.0008

Multiple r = .9897

Std Err Est = .668

F = 71.8507

Constant = -7.309712

Multiple Correlation Summary

	Multiple r	r-square
Unadjusted	.989722	.97955
Adjusted	.982811	.965917

Std Error of Estimate = .667964

Sample size = 11

portant, this study suggests that environmental factors strongly influence the undrained performance of JPCP. Therefore, the future use of current PCCP designs and development of alternative PCCP designs should address environmental factors that can contribute to poor PCCP performance in California.

REFERENCES

1. Wells, G. K. *Evaluation of Edge Drain Performance.* Caltrans Publication FHWA/CA/TL-85/15. California Department of Transportation, Sacramento, Nov. 1985.
2. Wells, G. K., and S. M. Wiley. *The Effectiveness of Portland Cement Concrete Pavement Rehabilitation Techniques.* Caltrans Publication FHWA/CA/TL-87/10. California Department of Transportation, Sacramento, Aug. 1987.
3. *Annual Average Daily Truck Traffic on the California State Highway System, 1971 through 1990.* Division of Traffic Engineering, California Department of Transportation, Sacramento.
4. *Monthly Normals of Temperature, Precipitation, and Heating and Cooling Degree Days 1951–80.* National Oceanic and Atmospheric Administration, Climatography of the United States 81 (By state). U.S. Department of Commerce, Sept. 1982.
5. Siegel, S. *Nonparametric Statistics.* McGraw Hill Publishing Co, 1956.
6. Neal, B. F. *Model Slab Faulting Study.* Caltrans Publication FHWA/CA/TL-80/23, California Department of Transportation, Sacramento, June 1980.
7. Armaghani, J., T. J. Larson, and L. L. Smith. Temperature Response of Concrete Pavements. Presented at 66th annual meeting of the Transportation Research Board, Jan. 1987.
8. *Pavement Management System, State of the Pavement.* California Department of Transportation, Sacramento, Jan. 1988.
9. Hallin, J. P., D. M. Mathis, and R. L. Lee. Performance Review of Concrete Pavement Restoration. Presented at 67th annual meeting of the Transportation Research Board, Jan. 1988.

Publication of this paper sponsored by Committee on Pavement Rehabilitation.

Comparison of Compaction Methods in Narrow Subsurface Drainage Trenches

GRAHAM R. FORD AND BARBARA E. ELIASON

Field investigation results of narrow-trench compaction methods with granular materials are presented. To determine what levels of compaction energy would produce target densities of at least 95 percent of standard Proctor, thus minimizing shoulder settlement above pavement edge drain trenches, a 200-mm (8-in.)-wide trench was excavated to four different depths: 300, 600, 900, and 1200 mm (12, 24, 36, and 48 in.). Fine filter aggregate was backfilled above a 75-mm (3-in.) inside diameter corrugated polyethylene pipe. Four compaction methods were evaluated: (a) one and two passes with a relatively low-energy modified plate compactor, (b) one and two passes with a high-energy vibratory wheel compactor, (c) one pass with a front-end loader tire, and (d) flooding with water. Sand cone densities and dynamic cone penetrometer tests were taken in each test section to determine how well the backfill was compacted. The high-energy wheel performed the best, producing satisfactory compaction to 300 mm (12 in.) with one pass and to 600 mm (24 in.) with two passes. It was the only method that actually achieved the desired target density. Slight pipe distortion was noted after two vibratory wheel passes at 300 mm (12 in.) deep, but no crushing was found. The vibratory ski performed poorly; in fact, one pass of the front-end loader tire gave generally better results than two passes with the vibratory ski. Water densification in the narrow trench was only slightly better than no compaction at all. Dynamic cone penetrometer testing generally correlated well with percent of Proctor compaction data, thus showing promise for evaluating compaction in narrow, granular-backfilled trenches.

The Minnesota Department of Transportation (Mn/DOT) typically installs 600,000 to 900,000 m (2 million to 3 million ft) of pavement edge drain per year and specifies the method in which these drains shall be backfilled and compacted (Figure 1 shows a typical drain section). Until research and on the basis of consultation with several compactor manufacturers, it was assumed that if the contractor followed a specified method for compacting these drains, satisfactory density and stability would be achieved. Current Mn/DOT specifications for backfill of these narrow trenches, defined here as up to 250 mm (10 in.) wide, state that the fill shall be a moist (approximately 3 to 5 percent moisture) fine filter aggregate (equivalent to a clean washed concrete sand). It shall be compacted with a vibratory plate compactor to which a shoe or "ski" has been attached that extends below the plate and down into the trench. The fabricated ski shall be narrower than the trench by 50 mm (2 in.), shall be 500 mm (20 in.) long, and shall vibrate at a minimum of 2,000 revolutions (blows) per minute (rpm). The impact force of the compactor shall be a minimum of 1815 to 2725 kg (4,000 to 6,000 lb) depending on the depth of the lift being compacted. Individual lift depths must not exceed 600 mm (24 in.).

Use of this method specification has resulted in Mn/DOT having occasional problems with settlement above the narrow trenches (Figure 2). The question arose as to whether satisfactory densities were being achieved with this method specification. Satisfactory density is defined here as 95 percent of standard Proctor density. Skok (*1*) states in his report on trench compaction, and Mn/DOT (along with most construction agencies) believes, that to minimize settlement, it is very important to compact trench backfill to at least 95 percent of standard Proctor. Conceivably, densities down to 90 to 92 percent of Proctor may minimize settlement in narrow trenches, but no attempt was made in this research to verify any particular minimum value.

To minimize potential safety hazards for vehicles due to shoulder settlement and to diminish the need for long-term maintenance, Mn/DOT undertook this study of compaction methods using fine filter aggregate (FFA) in narrow trenches. The goal was to determine the actual densities achieved at various depths with different compaction energies and methods and ultimately specify either a compaction method or a density that would minimize the potential for settlement in future trenching contracts.

Trench compaction has been studied in the past using wider trenches or more cohesive soils, but the authors are unaware of other research that duplicates the goals of this study. ASCE (*2*) studied the compaction of clay backfill in trenches. Farrar (*3*) researched settlement of road surfaces above reinstated sewer trenches approximately 1 m (3 ft) wide. Kersten and Skok (*4*) and Skok (*1*) studied backfill densities with various soils, equipment, and trench geometries in trenches generally wider than 0.6 m (2 ft). The authors contacted several manufacturers of compaction equipment in the search for other research of this nature, but without success.

FIELD RESEARCH

The soil in which the research trench was excavated was predominantly clay with an approximate near-surface density of 1410 kg/m^3 (87 lb/ft^3) at 20 percent moisture, against a standard Proctor density (ASTM T99) of 1640 kg/m^3 (101 lb/ft^3) at 18 percent optimum moisture and a modified Proctor (ASTM T180) of 1830 kg/m^3 (113 lb/ft^3) at 15 percent optimum moisture. The research trench was constructed in an agricultural field instead of along a roadway for safety reasons. The lower densities of the clay trench walls may lead to slightly lower compacted backfill densities than would have been found if

Minnesota Department of Transportation, Office of Materials Research and Engineering, 1400 Gervais Avenue, Maplewood, Minn. 55109.

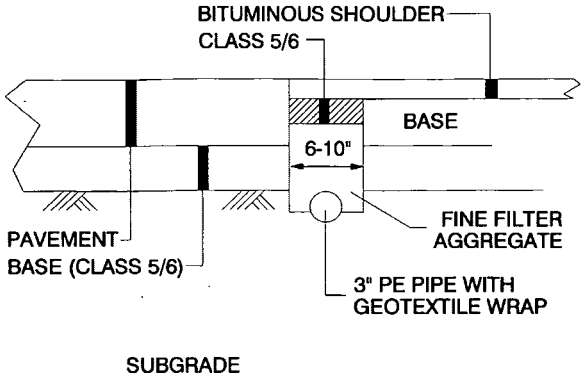

FIGURE 1 Typical drain section for Mn/DOT subsurface pavement edge drains.

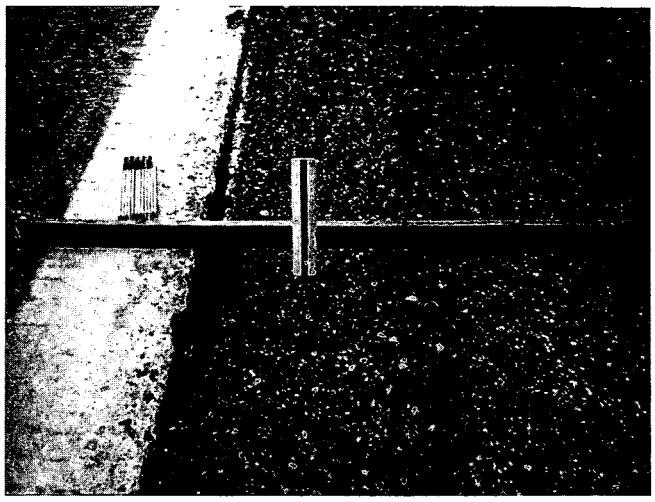

FIGURE 2 Settlement of approximately 30 mm (1.2 in.) that occurs when trench backfill is not compacted sufficiently.

the trench had been excavated into more typical higher density roadway grading materials.

A 75-mm (3-in.) inside diameter × 100-mm (4-in.) outside diameter polyethylene pipe (AASHTO M252) was mechanically laid in the bottom of the trench. The backfill material was a relatively clean sand, unprocessed, from a local pit (Belle Plaine sand). It had a standard Proctor density of 1950 kg/m^3 (120 lb/ft^3) at 11 percent optimum moisture and modified Proctor density of 2100 kg/m^3 (129 lb/ft^3) at 11 percent optimum moisture. The mechanical analysis of these two materials (Belle Plaine sand and native soil) as well as the Mn/DOT specified gradation band for FFA are shown in Figure 3. The Belle Plaine sand does not fully comply with Mn/DOT specifications for a FFA but was readily available at the research site. A short laboratory experiment was performed to correlate the field results of the "dirty" Belle Plaine sand to a more typical and cleaner (relative to the percentage minus 200) FFA. The results of that research are discussed in later sections.

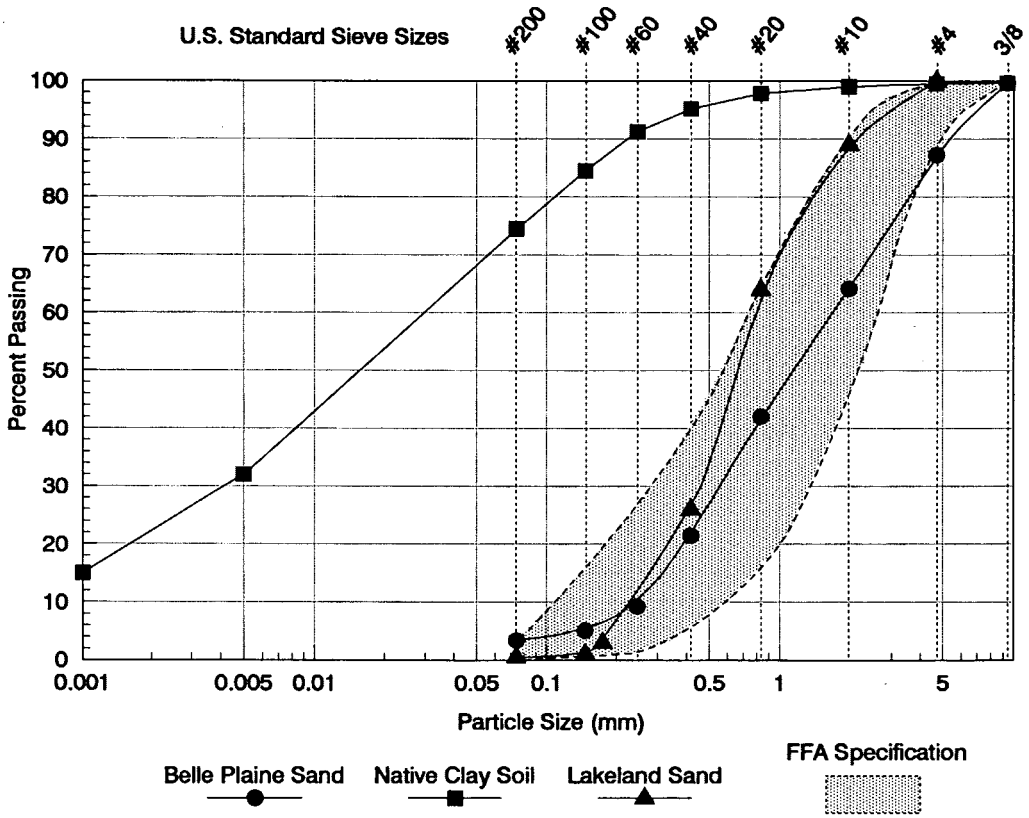

FIGURE 3 Mechanical sieve analysis of soils used and specification band for FFA.

Field Procedure

The research trench was constructed in an agricultural field just outside of Belle Plaine, Minnesota (65 km south of Minneapolis). The research was performed in fall 1991 and spring 1992. A standard Dynapac trenching machine with shield attachment was used to excavate a trench 105 m (343 ft) long by 200 mm (8 in.) wide. FFA was placed and compacted with an approximate moisture content of 5.5 percent. Figure 4 shows the trencher and backfilling equipment employed. The trench is continuous with four test cells, each 23 m long (75 ft), each of a different depth—300, 600, 900, 1200 mm (12, 24, 36, 48 in.)—and a transition zone between each cell (Figure 5). The transition zones received no compaction.

Each of the four test cells is divided into five test sections 4.6 m (15 ft) long and compacted with a different method or repetition of a method. The first test section in each cell was compacted with one pass of the low-energy vibratory ski, the second with two passes of the vibratory ski, the third with one pass of the higher-energy vibratory wheel, the fourth with two passes of the vibratory wheel, and the fifth with one pass of a front-end loader tire. All compactors traveled at an approximate speed of 15 to 18 m/min (50 to 60 ft/min), which is typical of trenching rates for Minnesota contractors.

The vibratory ski is a modified standard plate compactor with a "ski" attachment (Figure 6). The version used in this research was the Sakai plate compactor, Model PC8S with a 2633-kg (5,800-lb) rated force (per blow) operated at 3,400 rpm. The ski attachment extended 150 mm (5.75 in.) below the bottom of the plate, which was sufficient to prevent dissipation of energy onto each side of the trench. This was true even with the deepest trenches because minimal density change (compaction) was noted in the lower portions of the trench. Vibratory ski compaction was studied because it is currently the required method of compaction in Mn/DOT specifications.

FIGURE 4 Dynapac trenching machine, truck delivering filter aggregate, and shouldering attachment on front-end loader, which places filter aggregate into trench.

The wheel is a vibratory compactor made by the Vermeer Manufacturing Company, under the model name Ditcher Stitcher. It has a gross weight of 1170 kg (2580 lb) and has a rated force of 3629 to 7257 kg (8,000 to 16,000 lb) operating at 1600 rpm (Figure 7). The trench was compacted using the Vermeer wheel's maximum force. The compaction wheel itself has the ability to drop below ground level to a depth of 660 mm (26 in.). The Vermeer compactor was chosen for the research because a local contractor was using it and it was

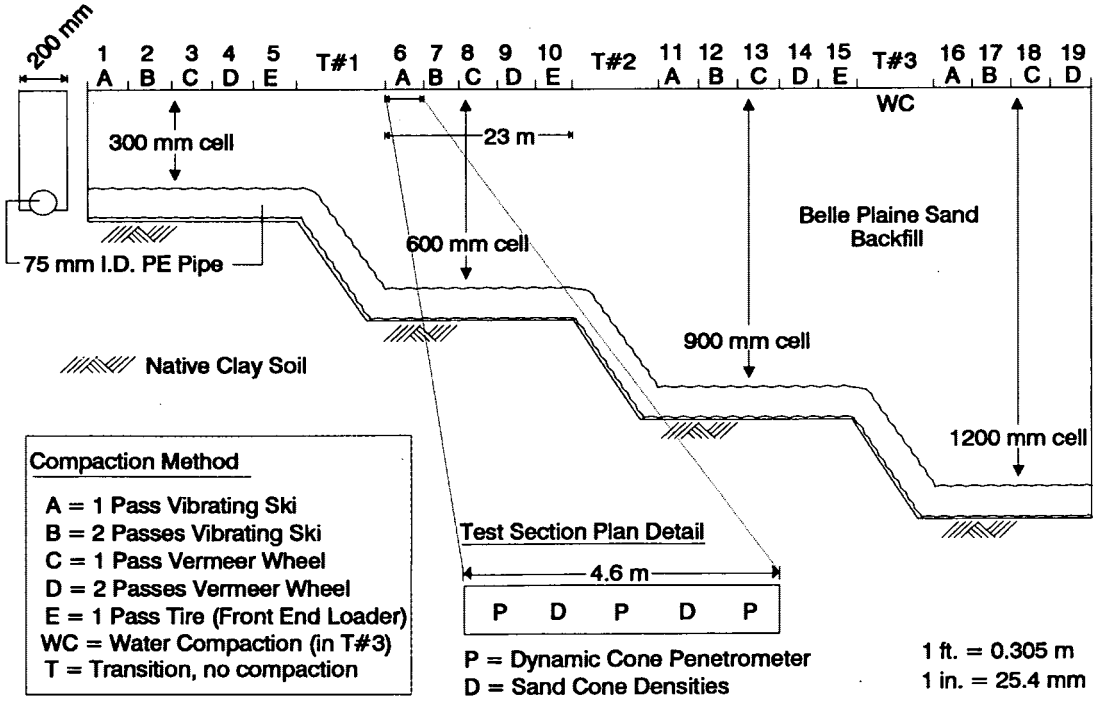

FIGURE 5 Testing layout of research trench.

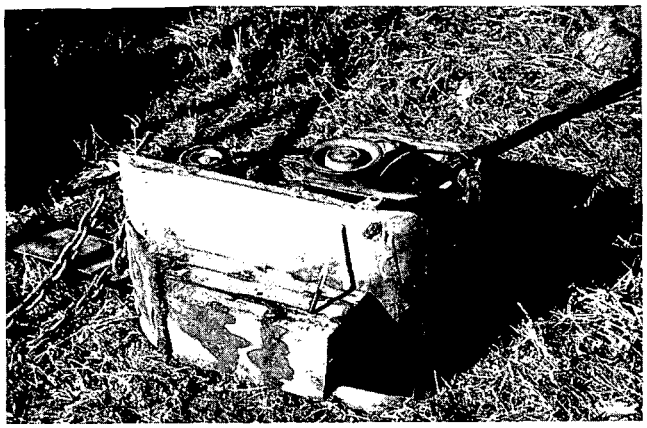

FIGURE 6 Sakai plate compactor modified into vibratory ski.

believed it represented the high end of the compaction equipment available locally. The following table presents the manufacturers' specifications for the various compactors discussed:

	Sakai PC8S "Ski"	*Vermeer*	*Stone S-52 "Ski"*
Rated force (kg)*	2633	3628–7257	2315
Frequency (rpm)	3400	1600	5400

* 1 lb = 0.454 kg

It was also decided to verify the compaction achieved by simply running a piece of heavy construction equipment, in this case the tire of a large front-end loader, over sand heaped 100 to 150 mm (4 to 6 in.) above the trench. This method of compaction was studied because of claims by contractors that densities as high as the vibratory ski could be achieved this simply.

The final method of compaction evaluated was the flooding of an area of the already backfilled trench with water. This phase was done because it is broadly speculated that flooding will give adequate densities in granular material. Transition 3 was chosen for this work because it was a deep section of undisturbed, uncompacted trench. To provide a reservoir to contain the water, the upper 350 mm (14 in.) of sand was removed, thus creating a trough 3.7 m (12 ft) long and 200 mm (8 in.) wide. The trough was flooded in two steps. The first time, 380 L (100 gal) were poured into the trough. The water was poured onto a piece of plastic at one end of the trough to avoid disturbing the surface soil and thus changing the water infiltration rate due to surface siltation. A half hour later an additional 190 L (50 gal) were applied for a total of 155 liters/m (12.5 gal/ft) of trench length. The water in the trough reached a maximum head of 180 mm (7 in.) each time water was added and percolation rates through the sand were relatively fast. Two quantities of water were used because no increase in density was noted using dynamic cone penetrometer (DCP) equipment after the first flooding. Before testing the water-densified section, it was verified that all excess water had passed through the backfill and drained out of the underlying perforated pipe, thus no further compaction would be expected.

FIGURE 7 Vermeer ditcher stitcher.

Testing Procedure

The consolidation of the soil after compaction was determined by two methods. The first was by sand cone density, AASHTO T191. These were run at roughly 150-mm (6-in.) vertical intervals to the top of the pipe and at either one or two location in each test section (Figure 5).

The second method used the DCP (*5*). It is a semidestructive testing device used to evaluate subgrade soil strengths. It consists of a scaled steel rod 1120 mm (44 in.) long with a penetrating cone at the tip (Figure 8). A sliding 8-kg (17.6-lb) weight with a drop distance of 575 mm (22.6 in.) is attached and provides the force to drive the rod into the soil. Gross weight of the DCP is 13 kg (29 lb). After each blow, the depth to which the rod has penetrated is read. Two or three DCP tests were taken in each test section (Figure 5). For purposes of this investigation, the DCP has not been actually calibrated to give soil strength and density, but rather to provide a relative indication of the compaction in the backfill sand. The moisture content of the trench backfill sand ranged from about 4 to 7 percent during testing (8 to 9 percent in the water compacted section). The authors are unaware of any research that has been done with the DCP to determine whether, for the same density, moisture changes in granular soils significantly alter the DCP test values.

To determine whether the polyethylene pipe laid in the bottom of the trench had been damaged by compaction, the end of the pipe from Test Section 4 was exposed and the diameter measured. In addition, a 65-mm (2.5-in.) probe was pushed through the length of pipe in the same section to check for crushing. Test Section 4 was chosen as representing the worst case condition because it was only 300 mm (12 in.) deep and had received two passes with the Vermeer wheel.

Results

The results of the sand cone densities and the DCP tests have been compiled by test cell depth and shown in Figures 9–12. The sand cone densities are listed to the left of the DCP values and represent percent of standard Proctor density. These numbers are plotted at the midpoint of each tested interval, usually 150 mm (6 in.). In Figures 9–12 an ^{A} next to a Proctor percentage indicates an average of two values for the same

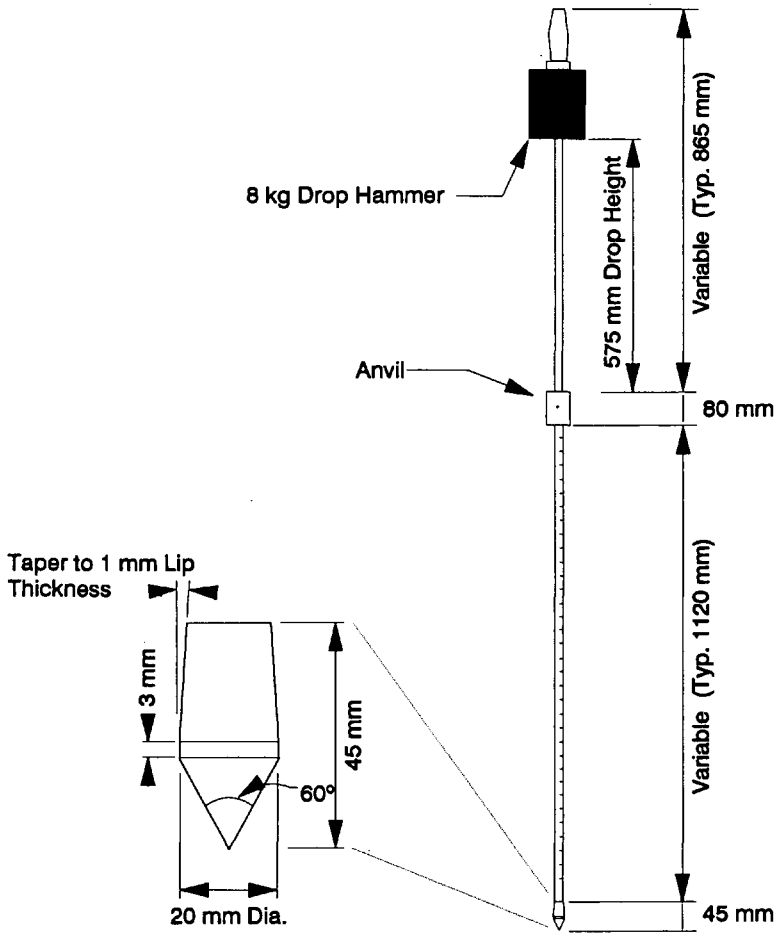

FIGURE 8 Diagram of DCP, standard South African design.

depth but in different locations in the test section. Where average values are shown for Proctor percentages, 60 percent are within ±1 Proctor percent of the values averaged, 80 percent within 2 percent, and 90 percent within 3 percent. Areas that have densities at or above the 95 percent Proctor target have been shaded.

The average density of the backfill placed in the trench without any compaction (labeled "none" on the graphs) is approximately 82 percent of standard Proctor. Higher densities were generally seen at depth due to the weight of the overlying sand. As expected, all compaction methods produced higher densities than no compaction at all.

Surprisingly, the low energy vibratory ski, which is the method currently specified by Mn/DOT for use in its narrow trenches, only gave one density reading greater than 95 percent standard Proctor—even after two passes—throughout the entire research trench. This indicates that Mn/DOT sees settlement of paved shoulders above some of the trenches because of the use of insufficient compaction energy and not as a result of inadequate construction procedures or inspections. The higher energy Vermeer wheel performed significantly better, producing densities around 95 percent of standard Proctor up to a depth of 300 mm (12 in.) with one pass and about 600 mm (24 in.) with two passes. Below 600 mm (24 in.), even with the Vermeer, compaction effectiveness dropped off significantly, as seen both by percent of Proctor and DCP blow count. That the Vermeer provided superior results with respect to the "ski" should not be unexpected because the rated force for the Vermeer is almost three times that of the Sakai compactor. Each also had different vibration frequencies (blows per minute), the possible effect of which was not evaluated here. It was also a surprise that one pass with the front-end loader tire generally outperformed the ski compactor.

After flooding a 3.7-m (12-ft) long and previously noncompacted section of the trench—Transition zone 3—with a total of 570 L (150 gal) of water—155 L/m (12.5 gal/ft)—the average density of the backfill was greater than the uncompacted sand but was still only 87 percent of standard Proctor (Figure 11). The volume of water used is greater than would or could typically be used during normal edge drain construction.

DCP blows are given in the bars on Figures 9 through 12. A line is drawn across the bars at the depth at which the DCP cone stopped. The number above the line indicates the number of hammer blows to that depth; a zero indicates penetration achieved due solely to the gross weight of the DCP because it was carefully set into the backfill. Zero penetration

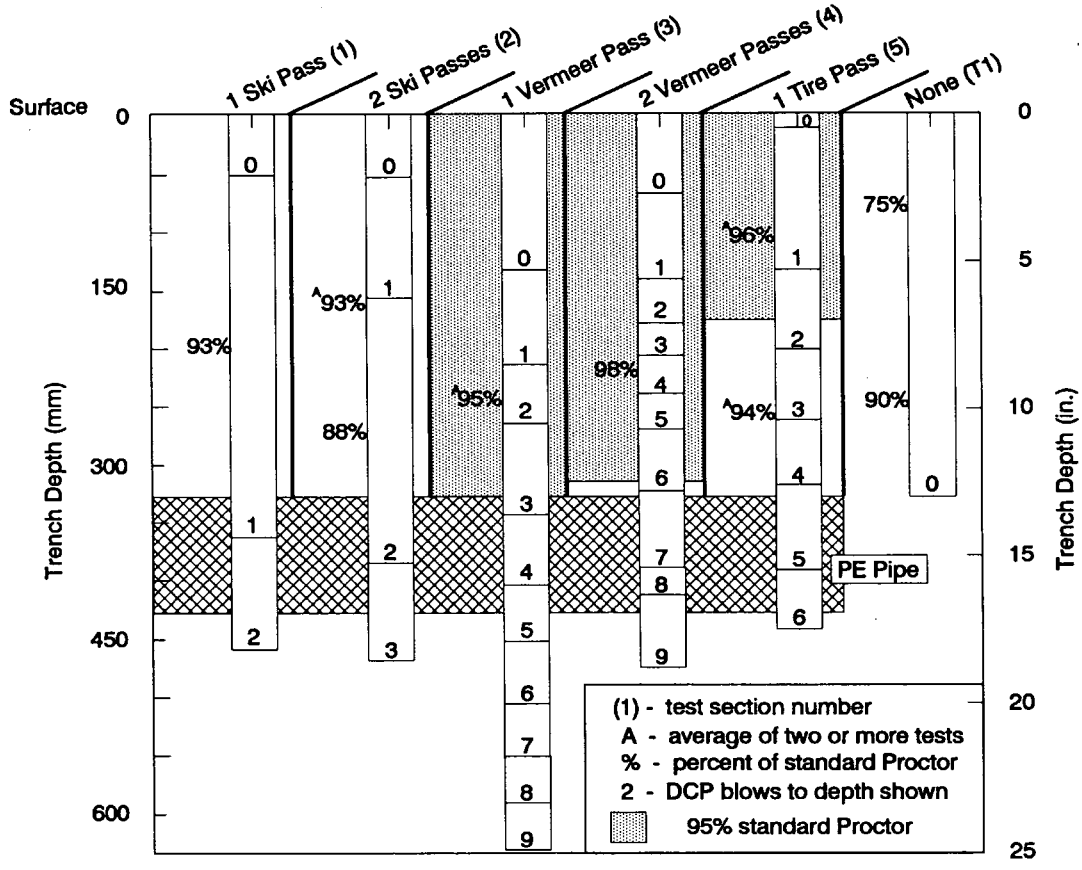

FIGURE 9 Field compaction results in 300-mm trench depth.

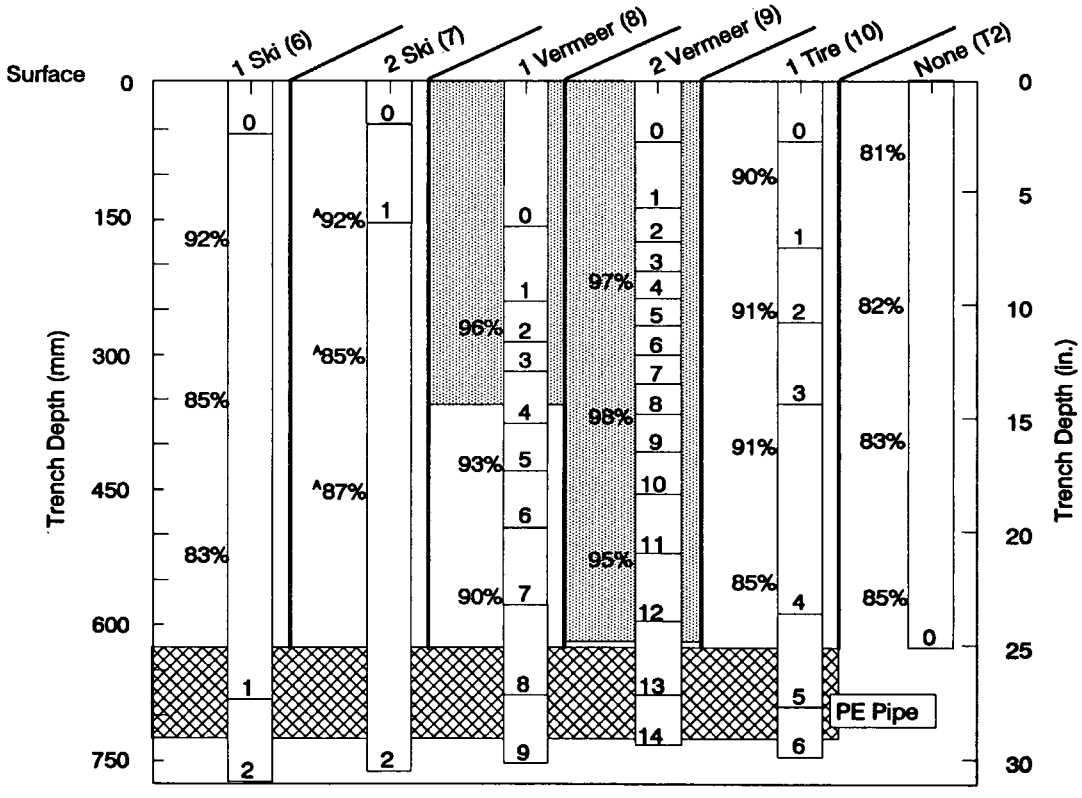

FIGURE 10 Field compaction results in 600-mm trench depth.

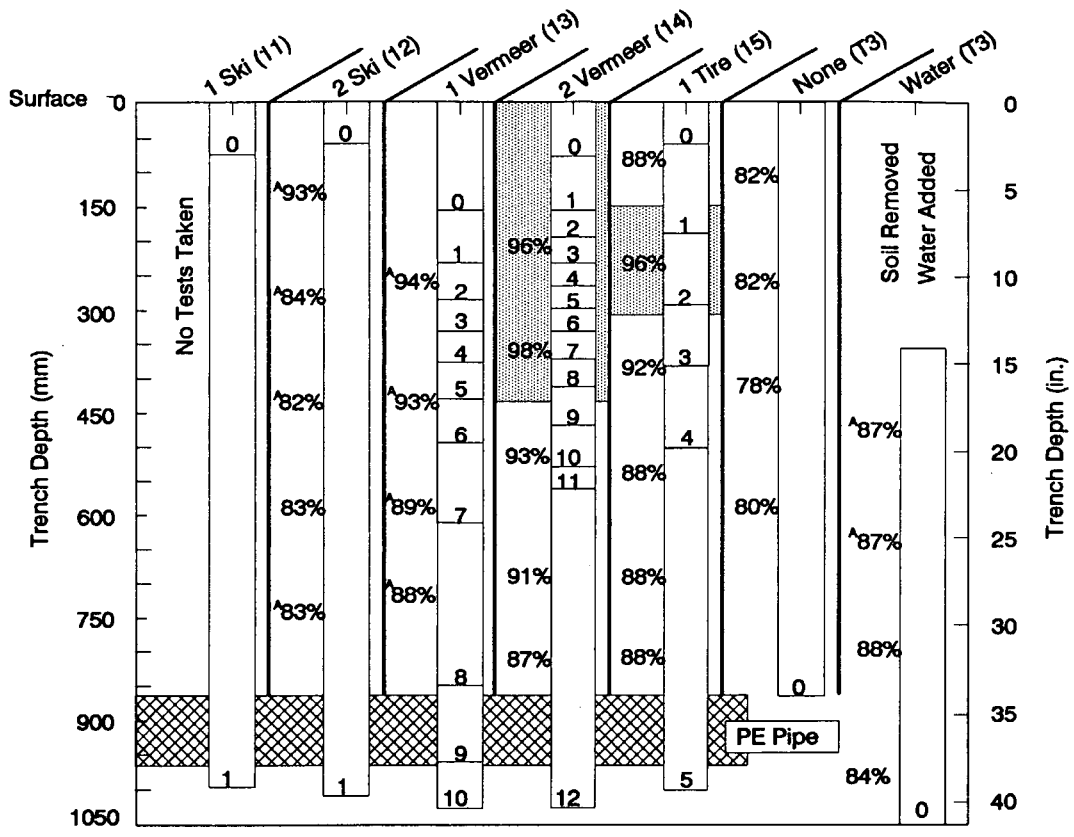

FIGURE 11 Field compaction results in 900-mm trench depth.

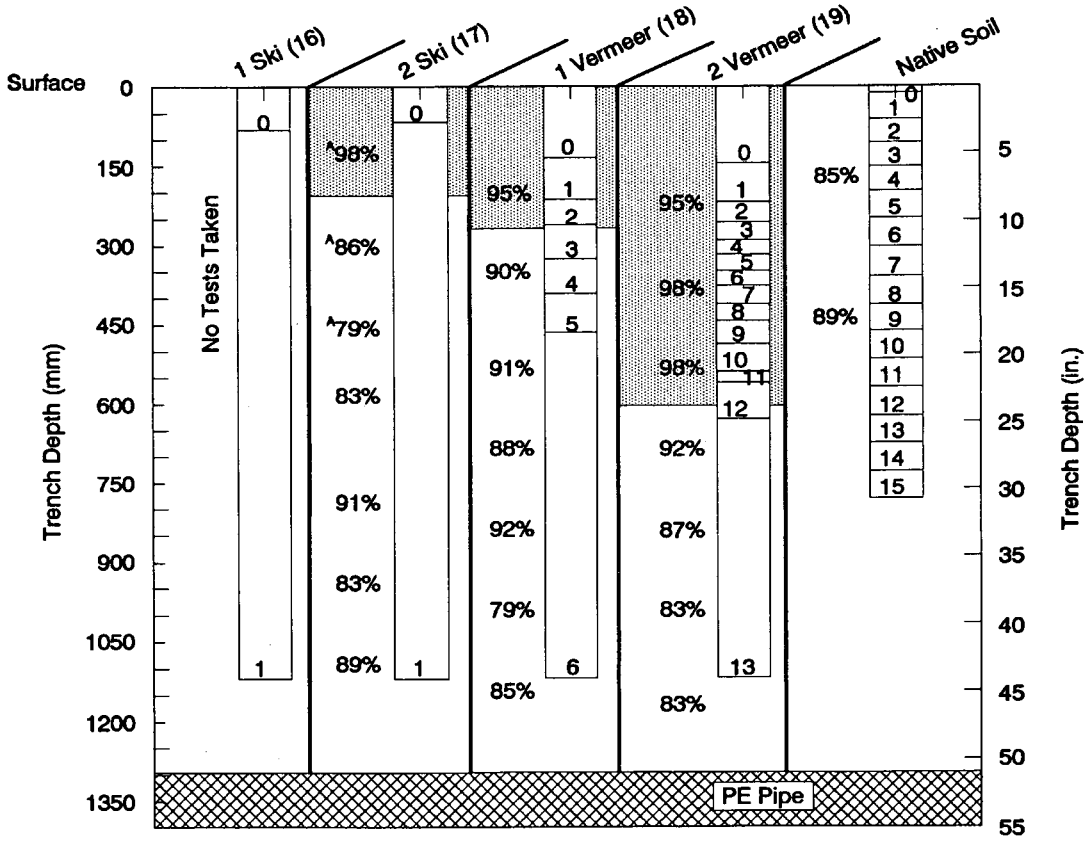

FIGURE 12 Field compaction results in 1200-mm trench depth.

points, which are shallower for two-pass test sections than one-pass test sections, are because before the second compaction passes, these sections were refilled with sand to the ground surface.

In the vicinity of the pipe, the DCP tip was driven through the pipe (with no apparent resistance) or in some instances possibly through the sand immediately next to the pipe without penetrating the pipe. Some of the plots show the DCP cone as stopping within the pipe itself, which did not actually occur in the field. This apparent anomaly is because two or three DCP tests are averaged within each test cell (some above the pipe and some at or below the bottom). Because the DCP can read a maximum 1120 mm (44 in.) below the ground surface, no data exist below this depth.

DCP penetration depths for equal blow counts were found to be quite consistent within each test section. For any blow count, roughly 70 percent of the two or three depths averaged are within ±25 mm (1 in.) of the average plotted and an additional 25 percent are within 50 mm (2 in.) of the average.

As would be expected, DCP values reflect compaction effectiveness, showing less penetration per blow the more compacted is the sand. Although a graphical method of showing the DCP data was chosen for this paper instead of the more conventional penetration per blow, the penetration index can be roughly calculated from the figures.

The polyethylene pipe was found to be distorted less than 2 mm (.0625 in.) when a 150-mm (6-in.) length of the pipe was carefully removed and the inside diameter of the pipe remaining in the ground was measured. Using a 65-mm (2.5-in.) probe, no resistance was encountered anywhere in the 4.6 m (15 ft) of pipe probed except in one isolated spot, yet the probe would still pass through. Therefore, although a maximum distortion of approximately 13 mm (0.5 in.) occurred, for the most part the pipe remained undamaged after two passes with the Vermeer wheel in the 300-mm (12-in.) test cell. Sand cone densities and DCP data for the in-place agricultural field clay are shown in the last column of Figure 12.

LABORATORY RESEARCH

As can be seen in Figure 3, the backfill that was used in the field research trench was not as "clean" as that normally specified by Mn/DOT for use in narrow trenches (about 4 percent minus 200 versus typically 2 percent minus 200). To give the results taken from the field more credibility, the slightly "dirty" Belle Plaine backfill was compared with a "cleaner" sand in the laboratory. The "cleaner" sand is identified as Lakeland sand. It had a standard Proctor density of 1800 kg/m^3 (111 lb/ft^3) at 13 percent optimum moisture and a modified Proctor density of 1880 kg/m^3 (116 lb/ft^3) at 12 percent optimum moisture. Its gradation is shown in Figure 3.

The Lakeland sand, with approximately 3 percent moisture content, was placed in 150-mm (6-in.) lifts into a plywood box measuring 200 mm wide × 600 mm long × 900 mm high (7.5 × 24 × 36 in.). The box was built to replicate a section of trench 900 mm (36 in.) deep. Each of the six lifts was compacted using a pipe-handled steel-plate hand tamper 75 × 150 mm (3 × 6 in.). The compaction effectiveness was determined by taking sand cone densities in the middle of the box and DCP tests on both sides. This procedure was then repeated using the Belle Plaine sand.

The results of this research (including Proctor densities) are shown in Figure 13. Although the gradations and sand cone density values differ, the DCP results and the percentage of standard Proctor for the two sands are quite similar.

CONCLUSIONS

The results of the research show that a relatively low-energy (force) vibratory ski, as currently specified by Mn/DOT, is not effective in achieving the 95 percent of standard Proctor density that Mn/DOT wants in the backfill of narrow trenches. One pass with a front-end loader tire over heaped sand gave generally better compaction than the vibratory ski, and compaction with water was only slightly better than no compaction at all. Two passes with the high-energy Vermeer vibratory wheel achieved the target 95 percent standard Proctor density without damage to the pipe and is thus the most effective method evaluated. The use of compaction equipment that will achieve densities of roughly 95 percent of standard Proctor should replace the vibratory ski method specification currently used by Mn/DOT.

It should be kept in mind that the energy imparted by the Vermeer wheel achieves the target density to a depth of 300 mm (12 in.) with one pass and 600 mm (24 in.) with two passes. Therefore, these lift heights should likely not be exceeded for this or similar energy equipment. Because the Vermeer wheel maximum reach is 660 mm (26 in.) below ground surface, this particular compactor, at the maximum energy level, appears to be suitable for satisfactorily compacting narrow highway trenches up to 1200 mm (48 in.) deep if the backfill is placed and compacted in two lifts.

The widely accepted concept of achieving satisfactory density with water may be true if the sand is placed under water or in a wider trench or larger area, but water appears to provide minimal benefit in narrow trenches of the type investigated. Even if flooding provided a satisfactory density increase, experience suggests that under field construction conditions the use of water is not realistic for several reasons: (a) drain outlets must be in place before water densification can be accomplished, (b) the water liberates and spreads fines over the surface of the sand, which seals and prevents rapid water infiltration into the trench, and (c) water runs downgrade along the trench and saturates discharge locations, making density difficult to achieve in the backfill soils.

Research in both the field and laboratory leads to the conclusion that granular materials anywhere in the FFA gradation band (Figure 3), even though they may differ slightly in gradation and Proctor density, are likely to exhibit similar percent of Proctor and DCP penetration indexes for similar compactive efforts. The following generalizations can be drawn between penetration indexes and percent of Proctor for this set of research data: (a) penetration indexes of 75 mm (3 in.) per blow or less generally indicate compaction at or above 93 percent of standard Proctor, (b) penetration indexes greater than 125 mm (5 in.) per blow generally indicate compaction at or less than 89 percent of standard Proctor, and (c) percent of standard Proctor values from 89 to 93 percent yield variable penetration index values, ranging from 50 mm (2 in.) to greater

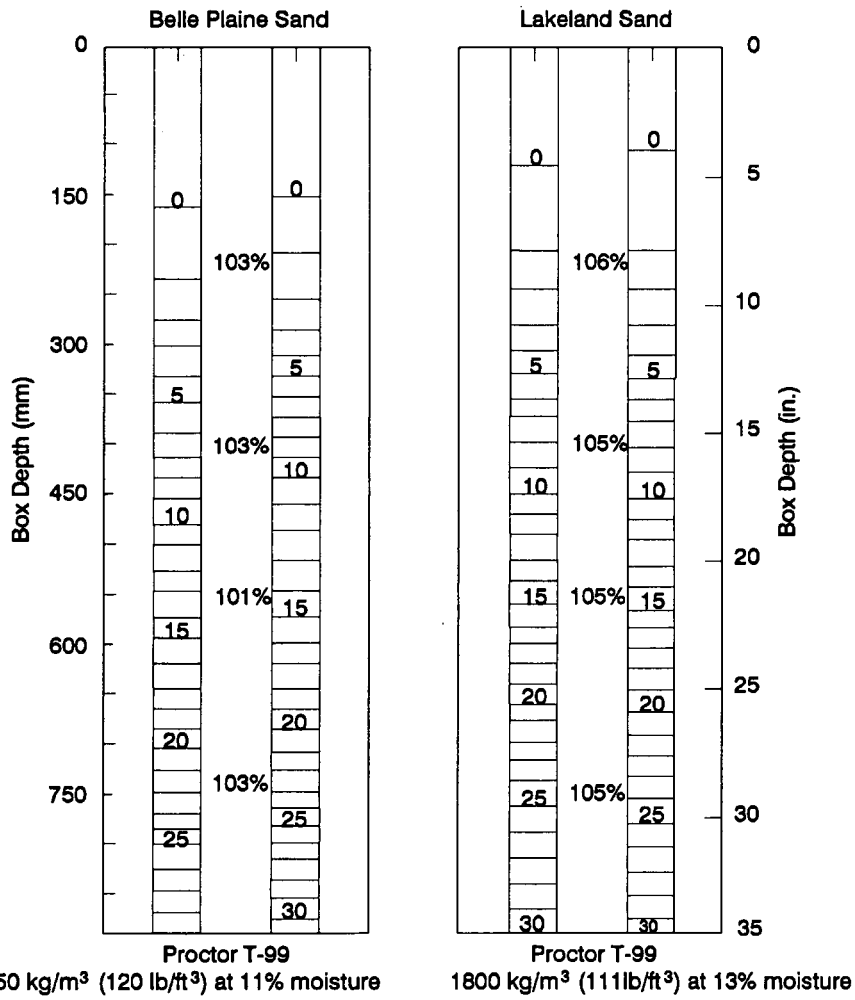

FIGURE 13 Laboratory compaction results in test box.

than 125 mm (5 in.) per blow, and thus are not easily distinguished by penetration index data. Using these general relationships, the DCP can be easily and quickly used by construction inspectors to evaluate and approve the use of different types of compaction equipment on the basis of field test installations. Depth of satisfactory compaction can also be easily verified. Such evaluations could be done on a project-by-project basis or possibly for specific types of equipment commonly used by contractors.

One issue for which this research does not provide a satisfactory answer is the possible effect of sidewall friction. In a trench deeper than 600 mm (24 in.), if the upper 600 mm (24 in.) are compacted to at least 95 percent of Proctor while the lower portion of the trench is not, will the sidewall friction of the upper portion still minimize long-term settlement, even with traffic vibrations and vehicle loading? Skok (*1*) reports that compaction to 95 percent of Proctor is most critical in the upper 600 mm (24 in.) because this is the area where the majority of the settlement occurs. It is possible that densities of 90 to 95 percent of Proctor below 600 mm (24 in.) may still yield minimal trench settlement.

These results likely apply to granular materials similar to those tested but should not be extended to significantly different granular materials, nongranular materials, or wider trenches without additional research. As a general conclusion and to paraphrase Skok (*1*), trench settlement can never be totally eliminated (regardless of compaction method and density achieved), only minimized to a satisfactory extent.

ACKNOWLEDGMENTS

The authors thank Chard Tiling and Excavating, Inc., of Belle Plaine, Minnesota, for providing the site, equipment, materials, and labor during the installation of the field trench. Without this assistance, the research could not have been accomplished. Thanks also to Mn/DOT's Physical Research Section for providing the DCP equipment and advice on its use and to George Cochran, physical research engineer, for advice and encouragement during the progress of the work.

REFERENCES

1. Skok, E. L., *Synthesis of Recent Trench Backfilling Studies*. Minnesota Highway Department Investigation 633. Department of Civil and Mineral Engineering, University of Minnesota, Sept. 1972.

2. *Committee on Backfilling in Public Rights-of-Way—Final Report.* ASCE, St. Louis Section, Missouri, April 1968.
3. Farrar, D. M., Some Measurements of Differential Settlement Above Reinstated Sewer Trenches. *Highways and Public Works*, Vol. 49, No. 1851, Feb. 1981, pp. 30–32.
4. Kersten, M. S., and E. L. Skok. *Backfilling Trench Excavations.* Minnesota Highway Department Investigation 610. Department of Civil and Mineral Engineering, University of Minnesota, June 1971.
5. Klimochko, D. The Application of the Dynamic Cone Penetrometer Test in Determining In-Situ Subgrade CBR. Presented at 44th Annual Conference of Western Association of Canadian Highway Officials, Saskatoon, Saskatchewan, Canada, April 1991.

Publication of this paper sponsored by Committee on Subsurface Drainage.

Hydraulic Requirements of Permeable Bases

JAMES A. CROVETTI AND BARRY J. DEMPSEY

To address the need for increased drainage within the pavement system, open-graded permeable materials (OGPM) are finding their way into standard design sections throughout the country. The design requirements of the OGPM to handle surface water infiltration are reported. Infiltration rates and required permeabilities of the OGPM are calculated for a range of conditions typical for pavement design. The effects of pavement geometry on required permeabilities, including cross slope, longitudinal gradient, and drainage layer thickness and width, are discussed. Analysis of selected materials, typical for use in Illinois, is completed to determine appropriate permeabilities.

The subject of drainage has been an integral part of pavement design since the early days of road building. Pursuant to this need, open-graded permeable materials (OGPM) have been used within portland cement concrete (PCC) pavement structures as long as these pavements have been built. The trend toward dense-graded aggregate base layers, both stabilized and unstabilized, that predominated the middle of this century lessened the use of these materials. However, in the past two decades there has been a resurgence in the use of OGPM within pavement structures. Highway agencies throughout the country have renewed efforts to evaluate OGPM, with the aim of developing pertinent design methodologies compatible with design specifications, climatic conditions, materials availability, and construction procedures. A research project initiated to address these topics was recently completed at the University of Illinois and the findings were published in a report entitled *Pavement Subbases* (*1*).

From a hydraulic perspective, a complete pavement drainage system is typically composed of many parts, including the base layers under the driving surface, longitudinal collector/transport systems located in the vicinity of the pavement edge, and sequential transverse outlet systems daylighted to surface drainage channels or attached to storm drains. Figure 1 gives a schematic illustration of the subdrainage components in a PCC pavement system. Basically stated, a positive drainage system should move water from the point of inception to the final exit through materials with sequentially lesser resistance (i.e., greater permeability) and greater capacity and should eliminate any conditions that would constrict flow.

This paper focuses on the first of these drainage components, the base layer under the driving surface. This layer is now constructed with OGPM to effectively transport surface water, which infiltrates the pavement surface through open cracks and joints to the remaining components of the drainage system. To intercept infiltrated surface water as quickly as possible, the OGPM layer is often placed immediately below the surface layer, as shown in Figure 1. Although it is possible for other sources of water, such as groundwater flow, artesian flow, and meltwater flow, to contribute to the total water to be drained by the OGPM, surface infiltration typically remains the dominant water source in structural pavement subdrainage design (*2*). To function properly as a drainage material, OGPM must be selected to meet the permeability and hydraulic gradient requirements of the pavement system.

J. A. Crovetti, Department of Civil Engineering, University of Illinois at Urbana-Champaign. Current affiliation: Marquette University, 1515 West Wisconsin Avenue, Milwaukee, Wis. B. J. Dempsey, University of Illinois, 1205 Newmark CEL-MC250, Urbana, Ill. 61801.

OBJECTIVES

The general objectives of this paper are to detail the properties of open-graded permeable materials (OGPM) that satisfy the permeability and hydraulic gradient requirements in pavements. The specific objectives are

- To relate pavement longitudinal grade and cross slope to permeability requirements of OGPM,
- To evaluate the hydraulic properties of various aggregates in Illinois pavement construction, and
- To discuss methods for evaluating the permeability of OGPM.

PERMEABILITY AND HYDRAULIC GRADIENT REQUIREMENTS IN PAVEMENTS

Surface Infiltration

Infiltration of water into a pavement system is a very complicated phenomenon. Theoretical transient flow studies in uniformly porous pavements have provided some insight into this complex problem (*3*). Generally stated, the amount of water that may infiltrate a given area of pavement surface depends on the permeability of the intact surface, the number of ingress channels (joints and cracks), and the quantity of water supplied. Research conducted by Ridgeway (*4*) indicates that the condition of the ingress channel (i.e., sealed or unsealed and debris filled, wide or narrow cracks/joints) and the type of base layer that underlies the pavement surface (i.e., open graded or dense graded) both play a role in defining the infiltration capacity of the joint/crack. For high capacity joints/cracks, high intensity, short duration storms are important. For low capacity joints/cracks, storm duration is more important than intensity.

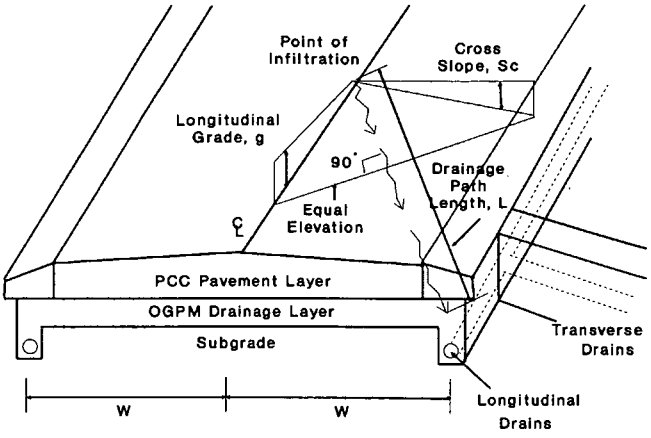

FIGURE 1 Typical pavement cross section.

Two separate methods for estimating surface infiltration rates in highway pavements are presented in the FHWA *Highway Subdrainage Design* manual (*5*). One approach recommended by Cedegren suggests calculating the infiltration by multiplying the 1 hr/1 year frequency precipitation rate by a standard coefficient based on pavement type. Throughout the United States, the 1 hr/1 year frequency precipitation rate varies from less than 0.5 cm/hr (0.2 in./hr) up to approximately 6.1 cm/hr (2.4 in./hr), which results in calculated infiltration rates approaching 0.5 cubic meters per day per square meter of pavement (m^3d/m^2) using this approach (0.5 m^3d/m^2 = 1.6 ft^3d/ft^2).

The second approach recommended in the FHWA manual (*5*) calculates the potential surface infiltration rate on the basis of the total length of cracks/joints per unit area of pavement and the infiltration capacity of the joints/cracks. For "normal" conditions, it is assumed that (a) the pavement surface layer is impermeable in uncracked locations, (b) continuous longitudinal joints separate at least two individual driving lanes and separate outer driving lanes and shoulders, and (c) transverse joints or cracks are regularly spaced. On the basis of those conditions, potential surface infiltration rates may be calculated using an equation of the form

$$q_i = I_c\left(\frac{N + 1}{W} + \frac{W_c}{W\,C_s}\right) \quad (1)$$

where

q_i = surface infiltration rate (m^3d/m^2),
I_c = crack infiltration rate (m^3d/m),
N = number of traffic lanes,
W_c = average length of transverse cracks and/or joints,
W = width of the OGPM layer, and
C_s = spacing of transverse cracks or joints.

Equation 1 may be rewritten in a more generic form as

$$q_i = I_c\left(\frac{Y}{W}\right) \quad (2)$$

where Y is the average length of cracks/joints per meter of pavement, which is numerically equal to $(N + 1) + (W_c/C_s)$.

A value of I_c = 0.223 m^3d/m (2.4 ft^3d/ft) is suggested for computations based on studies of saturated joints/cracks conducted by Ridgeway (*4*). It is important to note that this suggested value approximates the average infiltration rate measured through cracks in bituminous concrete pavements underlain by open-graded materials. Data presented by Ridgeway indicate wide variations in measured infiltration rates for these pavements with values ranging from 0.005 to 1.521 m^3d/m (0.05 to 16.37 ft^3d/ft). In addition, for tests conucted over saturated, unsealed joints and cracks in PCC pavements (PCC pavements were constructed over dense-graded base materials) measured infiltration rates varied from 0 to 0.181 m^3d/m (0 to 1.95 ft^3d/ft), with an average of 0.07 m^3d/m (0.74 ft^3d/ft). Also for one PCC test site with sealed joints, an infiltration rate of 0.116 m^3d/m (1.24 ft^3d/ft) was measured (*4*).

From evaluation of the Ridgeway data, it is observed that no one value of I_c can serve to quantify the spectrum of field conditions that may exist and that appropriate selection of I_c values should include an awareness of component pavement layers. Although further research is indicated, it may be generally concluded from collected data that (a) for PCC pavements the condition of crack/joint sealants does not play a significant role in altering surface infiltration rates over dense-graded materials and (b) the suggested value of I_c= 0.223 m^3d/m (2.4 ft^3d/ft) represents a reasonably conservative value for most cases where OGPM are to be considered.

When using Equation 1, it is important to recognize the relative sensitivity and interdependence of individual terms. For any given crack infiltration rate the total surface infiltration will increase as the number or length, or both, of included joints and cracks increase. Thus, as additional lanes are to be drained, the total infiltration will increase. However, when this total infiltration is averaged over the total width of the pavement to be drained, the net result is a reduction in the average infiltration rate, expressed in units of m^3d/m^2 (ft^3d/ft^2). This is because for one lane drainage two longitudinal joints are typically included, and each additional lane to be drained includes only one additional longitudinal joint. This reduced average infiltration rate, upon which required permeability will ultimately be based, does not result in a lower required permeability because there is a concurrent net increase in the length of the drainage path.

It must be recognized that the amount of water that passes through the OGPM base layer under each lane is not a constant value, as would be assumed during the averaging procedure detailed. The outside section of the OGPM base, which is below the lane closest to the longitudinal drain, must carry all of the infiltrated water from this lane in addition to water that infiltrates adjacent lanes that are drained toward this section. Therefore, the design infiltration rate for this outside OGPM base section should increase as the number of lanes to be drained increases to account for both infiltration and accumulated flow from the other lanes. In addition, the flow path length within this outside OGPM base section should remain constant, as determined from the pavements geometrics.

Flow Hydraulics

As water infiltrates the pavement surface it will flow both vertically and horizontally within the sublayers by following

the path of least resistance. The geometry of constructed pavement sublayers (e.g., thin, gently sloping layers with relatively large horizontal extent) typically results in a dominant horizontal flow component. The key factors controlling the time required to adequately drain a pavement system with predominantly horizontal flow include hydraulic gradient, flow path length, and permeability. The general orientation of the controlling geometric parameters is given in Figure 1.

The flow-path gradient is an important parameter during horizontal flow analysis. This slope is a function of pavement geometry and may be obtained using the equation

$$S = \sqrt{S_c^2 + g^2} \tag{3}$$

where

S = flow-path gradient (m/m),
S_c = cross slope (m/m), and
g = longitudinal gradient (m/m).

Figure 2 shows the potential range of flow-path gradients for a variety of longitudinal gradients and cross slopes (the flow-path gradient is independent of drainage layer width).

The length of the drainage path defines the distance the water flows from the furthest point of infiltration to the point of exit. This length is a function of the cross slope, the longitudinal gradient or slope, and the width of the drainage layer. The drainage path length is calculated using the equation

$$L = W\sqrt{1 + \left(\frac{g}{S_c}\right)^2} \tag{4}$$

where L is the length of the drainage path in meters and W is the width of the drainage layer in meters. Figure 3 shows drainage path lengths for drainage layer widths varying from 3.7 to 14.6 m (12 to 48 ft), or 1 to 4 lanes, for longitudinal gradients varying from 0 m/m to 0.05 m/m (0 to 5 percent), and for cross slopes varying from 1 to 2 percent. As shown in Figures 2 and 3, increasing the pavement cross slope from 1 to 2 percent will increase flow-path gradients and significantly reduce flow lengths for any given longitudinal gradient. The end result will be a reduction in drainage times. Equations 3 and 4 may be rewritten in the form

$$\frac{S}{S_c} = \sqrt{1 + \left(\frac{g}{S_c}\right)^2} \tag{5}$$

$$\frac{L}{W} = \sqrt{1 + \left(\frac{g}{S_c}\right)^2} \tag{6}$$

By comparing Equations 5 and 6, it can be seen that for any longitudinal gradient and cross-slope combination, $L/W = S/S_c$, indicating the proportional increase in drainage path length over the baseline value W is exactly equal to the proportional increase in the slope of the flow path over the baseline cross slope of the pavement.

Permeability Requirements

The surface infiltration described represents a source of water for which drainage must always be provided. In addition,

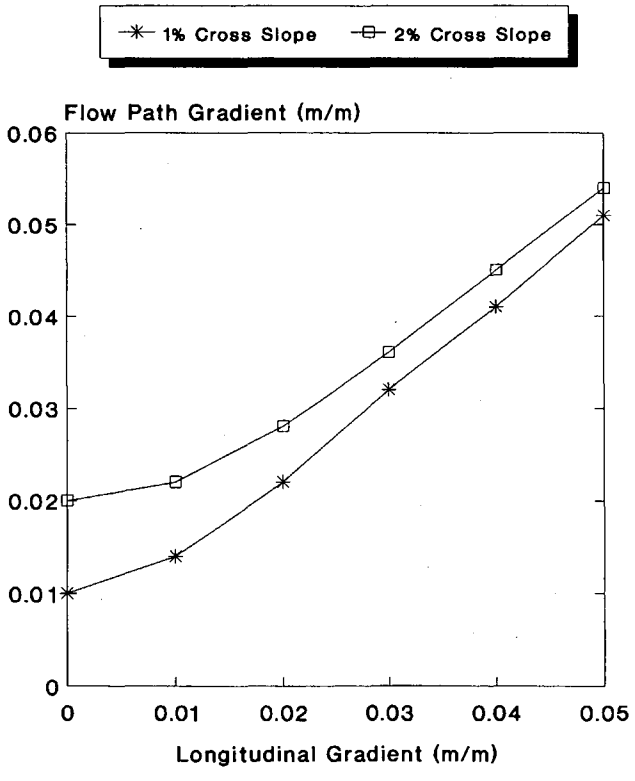

FIGURE 2 Flow path gradients.

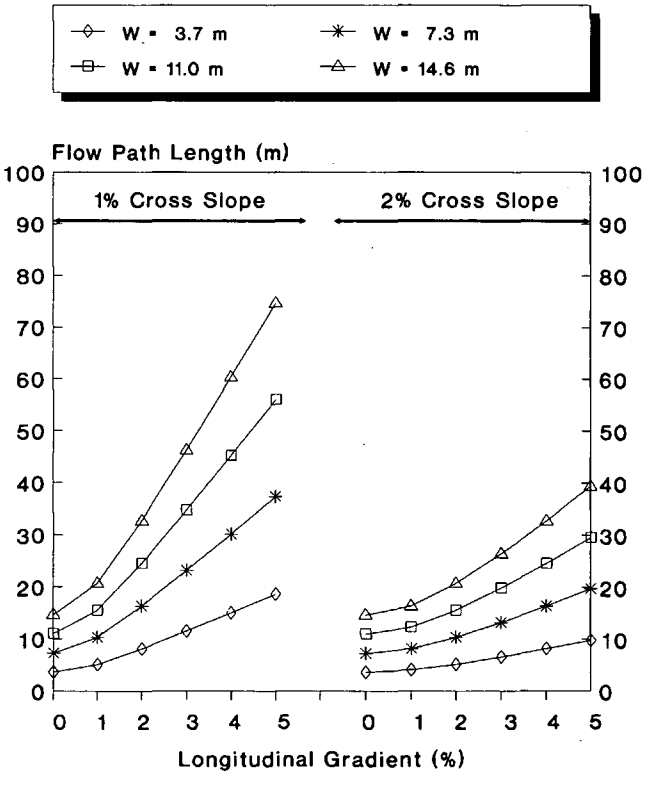

FIGURE 3 Drainage path lengths.

groundwater flow (either by gravity or artesian conditions) and meltwater (from surface ice, snow melt, ice lens development during frost action, or all) may provide significant increases to this design inflow that must pass through the drainage layer. The permeability requirements, which will be presented, account only for the surface infiltration rates caused by rainfall. In locations where other sources of water may be significant, adjustments to the permeability requirements will be warranted.

To effectively drain surface infiltration, the drainage layer must be designed with an optimal combination of thickness and horizontal permeability. The coefficient of transmissibility, defined as the product of thickness and permeability, controls the ability of the drainage layer to transmit water when flowing full or at a constant depth. It is often infeasible to design a drainage layer that will never become saturated; therefore, the design of the drainage layer is typically conducted to satisfy two conditions.

1. To provide adequate permeability to transmit all infiltrated water during rain under partially or fully saturated flow conditions and
2. To limit the time that the drainage layer is fully saturated to a relatively short duration of a few hours or less after the rain stops (*3*).

For any given design inflow, the required permeability will ultimately depend on the slope and length of the flow path. The FHWA design manual (*5*) includes a design nomograph for determining required permeability (partially saturated flow conditions) based on OGPM thickness, flow path length, flow path slope, and design rate of infiltration. By using this nomograph, required permeabilities were determined for a 10-cm (4-in.) drainage layer thicknesses with varying longitudinal gradient, cross slope, and drainage layer width combinations. Figure 4 gives the results of this analysis using a constant infiltration rate of 0.305 m^3d/m^2 (1.0 ft^3d/ft^2). The required permeabilities illustrated are directly proportional to design inflow rates and thus can be used to extrapolate any given design inflow rate. For example, the required permeability for a design inflow rate of 0.152 m^3d/m^2 (0.5 ft^3d/ft^2) would be exactly half of that required for a design inflow of 0.305 m^3d/m^2 (1.0 ft^3d/ft^2).

Figure 4 shows how the permeability requirements of the drainage layer can be significantly reduced by increasing cross slopes from 1 to 2 percent. One proposed solution for obtaining this increased cross slope within the drainage layer while still maintaining a finished pavement surface cross slope of something less than 2 percent is simply to grade the prepared subgrade layer with a 2 percent cross slope. Assuming the surface cross slope of the compacted OGPM layer will be less than 2 percent (equal to the finished pavement surface), the net result will be to provide for a variable thickness OGPM layer that becomes thicker toward the edge. This solution also provides for increased flow capacity in the critical pavement edge locations.

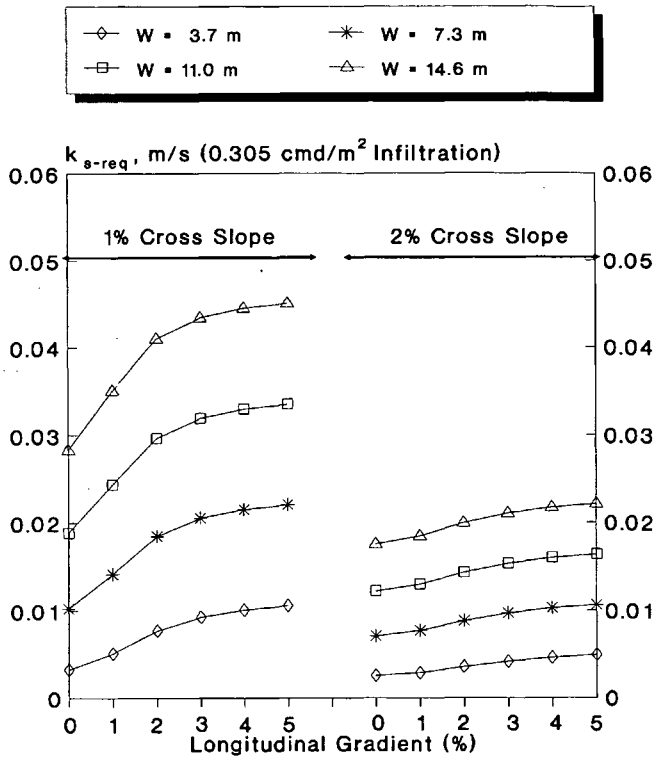

FIGURE 4 Required permeability for 10-cm OGPM.

Permeability Measurements

Throughout the years, a wide variety of theoretical and empirical equations has been presented for estimating the coefficient of permeability of porous media (*6–8*), or more correctly the saturated hydraulic conductivity, k_s. It is desirable to evaluate the hydraulic conductivity through field or laboratory testing, but it is often necessary to estimate this quantity on the basis of correlations with material properties such as grain size characteristics, dry density, and porosity or void ratio.

Permeability Estimation Based on Gradation Analysis

One simple method for obtaining estimates of the hydraulic conductivity of materials uses an analysis of the gradation band of the material. A figure developed by Cedegren (*9*) and Cedegren et al. (*10*) is provided in the FHWA manual (*5*) as an aid to estimating the hydraulic conductivity of selected materials. Another simple gradation-based analysis method, which is also included in the FHWA manual (*5*), was developed from statistical correlations between measured hydraulic conductivities and properties known to influence hydraulic conductivity (*11–15*). The most significant properties found were effective grain size, D_{10}, porosity, n, and percent passing the No. 200 Sieve, P_{200}. The percentage passing, P_{200}, accounted for over 91 percent of the variation in the hydraulic conductivities measured. A nomograph is provided that graphically solves the equation

$$k_s = \frac{6.214 \times 10^5 D_{10}^{1.478} n^{6.654}}{P_{200}^{0.597}} \quad (7)$$

The character of the fines (e.g., plastic, nonplastic), compacted density, and hydraulic gradient may significantly alter

in-place permeability. Therefore, it is suggested that the estimation methods described be used only to establish trial gradations targeted to achieve desired permeabilities rather than for final design. (Graphical procedures currently employed in the FHWA manual yield permeability estimates in units of feet per day (fpd). To convert to SI units of meters per second (m/sec), use the relation 1 fpd = 3.528 μm/sec.)

Equation 7 was used to analyze standard Illinois DOT gradation specifications suitable for use as OGPM or filter materials and for the AASHTO #57 gradation (the AASHTO #57 gradation is used for OGPM in some states). Figure 5 shows the mid-range gradation bands for these materials. The fine, mid-range, and coarse specification limits of the materials were analyzed in each case. Table 1 gives the results of this analysis and indicates how the hydraulic conductivity may vary significantly between the fine and coarse limits of most of the gradation specifications. Actual laboratory measurements of permeability for these materials are discussed later.

The FHWA *Highway Subdrainage Design by Microcomputer* manual, developed at the University of Illinois (*16*), includes a software program DAMP (Drainage Analysis & Modeling Programs). The DAMP program provides computerized solutions for the design charts and equations included in the FHWA manual. The program incorporates Barber and Casagrande's equations for calculating drainage times to various saturation levels, along with analysis methodology for determining AASHTO drainage coefficients. This program was used to determine the estimated drainage time from complete saturation to 85 percent saturation for each of the materials. These values, which are also included in Table 1, are important because many granular materials experience significant strength loss and high deformations as saturation levels exceed 85 percent (*17,18*). It should be noted that the Barber equations tend to produce slightly longer drainage times and some researchers believe these are more appropriate than the Casagrande equations when analyzing base course drainage. It should also be noted that calculated drainage times assume an initially saturated medium, which is a condition contrary to the partially saturated flow regime assumed during the determination of hydraulic requirements of existing methods (*5*).

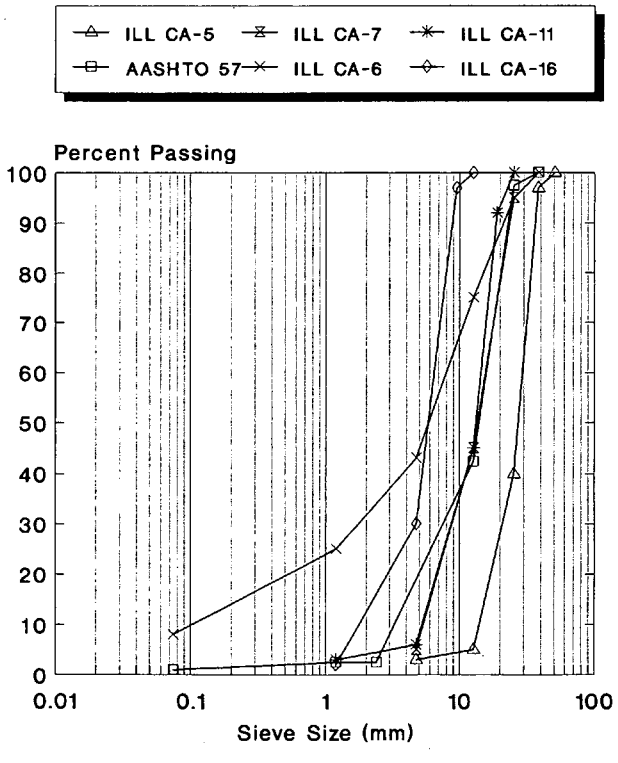

FIGURE 5 Midrange gradation bands for selected materials.

Permeability Measurement from Laboratory Testing—Constant Head

Darcy's law for saturated steady-state flow may be used to estimate the hydraulic conductivity of materials using the equation

$$Q = k_s i A \tag{8}$$

where

Q = volumetric flow rate (m^3/sec),
k_s = hydraulic conductivity (m/sec),
i = hydraulic gradient (m/m), and
A = cross-sectional area of flow (m^2).

Equation 8 can be rewritten in the form

$$k_s = \frac{Q}{i A} \tag{9}$$

and used to compute hydraulic conductivity based on flow parameters obtained during constant head permeability testing. ASTM Test Method D2434-68 Standard Test Method for Permeability of Granular Soils (Constant Head) also uses this relationship. Assuming that saturated flow, constant head conditions exist in the field, the potential exists to use Equation 9 to directly calculate required permeability of a porous medium based on design infiltration and geometric parameters previously discussed.

Research conducted as part of IHR Project 525 Pavement Subbases (*1*) indicated the usefulness of a constant head permeability device that would more closely represent field conditions by producing water flow perpendicular to the direction of compaction of a large OGPM sample. To satisfy this requirement, the flow chamber given in Figure 6 was fabricated on the basis of a previously built apparatus used for measuring in-plane flow through geocomposites and geotextiles. The flow chamber is equipped with a removable mold that allows for the placement of material samples with cross-sectional areas up to 0.09 m^2 (1 ft^2) and lengths up to 0.91 m (3.0 ft). The hydraulic gradient across the sample can be varied from 0 m/m up to 4 m/m by adjusting water flow or downstream weir heights, or both.

During testing, saturated samples were subjected to flows with hydraulic gradients ranging from near 0 to more than 1.0 m/m. The upstream head, downstream head, and flow height above the V-notch weir were measured with a Lowry point gauge capable of reading to the nearest 0.3 mm (0.001 ft). The volumetric flow rate through the sample was directly

TABLE 1 Calculated Permeabilities and Drainage Times for Selected Materials

Material Designation	D10 (mm)	P200 (%)	Saturated Permeability (m/s)	Drainage Time to 85% Saturation: Barber Equations (hrs)	Drainage Time to 85% Saturation: Casagrande Equations (hrs)
OGPM Materials					
IDOT - CA5					
Fine	12.9	6	2.68E-02	0.170	0.150
Midrange	14.1	3	4.63E-02	0.090	0.080
Coarse	20.4	0	6.00E-01	0.005	0.004
IDOT - CA7					
Fine	4.7	10	4.42E-03	1.210	1.160
Midrange	5.3	5	8.06E-03	0.630	0.590
Coarse	6.4	0	1.06E-01	0.030	0.030
IDOT - CA11					
Fine	2.8	6	2.87E-03	1.940	1.890
Midrange	5.2	3	1.07E-02	0.460	0.420
Coarse	6.5	0	1.23E-01	0.030	0.030
AASHTO #57					
Fine	2.7	2	5.08E-03	1.040	0.990
Midrange	3.2	1	1.00E-02	0.490	0.460
Coarse	4.6	0	7.06E-02	0.060	0.050
Filter Materials					
IDOT - CA6					
Fine	0.074	12	7.06E-06	788.000	950.000
Midrange	0.1	8	1.76E-05	462.000	557.000
Coarse	1.2	4	9.70E-04	6.360	6.480
IDOT - CA16					
Fine	1.45	4	1.35E-03	4.400	4.420
Midrange	1.75	2	2.69E-03	2.080	2.030
Coarse	2.91	0	3.53E-02	0.130	0.110

Saturated permeabilities calculated assuming dry density = 1.76 metric tons per cubic meter

1 m/s = 2.77 E+05 ft/day

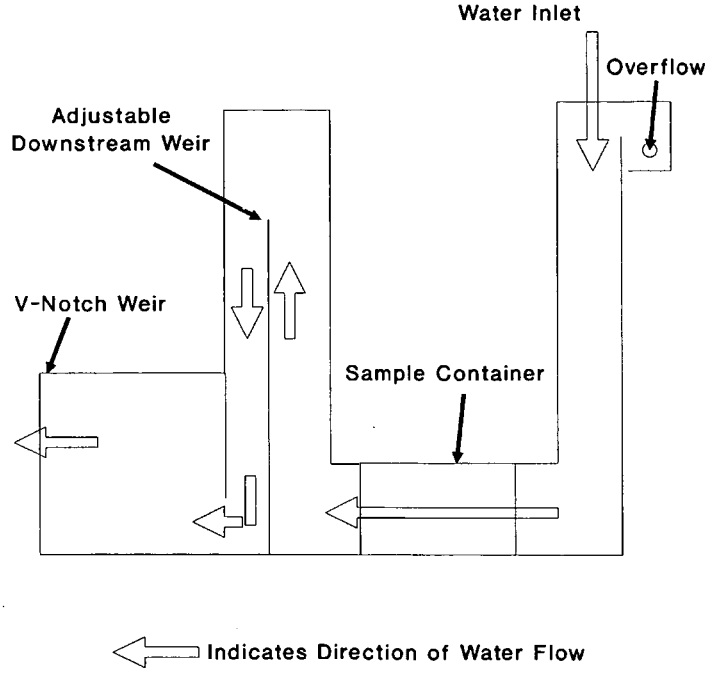

FIGURE 6 Schematic of IHR-525 flow chamber.

calculated based on V-notch weir flow heights. Hydraulic conductivities of the various materials were calculated using Equation 9. Figure 7 gives the results of tests conducted on typical Illinois DOT gradation specifications. It is interesting to note that a significant drop in hydraulic conductivity (approximately 50 percent) occurs as the hydraulic gradient is increased. This is most likely caused by turbulence within the sample, which both restricts flow volume and causes a divergence from the assumed laminar flow conditions on which Darcy's equation is based. This trend, which occurs under hydraulic gradients well in excess of typical in situ conditions, was typical for all of the materials tested.

Permeability Measurement from Laboratory Testing—Falling Head

The saturated hydraulic conductivity of a material may also be determined under falling head conditions using the equation

$$k_s = \left(\frac{a\,l}{A\,t}\right) \ln\left(\frac{h_1}{h_2}\right) \tag{10}$$

where

a = cross-sectional area of reservoir (m^2),
l = length of specimen (m),
A = cross-sectional area of specimen (m^2),
h_1 = head loss across specimen at time t_1,
h_2 = head loss across specimen at time t_2, and
t = elapsed time ($t_2 - t_1$).

Various types of falling head apparatus have been fabricated and used by states to quantify the hydraulic conductivity of aggregate samples. On the basis of the particular dimensions of the apparatus used, hydraulic conductivity is typically determined directly using the equation

$$k_s = \frac{B}{t} \tag{11}$$

where B is the permeameter constant, which is numerically equal to $(al/A)*\ln(h_1/h_2)$.

The New Jersey DOT fabricated a falling head permeameter assembly (*19*) similar to that shown in Figure 8, which reportedly was used successfully for materials having hydraulic conductivities ranging from 3.528×10^{-4} to 7.1×10^{-2} m/sec (100 to 20,000 fpd).

Longitudinal Drainage Requirements

The longitudinal drain system is typically composed of three components: a geotextile filter fabric wrapping, an aggregate trench backfill, and a perforated pipe. As a system, the fabric wrapping acts as a protection against subgrade intrusion, the aggregate trench backfill as an envelope/permeable medium, and the pipe as a drainage conduit. For this system to perform adequately, the following conditions should be met:

1. The filter fabric must satisfy filtration requirements dictated by the particle size distribution of the subgrade materials.

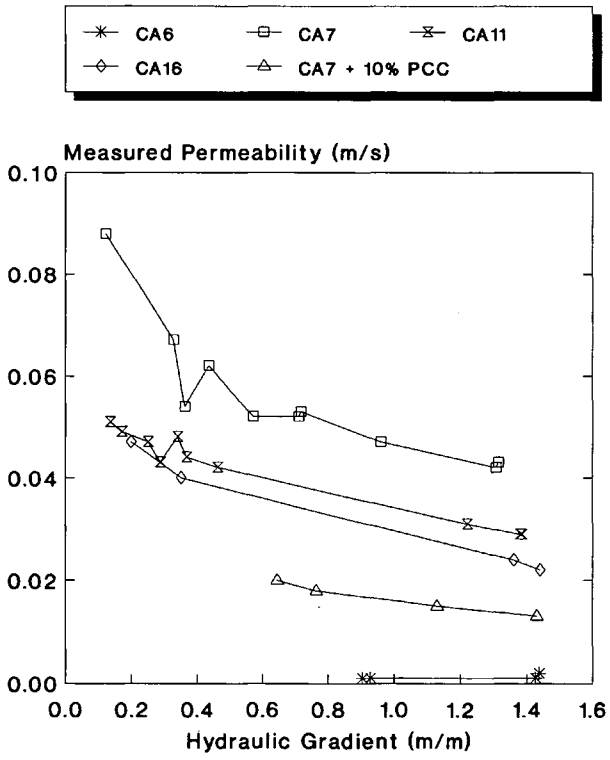

FIGURE 7 Measured permeabilities using IHR-525 flow chamber.

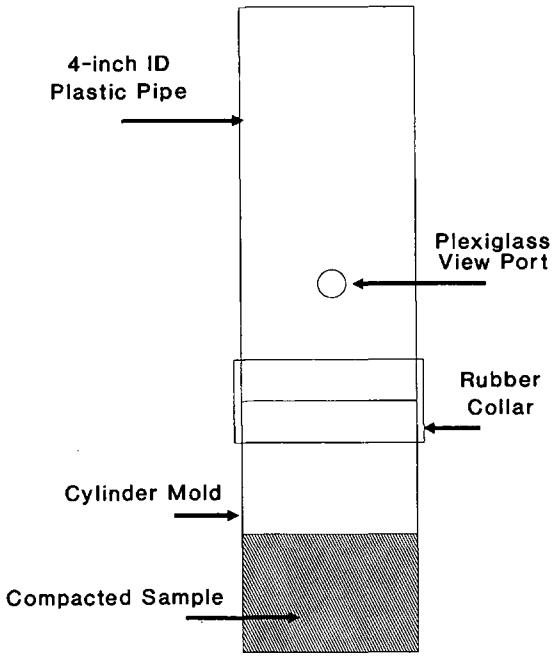

FIGURE 8 Schematic of New Jersey DOT falling head permeameter.

2. The aggregate trench backfill should have a hydraulic conductivity at least as great as the OGPM base layer.
3. The pipe must have sufficient dimensions and perforations to handle expected inflow.

Condition 1 may be satisfied using a number of design criteria (*20–22*). As an example, Carroll (*21*) suggests selecting a filter fabric with an apparent opening size (AOS), which is less than 2 or 3 times subgrade particle size for which 85 percent of the subgrade is finer (D_{85}).

Condition 2 may be satisfied by selecting aggregate backfill materials identical to those used for the OGPM base layer. Care must be exercised to ensure that the trench backfill material is composed of high permeable materials, otherwise a damming effect may result that would restrict flow within the OGPM base layer.

Condition 3 is typically satisfied using a design nomograph presented in the FWHA design manual (*5*). The use of this nomograph to determine the required pipe size uses three basic input values: the flow rate into the drain, q_d (ft^3d/ft), the distance between transverse outlets (ft), and the pipe gradient (ft/ft). The first of these inputs is calculated based on q_n, the net design inflow (ft^3d/ft^2) multiplied by L, the length of the flow path (ft), providing the proper units of ft^3d/ft of pipe. The remaining inputs are determined directly from design conditions. (English units were used to match input values used within the nomograph.)

The equation $q_d = q_n * L$ for calculation of flow rate into the drain can increase the conservative value of inflow for drainage design. As presented, the length of the flow path is used. In reality, the width of the drainage layer, W (meters or feet) should be used. The reason for this statement can be explained in two ways. First, in the initial calculations for inflow, the units of cubic meters per day per square meter (cubic feet per day per square foot) are obtained by dividing the inflow rate, with units of cubic meter per day per meter of pavement, by the width of the drainage layer, with units of meters (feet), to produce units of cubic meters per day per square meter (cubic feet per day per square foot). It would therefore be logical to multiply by the width of the drainage layer (meters or feet) to revert back to inflow rate in units of cubic meter per day per meter (cubic foot per day per foot of pavement). Second, the required pipe size is determined from the inflow quantity per unit length of pipe. The inflow quantity can be envisioned as the quantity of inflow, in units of cubic meters per day per square meter (cubic feet per day per square foot), multiplied by the surface area accepting this inflow rate, square meter per meter (square foot per foot), which results in inflow quantities with units of cubic meter per day per meter (cubic foot per day per foot). For the baseline case, where $g = 0$ m/m (0 ft/ft), the surface area accepting the inflow is a rectangle with a length equal to the width of the drainage layer, W, and a width equal to the unit pavement length (AREA = $W * 1$). If a longitudinal gradient is involved, the drainage area accepting inflow becomes a parallelogram, with an average length equal to the flow path length, L, and a width equal to W/L (AREA = $L * W/L = W$). Figure 9 shows this concept. Therefore, because the surface area accepting inflow remains constant regardless of longitudinal gradient, the design inflow rate into a unit length of pipe should also remain constant.

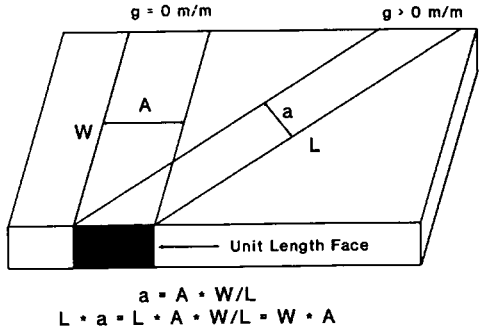

FIGURE 9 Surface infiltration areas.

The implication of the present method is that for those cases where $g > 0$ m/m, using the design nomograph with flow rate equal to $q_n * L$ will result in required pipe sizes larger than necessary. This error can be eliminated by replacing the flow path length, L, by the width of the drainage layer, W, in the equation. This will result in constant pipe inflow quantities throughout the length of any given project, regardless of longitudinal gradient, as long as the width of the drainage layer remains constant.

SUMMARY AND CONCLUSIONS

This paper focused on the permeability aspects of OGPM necessary for various surface infiltration rates. Different methodologies have been presented for the calculation of surface infiltration and for the determination of required permeabilities. It has been shown that pavement geometry, including cross slope, longitudinal gradient, and drainage layer thickness and width, play an important role in these calculations. It is apparent that there is no magic number that can be given for a required permeability that will satisfy all conditions while still maintaining a measure of economy. For conditions that prevail in Illinois, typical permeability requirements for Interstate highway design would range from approximately 3.5×10^{-3} m/sec to 10.6×10^{-3} m/sec (1,000 to 3,000 fpd) when designing a 10-cm (4-in.) base layer thickness and a drainage width of 3.6 m (12 ft). This required permeability may be drastically increased under adverse conditions of steep slopes, super elevations, or multiple lanes, or all three.

Permeability requirements of OGPM represent one important function that must be considered in design; however, the provision for permeability must be balanced by the quality of support provided by the OGPM to the surface layer. Although this topic is beyond the scope of this paper, items for further study include

1. Density requirements necessary during placement of the OGPM,
2. Construction stability of the OGPM needed to ensure proper placement of surfacing materials without loss of permeability,
3. Evaluation of the degradation of OGPM during service to determine whether support conditions deteriorate over time, and

4. Investigation of OGPM hydraulic conductivity to determine whether it changes significantly over time because of degradation, intrusion, and other factors.

ACKNOWLEDGMENTS

This paper was based in part on findings from the research study *IHR525 Pavement Subbases*, conducted at the University of Illinois at Urbana-Champaign under the sponsorship of the Illinois Department of Transportation and in cooperation with FHWA, U.S. Department of Transportation.

REFERENCES

1. Crovetti, J. A., and B. J. Dempsey. *Pavement Subbases*. Civil Engineering Studies, Transportation Engineering Series 64, Report UILU-ENG-91-2005. University of Illinois at Urbana-Champaign, May 1991.
2. Cedegren, H. R. *Seepage, Drainage and Flow Nets*. John Wiley and Sons, New York, 1968.
3. Jackson, T. J., and R. M. Ragan. Hydrology of Porous Pavement Parking Lots. *Journal of the Hydraulics Division*, ASCE, Vol. 100, No. HY12, Dec. 1974.
4. Ridgeway, H. H. Infiltration of Water Through the Pavement Surface. In *Transportation Research Record 616*, TRB, National Research Council, Washington, D.C., 1976.
5. Moulton, L. K. *Highway Subdrainage Design*. Report FHWA-TS-80-224. FHWA, U.S. Department of Transportation, 1980.
6. Lambe, T. W., and R. V. Whitman. *Soil Mechanics*. John Wiley and Sons Inc., New York, 1969.
7. Leonards, G. A. *Foundation Engineering*. McGraw-Hill Book Company, Inc., New York, 1962.
8. Loudon, A. G. The Computation of Permeability from Simple Soil Tests. *Geotechnique*, Vol. 3, 1953.
9. Cedegren, H. R. *Development of Guidelines for the Design of Pavement Subdrainage Systems, Phase I, Final Technical Report. Appendix A—Literature Review Abstracts*. March 1971.
10. Cedegren, H. R., J. A. Arman, and K. H. O'Brien. *Development of Guidelines for the Design of Subsurface Drainage Systems for Highway Pavement Structural Sections*. Final Report. FHWA, U.S. Department of Transportation, Feb. 1973.
11. Lane, K. S., and D. E. Washburn. Capillarity Tests by Capillarimeter and by Soil Filled Tubes. *HRB Proc.*, 1946.
12. Barber, E. S., and C. L. Sawey. Highway Subdrainage. *Public Roads*, Vol. 26, No. 12, Feb. 1952.
13. Yemington, E. G. A Low-Head Permeameter for Testing Granular Materials. In *ASTM Special Technical Publication 163: Permeability of Soils*, ASTM, Philadelphia, Pa., 1962.
14. Chu, T. Y., D. T. Davidson, and A. E. Wickstrom. Permeability Tests for Sands. In *ASTM Special Technical Publication 163: Permeability of Soils*, ASTM, Philadelphia, Pa., 1963.
15. Smith, T. W., H. R. Cedegren, and C. A. Reyner. Permeable Materials for Highway Drainage. In *Highway Research Record 68*, HRB, National Research Council, Washington, D.C., 1964.
16. Carpenter, S. H. *Highway Subdrainage Design by Microcomputer, DAMP Users Manual and Technical Guide*. Report FHWA-IP-90-012. FHWA, U.S. Department of Transportation, 1990.
17. Haynes, J. H., and E. J. Yoder. Effect of Repeated Loading on Gravel and Crushed Stone Base Material Used in the AASHO Road Test. In *Highway Research Record 39*, HRB, National Research Council, Washington, D.C., 1963, pp. 82–96.
18. Thompson, O. O. *Evaluation of Flexible Pavement Behavior with Emphasis on the Behavior of Granular Layers*. Ph.D. thesis. Department of Civil Engineering, University of Illinois, Urbana, 1969.
19. Kozlov, G. S. *Improved Drainage and Frost Action Criteria for New Jersey Pavement Design, Volume III, Road Surface Drainage Design, Construction and Maintenance Guide for Pavements*. Final Report. Division of Research and Demonstration, New Jersey Department of Transportation, March 1984.
20. Report of Task Force 25. Joint Committee of AASHTO-AGC-ARTBA, Dec. 2, 1983.
21. Carroll, R. G., Jr. Geotextile Filter Criteria. In *Transportation Research Record 916*, TRB, National Research Council, Washington, D.C., 1983.
22. Giroud, J. P. Filter Criteria for Geotextiles, *Proc., 2nd International Conference on Geotextiles*, Vol. 1, Las Vegas, Nev., Aug. 1982.

Publication of this paper sponsored by Committee on Subsurface Drainage.

Methodology for Inspection of Collector Systems

ZUBAIR AHMED AND THOMAS D. WHITE

Edge drains are a vital component of pavement drainage systems. In Indiana, performance problems exist with the types of drains used. A study was initiated to inspect and evaluate existing and retrofitted subdrainage collector systems through external visual inspection in combination with a probe for internal inspection. Distresses and deficiencies observed in construction are listed and have been compiled on video. A methodology for inspection is presented that can be used by highway agencies in monitoring the condition, need for maintenance, and performance of collector systems.

The concept of positive drainage for highway pavements is not new. It involves reducing the amount, duration, and extent of moisture present in a roadway base, subbase, and subgrade. In the absence of an effective subdrainage system, moisture-related damage reduces the performance of both flexible and rigid pavements.

In flexible pavements, the continued presence of moisture in conjunction with heavy vehicle loads may result in stripping of asphalt from aggregate, potholes, and alligator cracking. In concrete pavements, moisture may result in loss of support, degradation of the base material, and concrete deterioration.

If pavements are provided with a means for efficient internal drainage, water-related damage is significantly reduced. Internal drainage not only increases the life of the pavement, but also minimizes the cost of maintenance and rehabilitation.

A number of research studies have been conducted to improve the material properties associated with drainage of base and subbase layers (*1,2*). These studies have resulted in the development of permeable open-graded drainage layers having a low percentage of fines. Mathis (*3*) has compiled a list of the gradations and permeabilities of open-graded base courses used by different highway agencies.

One facet of the drainage system that has not been emphasized is the collector system, which receives water from the base or subbase layers and discharges it outside the pavement system through outlet pipes. Cedergren and O'Brien (*4*) and Moulton (*5*) have prepared guidelines and procedures for the design and construction of collector systems. But, literature on inspection procedures, cleaning, and maintenance of edge drains is limited. Dempsey et al. (*6*) have described a system for jet cleaning conventional pipe edge drains. California (*7*) has standard plans incorporated into the specifications for cleaning and inspection of edge drains.

Z. Ahmed, Civil Engineering Department, NED University of Engineering and Technology, Karachi, Pakistan. T. D. White, School of Civil Engineering, Purdue University, West Lafayette, Ind. 47907.

To maintain subdrainage effectiveness, edge drains should be inspected inside and outside. This research focuses on the inspection of existing subdrainage collector systems.

PURPOSE AND SCOPE

This portion of a larger study on subdrainage is aimed at observing and recording the distresses around and within the existing subdrainage collector systems. Results of the study will help the Indiana Department of Transportation (INDOT) better plan the construction and maintenance of edge drains.

Objectives

The objectives of the study included

1. Inspecting existing types of edge drains in Indiana in regard to performance and operation,
2. Monitoring the conditions inside edge drains by means of a video probe, and
3. Developing a methodology for inspection of edge drains.

Basis

For the study, a comprehensive field survey was initiated to locate sections with the two basic types of subdrainage collector systems used in the state. These are the perforated pipe edge drains and prefabricated edge drains or fin drains. To achieve a comparative evaluation of the performance of the drains, drains 10 years and older and those placed for newly built road sections less than 4 years old were incorporated into the study.

A total of 70 pipe and fin drains were inspected through the outlet pipes, and visual and camera observations were recorded. This paper summarizes the findings of the inspections and gives a detailed step-by-step procedure used for this purpose. An edited video of significant observations made during the inspection was prepared as part of the study.

INSPECTION OF EXISTING SUBDRAINAGE SYSTEMS

Site Information

Before inspection of the edge drains, site specific information was needed for the pavement subdrainage sites selected for

investigation. This was achieved through project log records and construction plans. The log records provided information on the highway classification, route number, county and district in which the section was located, project and contract numbers, and project location.

The construction plans helped determine the location of the edge drain in the pavement section and type and size of edge drain used. Edge drain design, placement, and construction practice vary. A typical pipe edge drain design used in Indiana for both old and new construction projects is shown in Figure 1. This consists of a trench 350 mm wide × 600 mm deep. A perforated edge drain pipe is placed at the bottom of the trench to a required depth and the trench backfilled with open-graded aggregate. Lining the trench or wrapping the pipe with geotextile is not practiced. For retrofit and overlay projects, a geocomposite fin drain is used and connected to the outside by a 100-mm diameter plastic outlet pipe (Figure 2). The pipe edge drains are located either at the edge of the pavement under the shoulder or at any intermediate point under the shoulder, whereas fin drains are next to the pavement at the pavement-shoulder joint. Location of the drain helps determine in advance the length of the outlet pipe that the inspection probe has to traverse before making a bend into the collector pipe.

Condition Evaluation

Inspection of edge drains was preceded by an evaluation of pavement conditions of surveyed sites. The objective was to quantify the extent of deficiencies affected by the presence of moisture and imperfect functioning of existing drainage facilities. Evidence of distresses, such as pumping, alligator cracking, and joint cracking, could be related to drainage.

Pavement condition surveys were performed using the distress identification procedure developed by Shahin and Kohn (*8*). Generally, condition surveys were not conducted on newly constructed or overlaid sections. However, water stains from pumping and bleeding of water from overlaid concrete pavement sections were noted at sites where edge drain outlets were buried or clogged.

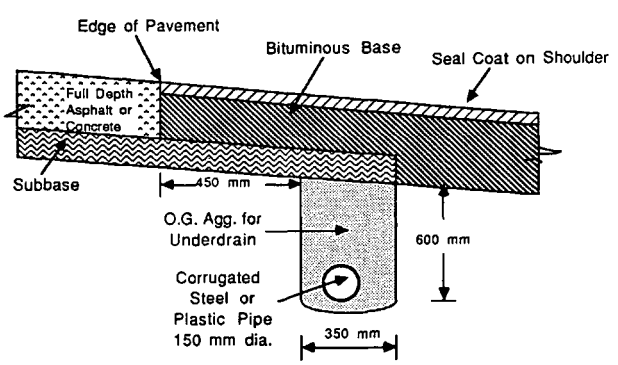

FIGURE 1 Cross section of pipe edge drain used in Indiana.

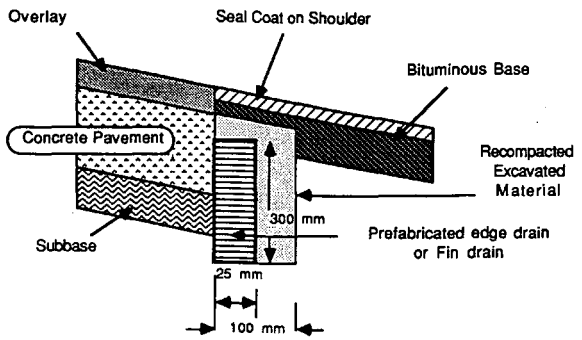

FIGURE 2 Cross section of fin drain used in Indiana.

Equipment for Inspection

Borehole Camera System

Internal inspection of collector systems is conducted with a videoimagescope or borehole camera. For this project, a market survey was made to find a camera system that would allow effective inspection of either 100- or 150-mm diameter edge drains or outlet pipes, or both. Four systems were considered.

Two Olympus camera systems were evaluated. The first system consists of a 20-mm diameter videoimagescope pushed inside a pipe edge drain through the outlet pipe to a working length of 22 m. It has an interior 100 degree field of view that can be recorded on video.

The second Olympus system allows a single-lens reflex camera to be attached to a rigid borescope. This system can be used to pierce the fabric of the prefabricated edge drain and record an interior view of the drain.

The PLS system uses a compact television probe 76 mm long with an outside diameter of 40 mm. It comes with 46 m of camera cable, camera guide skids, push rod and reel, and a control unit that includes a 230-mm color television monitor/recorder. The system comes with two light heads, which are interchangeable. A view of the system is shown in Figure 3.

The final system considered (Cues) has a black-and-white camera system with a built-in, field replaceable lighting system. The camera is 70 mm in diameter tapering to 21 mm at the ends and is mounted on a skid assembly. This system also comes with 46 m of push cable mounted on a rotating drum and has to be connected to an external video recorder to record the image seen from the television housed in the control unit.

A decision to purchase the PLS system was based on the length of the cable available, the color image capability, and the provision of the push rod and reel, which would help the probe manually through the pipe in the absence of a motorized unit. For inspection of fin drains, an Olympus borescope by Monsanto (Figure 4) was used for inspection of fin drains. Monsanto participated in the inspection of its fin drain product.

A trial run was made in the laboratory with a T-type pipe joint before field application. This step was taken to develop techniques for camera operation, insertion, and extraction. Two problems were encountered. One problem was that the guide attached to the camera head could not be easily ma-

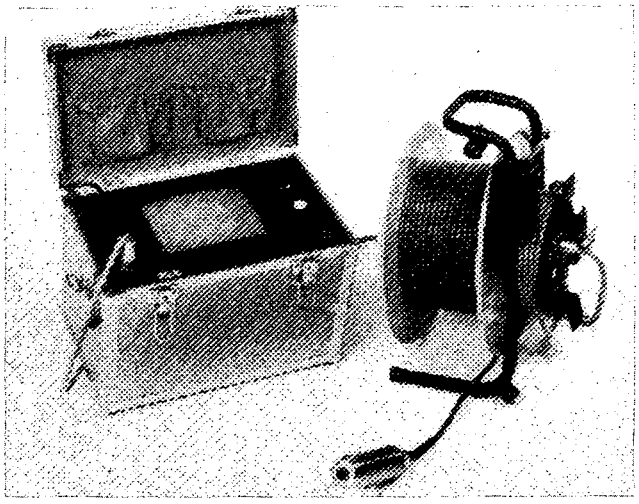

FIGURE 3 Inspection system for pipe edge drains (PLS Corporation).

neuvered through the 90 degree bend. The guide with attached camera was forced through the bend, but could not be extracted. The second problem was that the guide, because of its smaller diameter, "walked" up the sides of the pipe wall while being pushed. Another problem was that, for corrugated pipes, the probe would not ride smoothly over the corrugations, which resulted in a distorted image. Modifications were subsequently made to the guides that are shown in Figure 5.

Auxiliary Equipment

Equipment used for field inspection, in addition to the camera system, was a generator, weed eater, metal detector, and miscellaneous tools and equipments (shovels, crow bars, tapes, etc.). To operate the camera with both types of light heads, a portable generator with a minimum 750 W rating is required. For this study, a Honda generator with a maximum 1000 W output was used. The unit is compact, quiet, and easy to transport.

A weed eater can be effective in clearing the area around the outlet pipe. For most of the drains inspected, tall grass

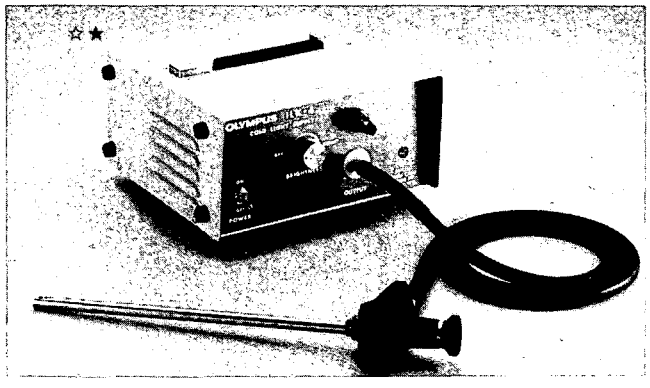

FIGURE 4 Inspection system for fin drains (Olympus Corporation).

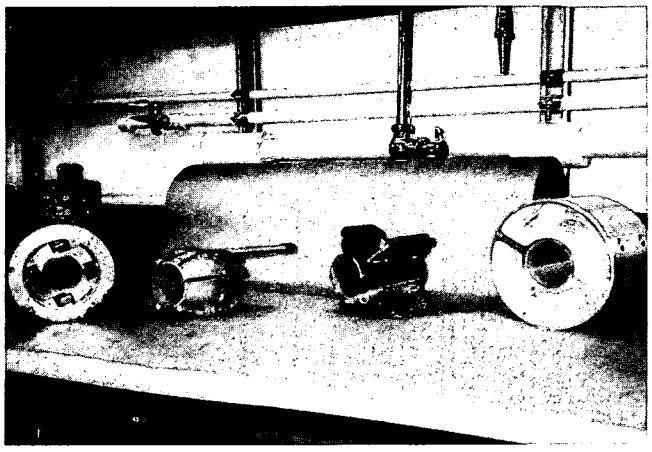

FIGURE 5 Types of guide sleeves used.

and vegetation were encountered, which not only obstructed the flow of water but also made it difficult to inspect the outlet.

During the initial survey to locate edge drain outlets, considerable difficulty was encountered on highway sections in service for more than 10 years. In some cases, outlets were not marked and were not found at the stations listed on the construction plans. Outlets were found buried by landscaping of adjacent areas. To offset this problem, a metal detector was used successfully.

Visual Observations

Drain inspection was carried out through visual and camera observations. A visual observation of the condition of the outlet pipe opening and the surrounding area was made. A number of problems were encountered and are discussed.

Outlet Pipe Slope

A general check of outlet pipe slope was made by measuring the vertical depth of the outlet pipe from the pavement surface and checking this measurement with construction plans. In the case of flat terrain or longitudinal grades of less than 1 percent, the outlets were found to have a negative or reverse slope. For this condition, ponded water was observed through camera inspections.

Outlet Condition

A frequent condition found was that the pipes were exposed for some length (Figure 6) or the outlet was crushed (Figure 7). Crushed outlet pipes become clogged over time, rendering the drainage system ineffective. Crushing is associated with erosion of soil on flat slopes from around the outlet and subsequent operation of mowing equipment on the embankments.

Markers and Rodent Screens

In most cases, outlet markers were not present or were bent or lying beside the outlet pipes. Rodent screens on outlet

FIGURE 6 View of exposed and damaged outlet pipe.

pipes were present in most of the inspected highway sections. Three outlet screen designs were found. The most common was a mesh-type screen, followed by spiral and spear types. The spear-type screen (Figure 8) did not cover the outlet and could be easily lifted, allowing rodents and small animals access to the pipe.

Vegetation

A main difficulty in edge drain inspection is the growth of vegetation around the outlet pipe. Moisture is retained around the pipe, rendering placement of equipment for inspection difficult. The standing grass around the outlet creates a barrier for flow from the outlet pipe. Accumulation of sedimentation and vegetation growth progressively blocked the pipe from outside. When vegetation was removed, any water standing in the outlet pipe started flowing.

Headwall and Erosion Control Apron

The presence of a headwall and erosion control apron or riprap protection around outlet pipes was observed to have a positive effect on the water outflow. In the absence of this

FIGURE 7 View of crushed outlet pipe.

FIGURE 8 Spear-type rodent screen.

protection, the soil around the outlet pipe erodes (Figure 9), exposing the pipe. The connection between the outlet pipe and the headwall may also be broken. A headwall or lined ditch at the outlet was found to be effective in restricting vegetation growth.

Camera Observations

The second stage in the inspection process involved the use of the camera systems for internal observations of pipe edge drains and geocomposite fin drains and the corresponding outlet pipes. Pipe edge drains were inspected by means of the PLS camera system. The same system was used to inspect outlet pipes for fin drains. Different-colored plastic tape was tied to the camera cable and push rod at 3-m intervals to determine the length of probe travel. This helped ascertain the distance to distresses described later and to points at which resistance was met.

Prefabricated edge drains were inspected with the equipment and personnel provided by INDOT and Monsanto Company staff. First a section of shoulder about 380 mm^2 was excavated next to pavement-shoulder joint. The excavation was made to a depth just above the top of the drain, and manual excavation was then used to expose the top of the fin

FIGURE 9 Erosion around newly constructed outlet pipe.

drain. The shaft of the Olympus borescope was inserted through the fabric into the core. Visual inspection was first made of the conditions inside the core, and a photographic record subsequently made with a reflex camera fitted to the borescope with an adapter. The condition and distresses observed for both types of drainage systems are described.

Joint Connections

Inspection of pipe interiors revealed the joint connections to be the most distressed part of the system. Specifications require the coupling to be flush with the pipe, but in some cases inspections revealed the absence of couplings and connections made by bending the pipe ends and forcing the bent end into the adjacent section. Plant roots were often observed penetrating such connections into the pipe.

Flow of Water

In newer sections (those built within the last 2 or 3 years), water was found to be flowing freely inside both the edge drain and the outlet pipes. In older sections, standing water with fine particles in suspension was observed where there was a sag in the pipe along its length or negative slopes for some outlet pipes. This could be attributed to either improper care during construction, as a result of settlement, or loads from vehicles or mowing equipment. Inspections made immediately after a rain showed water flowing with high velocity in sections having a positive slope for outlet pipes or at sag points along the highway. This helped flush out fine particles entering the drain through slots and openings.

Pipe Corrosion

Most of the corrugated steel pipe edge drains viewed through the camera showed significant corrosion. This can be attributed to dissolved salts or other chemicals. This type of distress becomes more severe when there is standing water inside the pipe, because it allows time for the chemicals in water to react with the pipe metal. In some of the inspected pipes, the severity of the corrosion resulted in development of cavities and openings in the pipes. These openings allowed material to enter the pipe and, without flow for a period of time, the pipe system becomes plugged. In one of the inspected drains, gravel used in the embankment was being transported out of the pipe (Figure 10). Plastic pipes inspected were free from this form of distress.

Sedimentation in Fin Drains

Some of the fin drains inspected through the camera showed sedimentation at the bottom of the fabric. Typically the fin drains are 300 mm high. However in several cases the shaft of the borescope could not be pushed beyond a depth of 250 mm. This was because of sedimentation. A section of the fin drain was removed from along Interstate 65. The cut section of the drain, which had been in place for 4 years, showed

FIGURE 10 Gravel from punctured outlet pipe.

sedimentation deposits to a depth of 75 mm (Figure 11). This section of I-65 has a dense-graded aggregate base. Fin drains installed along I-65, having bituminous stabilized subbases, showed less of this problem and water flowed freely immediately after rainfall events.

Fin Drain Buckling

Fin drain buckling was observed at most inspection sites. The cuspations of the drain core would appear to arch along the horizontal plane. This was more pronounced at transverse joints along concrete pavements. Sections exposed at the joint showed the width of the adjacent concrete slabs varying by 25 to 50 mm. Because the drain is placed immediately adjacent to the pavement-shoulder joint, projection of adjacent slabs causes the drain to bend in a horizontal plane (Figure 12). This in turn reduces the core flow capability of the drain.

A form of fin drain distress observed in the vertical plane is termed J-buckling (Figure 13). This is attributed to the design of the Monsanto fin drain. The drain core has a perforated base on one side with cuspations projecting from the base. The fabric is wrapped around the core. The cuspated side of the core is susceptible to buckling when loaded vertically. Such a vertical load is applied during trench backfilling

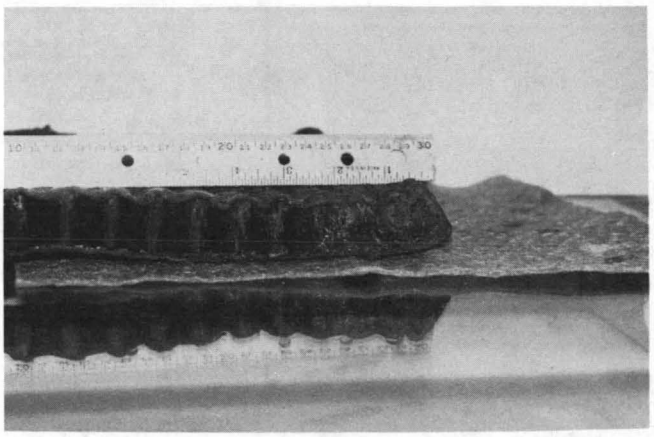

FIGURE 11 Sedimentation deposits in exposed fin drain.

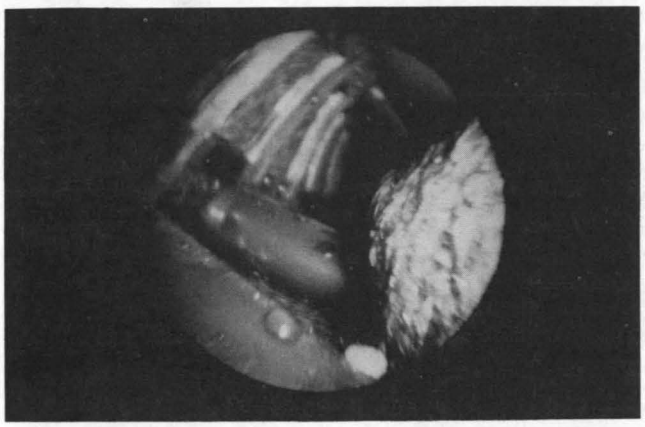

FIGURE 12 Fabric intrusion and roll over of fin drain.

and compacting. Also, outlet pipe connections are not made at the same time the drain is installed. Thus the trench has to be reexcavated at the point of joint connections to connect the outlet pipes. Backfilling and compaction result in the drain buckling along its bottom edge, especially at the joints. This was seen with the PLS camera system while checking the fin drain outlet pipes.

Connector Angle

The type of edge drain to outlet pipe connector will have a significant impact if future inspection, maintenance, and cleaning of the pipes are to be attempted. The connector angle has to be large enough not to restrict movement of the inspection camera probe. This is true as well for injection cleaning equipment, which may be used to clean the interior of the pipe through outlet pipes or clean-out ports. Evaluation of the existing drain connectors through the camera system has shown that the probe could be easily moved into a pipe edge drain through the outlet connector if a Y-connector is used instead of a T-connector. For new edge drains inspected, it was observed that connectors sweeping a 60 degree angle on a horizontal plane proved to be the most efficient for movement of the camera through the joint.

FIGURE 13 View of J-buckling in exposed fin drain.

EDGE DRAIN INSPECTION PROCESS

A detailed account of equipment and processes used to inspect pavement subdrain collector systems has been given. Various types of distresses and deficiencies in construction observed both visually and with the camera system have been described. A summary of the proposed inspection process will include

- Site information (inventory and as-built records),
- Condition evaluation of roadway,
- Visual and camera observations, and
- Information logging.

Site Information

Accurate site information is vital to the inspection procedure. Information on the route, location, direction, project and contract numbers, and year of construction can be obtained through inventory numbers, and year of construction can be obtained through inventory data maintained by the state highway agency. Construction plans help determine the exact locations of the outlets. This information is useful for periodic inspections of the same section.

Condition Evaluation

A general observation of the pavement condition before drainage inspection will give an indication of problems associated with trapped moisture. The observations will supplement those made by visual and camera observations.

Visual and Camera Observations

The features and geometrics of the outlet pipes are observed visually and noted, as well as any unusual feature that would help assess the effectiveness or problem areas associated with a collector system. Internal observations of the drains are made using an appropriate camera system.

Information Logging

For ease and convenience of recording information, a standard inspection report form has been developed. A completed sample form is shown in Figure 14. This form helps organize data. Supplemental information in the form of photographs also helps document deficiencies not listed or recorded. A final report should include the inspection report form, photographs, narrative descriptions, and other relevant information. This will provide a permanent record to be used for reference in periodic inspections of both existing and retrofitted drains.

CONCLUSIONS

A procedure for inspecting subdrainage collector systems has been described. Performance of existing and retrofitted subdrainage systems can be monitored effectively with a camera

COLLECTOR SYSTEM INSPECTION FORM

SITE INFORMATION

DISTRICT VINCENNES COUNTY CRAWFORD HWY No. I-64 DIRECTION EB

PROJECT No. I-64-2(38) CONTRACT No. R-10230 CONTRACT LENGTH 4.6 (MILES)

PROJECT LOCATION FROM PERRY-CRAWFORD CO. LINE TO 1.5 MILES WEST OF SR-37

DATE OF INSPECTION 9/9/90 INSPECTED BY Z. AHMED & N. KHAN

DRAIN No. 2 DRAIN LOCATION 2ND DRAIN FROM PERRY CO LINE SIGN

DISTANCE FROM PREVIOUS DRAIN _____ (IN FEET) 0.2 (IN MILES)

OBSERVATIONAL INFORMATION

LOCATION OF COLLECTOR: (1) END OF PAVEMENT 2. END OF SHOULDER 3. INTERMEDIATE POINT

TYPE OF COLLECTOR SYSTEM: [✓] UNDERDRAIN OR K-PIPE [ ] FIN OR X-DRAIN

TYPE OF UNDERDRAIN PIPE: (CIRCLE ONE) (1) CORRUGATED STEEL 2. BITUMINOUS COATED CORRUGATED STEEL 3. PLASTIC CORRUGATED 4. CLAY 5. OTHER _____

TYPE OF OUTLET PIPE: (CIRCLE ONE) 1. CORRUGATED STEEL (2) BITUMINOUS COATED CORRUGATED STEEL 3. PLASTIC PLAIN 4. PVC CORRUGATED PLASTIC 5. OTHER _____

VERTICAL DEPTH OF OUTLET PIPE FROM PAVEMENT SURFACE 2.5 (FEET)

SIZE OF OUTLET PIPE:	(6" DIA.)	4" DIA.	OTHER _____
SLOPE OF OUTLET PIPE:	FORWARD	REVERSE	(FLAT)
CONDITION OF OUTLET OPENING:	(FULL SIZE)	PARTIAL	DAMAGED
SCREEN PRESENT:	(YES)	NO	TYPE MESH
OUTLET MARKER PRESENT:	(YES)	NO	CONDITION BENT
HEAD WALL PRESENT:	YES	(NO)	CONDITION _____
EROSION CONTROL APRON PRESENT:	(YES)	NO	TYPE LINED DITCH
CONDITION OF VEGETATION ON EMBANKMENT:	(MOWED)	NOT MOWED	
MOVEMENT OF PROBE:	FREE	(PARTIAL)	BLOCKED
WATER PRESENT INSIDE DRAIN:	(YES)	NO	
IF YES:	FREE FLOWING	(STANDING)	

DISTANCE TRAVERSED BY PROBE 54 (FEET)

CAMERA OBSERVATIONS: CORROSION OBSERVED ON SIDE WALLS; STANDING WATER AT SAG OF PIPE FROM 50 FT. ONWARDS. NO BLOCKAGE OBSERVED

ADDITIONAL OBSERVATIONS: SECTION AT START OF DOWNHILL SLOPE

FIGURE 14 Sample of completed inspection report form.

system. The information will lead to improved pavement maintenance, design, material specifications, construction specifications, and performance of subdrainage systems.

The camera system can serve as a valuable tool for inspection of newly built drains before the project is handed over by the contractor to the state agency. Damage or distress due to construction practices can be located. Modifications of the original camera equipment will result in a more efficient and trouble free operation.

Inspection of both old and new edge drain installations resulted in the following conclusions:

1. Edge drains are effective in removing infiltrated water if care is taken during construction regarding slope, backfill compaction, and outlet treatment.

2. Mesh-type screens are more effective than other designs in preventing rodents and small animals from getting into the outlet pipes and edge drains.

3. Treatment of the area around the outlet pipe contributes significantly to proper functioning of the collector system. Vegetation growth, sedimentation, and erosion around outlet openings are impediments to effectiveness of the system. Riprap protection or concrete pads around the outlet area will minimize this effect and protect the outlet pipe from damage caused by mowing equipment.

4. Edge drains on flat grades or at minimum slopes were observed to have the most problem with clogging. This can be remedied through the use of a clean-out assembly using high water pressure. For pipe edge drains, inspection and jet cleaning can be done through outlet pipes. For fin drains, a

vertical plastic or steel port placed halfway between outlets can be used to clean the drain core.

5. Smooth-walled plastic outlet pipes perform better than corrugated steel pipes because corrosion and sedimentation are more pronounced in the latter.

6. Care is required in backfilling and compacting trenches to avoid sags and collapse of pipe and fin drains.

7. The type of fin drain inspected in this study has a tendency to buckle, and the use of an improved product is recommended.

8. To facilitate inspection and cleaning of edge drains it is recommended that outlet pipes be connected with a 60 degree minimum angle for Y- or L-connections, and no T-connections should be allowed.

REFERENCES

1. Strohm, W. E., E. H. Nettles, and C. C. Calhoun, Jr. Study of Drainage Characteristics of Base Course Materials. In *Highway Research Record 203*, HRB, National Research Council, Washington, D.C., 1967, pp. 8–28.
2. Moynahan, T. J., and Y. M. Sternberg. Effects on Highway Subdrainage of Gradation and Direction of Flow Within a Densely Graded Base Course Material. In *Transportation Research Record 497*, TRB, National Research Council, Washington, D.C., 1974, pp. 50–59.
3. Mathis, D. Permeable Base Design and Construction. *Proc., 4th International Conference on Concrete Pavement Design and Rehabilitation*, Purdue University, West Lafayette, Ind., 1989, pp. 663–669.
4. Cedergren, H. R., and K. O'Brien. *Development of Guidelines for the Design of Pavement Subdrainage Systems: Literature Review Abstracts*. Final Technical Report. FHWA, U.S. Department of Transportation, 1971.
5. Moulton, L. K., *Highway Subdrainage Design*. Report FHWA-TS-80-224. FHWA, U.S. Department of Transportation, 1980.
6. Dempsey, B. J., S. H. Carpenter, and M. I. Darter. *Improving Subdrainage and Shoulders of Existing Pavements*. Report FHWA-RD-81-0781. FHWA, U.S. Department of Transportation, 1982.
7. Wells, G. K., *Evaluation of Edge Drain Performance*. Office of Transportation Laboratory, California Department of Transportation, Sacramento, Nov. 1985.
8. Shahin, M. Y., and S. D. Kohn. *Pavement Maintenance Management for Roads and Parking Lots*. Technical Report M-294. U.S. Army Corps of Engineers, 1981.

Publication of this paper sponsored by Committee on Subsurface Drainage.

Drainage and Backfill Provisions for Approaches to Bridges

S. ABDOL CHINI, AMDE M. WOLDE-TINSAE, AND M. SHERIF AGGOUR

Approaches to bridges are designed to provide a smooth and safe transition from the highway pavement to the bridge deck. Generally this transition area, regardless of pavement type, has provided poor riding quality. Despite widespread occurrence of bridge approach problems, only a few research studies have been performed on the subject, most of which have been limited to problems associated with specific bridge sites. The few comprehensive studies done in this area have not suggested a design or specification to rectify the problem. A state-of-the-art and state-of-practice study that covers published and unpublished work in the United States and overseas was conducted. It included a comprehensive literature review and survey of state highway agency design and construction practices currently in use at approaches to bridges. The literature indicated that most problems occurring at bridge approaches can be associated with differential settlement between the highway pavement and bridge deck, and poor design of both bridge and pavement components. On the basis of the literature review and survey of highway agencies, critical items in design and construction of bridge approaches are summarized and recommendations on drainage systems and approaches to embankments are made. Points regarding the control of water around abutments and under approach pavement are summarized. Recommendations on materials, compaction, and construction for approach embankments are made.

Pavement irregularities adjacent to bridges are unpleasant, unsafe, destructive to vehicles, and may cause excessive impact loading on the bridge. In addition, in high traffic volume areas, these surface faults require costly maintenance that usually involves mudjacking or patching the approach pavement. Maintenance operations are costly to the traveling public in time and money. Shutting down lanes to perform repairs causes long lines of backed up vehicles, which in turn may cause costly accidents.

Parts of the roadway that may contribute to a poor-riding bridge approach are the bridge deck and abutment, roadway pavement, base, subbase, subgrade, embankment, and embankment foundation. Poor riding qualities are usually caused by differential settlement between highway pavements and the bridge deck. The biggest contributors to such differential settlements are subsidence of the original ground below the fill and settlement within the fill mass. Other factors that may contribute to a vertical change in the constructed profile are the fill height, type of abutment, age, abutment skew, settlement period, and traffic count. Abutment backfill material, drainage, and construction methods are critical items in building and maintaining good bridge approaches. Difficulty in obtaining uniform compaction of the fill, especially near the abutment area, may also cause uneven settlement.

Despite the widespread occurrence of bridge approach defects, only a few research studies have been performed on the subject. Most of these studies have been limited to problems associated with specific bridge sites (*1–6*). Because of the complexity of the problem, these types of studies have often led to conflicting observations or conclusions. A NCHRP comprehensive study conducted in 1969 summarized the existing information on the design and construction of bridge approaches and provided a better insight into the problem (*7*). The study was revised and updated in the 1990 NCHRP Synthesis 159 (*8*) to cover the new construction techniques and materials developed since the 1969 report.

A comprehensive literature review on design and construction practices currently used at approaches to different types of bridges was conducted. On the basis of findings of the literature review, a questionnaire was prepared and sent to state highway agencies and 20 countries overseas to study current design and construction practices in bridge approaches. The literature search of pertinent publications (*9–14*) indicated that the critical items in the design and construction of bridge approaches are embankment foundation, embankment and backfill materials, drainage systems, and construction methods.

This paper compiles the different problems encountered at approaches to bridges, summarizes corrective measures used or suggested, and makes recommendations on drainage systems and approach embankments.

EMBANKMENT FOUNDATION

Where compressible layers exist in the embankment foundation, proper design and construction techniques must be used to minimize postconstruction consolidation. Some of the construction measures used to stabilize foundation materials (*2,3,7,10*) are summarized in the following sections.

Use of Surcharge

Densification and preconsolidation of weak and compressible soils (saturated soft clays, compressible silts, organic clays, and peats) by preloading are the most widely used methods to reduce the magnitude of settlement after construction. The effectiveness of preloading before construction of the approach pavement depends on the time available for consolidation under the surcharge load and the actual rate of settle-

S. A. Chini, Department of Technology, University of Maryland Eastern Shore, Princess Anne, Md. 21853. A. M. Wolde-Tinsae and M. S. Aggour, Department of Civil Engineering, University of Maryland, College Park, Md. 20742.

ment. Thus, it is important to construct the embankment and surcharge as early as possible to provide enough time for consolidation before removal of the surcharge load.

The increase in stresses produced by the surcharge loading must not cause shear failure within the foundation materials. Sometimes embankment and surcharge loading may need to be placed in increments, corresponding to the strength gain, to avoid an increase in shear stress between weak foundation sublayers.

The surcharge should be compacted to the embankment standards because, as settlement occurs, the lower part of the surcharge becomes the top layer for the embankment of the grade elevation. Usually the surcharge height varies from 1 to 3 m (3 to 10 ft) depending on the soil conditions at the site.

Use of Drains

If the use of surcharge is not economical or the time required for surcharging is greater than the time available, vertical drains may be used to increase the rate of settlement. Vertical drains are effective in thick homogenous layers of clay where primary consolidation is the major part of the settlement (*5*). In peat and organic clays where settlement behavior is dominated by secondary consolidation, vertical drains are unnecessary.

Before the 1980s, sand drains—vertical columns of sand that provide a pathway for the excess water—were used successfully to accelerate the removal of water from foundation soil. In the early 1980s, prefabricated wick drains began to replace sand drains in the United States. The wick drains could be installed much more quickly and economically and provided more reliable drainage.

Prefabricated wick drains consist of a formed polymeric core surrounded by a geotextile filter fabric. They are installed vertically to depths of 45 m (150 ft) with modern wick installation rigs that use vibration and hydraulic crown to achieve high installation rates. A horizontal sand filter-blanket must be constructed beneath the embankment (above the vertical drains) to carry the excess water away. Today prefabricated drains completely replace sand drains.

Waiting Periods

If the analysis shows that excessive time is required to obtain an acceptable percentage of consolidation of the embankment foundation, additional time may be necessary for consolidation before construction of the approach pavements. The design and construction methods used in bridge approaches have a great influence on the rate of consolidation. For instance, the embankment and surcharge should be constructed before the construction of the abutment to provide more time for stabilization of the embankment foundation. However, in some cases in which embankments are on a highly compressible foundation, it is necessary to extend this period.

Removal of Unsatisfactory Material

When a soft compressible material is encountered in the embankment foundation, the rate of consolidation and the foundations ability to carry the loads may be questionable. A common practice is to remove a part or all the unsatisfactory material and replace it with rock or suitable well-compacted material. This method may not be practical or economical if the analysis shows that more than 3 or 5 m (10 or 15 ft) of the foundation depth must be removed (*10*).

Existing structures or rivers, or both, near the site may sometimes limit the dimensions of the foundation soil that can be removed. However, partial removal or stripping of the upper layers of very soft compressible soils will reduce the secondary consolidation of the soil (*7*).

Use of Lightweight Embankment Material

In cases in which the foundation's ability to carry the embankment load is limited, reduction in the approach-fill weight near the abutment may be necessary to reduce the settlement and movement of the underlying soft soils to an acceptable level. Lightweight fill, such as furnace slag, expanded shale, coal waste refuse, lightweight concrete, sawdust, bark, polystyrene foam, or other materials having small unit weights, may be used (*6*). The type of material used depends on its availability, cost, time required for construction, environmental concern, and existing conditions of the foundations. To avoid or minimize the acidity and corrosive effects, such materials should be encapsulated in geomembrane liners.

Dynamic Compaction

Dynamic compaction is another method applied in bridge approaches with loose, clean, coarse-grained deposits. In this method soil compaction is achieved by the repeated dropping of a heavy weight on the ground surface. Typically, weights ranging from 5.5 to 27.5 Mg (6 to 30 tons) are dropped from heights of 9 to 23 m (30 to 75 ft) at each point on a predetermined grid pattern (*8*).

The effective depth of dynamic compaction depends on the impact energy, soil type, and degree of saturation. Common effective depth is 12 m (40 ft), but higher effective depth can be achieved by increasing the impact load.

APPROACH EMBANKMENTS

Problems associated with embankments of bridge approaches are generally attributed to volume changes of the soil within the approach embankment. Highway designers usually permit the use of locally available soils in design of the highway embankment to reduce project costs. Substantial amounts of settlement of such materials may not affect the performance of the highway. Highway structures, on the other hand, are designed for little or no settlement to maintain specified highway clearances and ensure integrity of structural members. The approach embankment must therefore provide a smooth transition between roadway and structure and requires special materials and placement criteria to prevent internal consolidation.

Volume changes within the approach embankment may result from the rearrangement of soil particles, loss of moisture (shrinkage), increase in moisture (swelling), or ice and

frost action. Although roughness at bridge approaches is generally due to settlement of the embankment, in practice, roughness caused by swelling is also encountered. In cold climates, the uplift force could also be caused by the growth of ice lenses between the soil particles when frozen materials are incorporated in embankments.

Two parameters that affect the embankment performance are (a) suitability of various soil types as bridge approach embankment material and (b) proper compaction specification to be followed for a given soil type.

Material

Where embankments are composed in part or entirely of compressible materials, embankment settlement may contribute significantly to approach pavement settlement.

Primary consolidation of the soil involves a gradual escape of water from voids of the loaded soil. The time for settlement is controlled by the soil properties (compressibility, permeability, stress history, and void ratio) and by the geometry of the soil mass. For embankments consisting of granular soils, which have small void ratios and large permeabilities, this compression occurs rapidly within a few months and is completed before construction of approach pavement. However, where silty sand and silt exist, completion of primary compression requires 1 to 3 years. Where clay exists, several years may be required for complete consolidation. Hence, settlement of the approach pavement may be significantly affected where embankments are composed of soft clay.

Most approach embankments are constructed of materials readily available from roadway excavation or a convenient borrow site. However, there is a need to place restrictions on the type of fill material used behind bridge abutments. The survey of state highway agencies in this study (*15*) showed that at least 15 states specify select materials for bridge approach embankment. A typical suggested approach embankment cross section for a bridge on spread footing (*16*) is shown in Figure 1. FHWA (*16*) specifies select material to conform to the following requirements:

1. Gradation:

Sieve Size	*Percentage Passing by Weight*
100 mm (4 in.)	100
425 μm (No. 40)	0 to 70
75 μm (No. 200)	0 to 15

2. Soundness: the material shall be substantially free of shale or other soft, poor durability particles.

Compaction

The lack of proper compaction, due to either improper compaction specification or negligence in specification enforcement, is a major source of differential settlements within the bridge approach system. This is particularly true in confined areas near the abutment where only small compaction equipment can be used.

Studies by Road Research Laboratory (*17*) show that density of compacted soil varies for different thicknesses of lifts, and higher densities cannot be obtained throughout relatively thick lifts. As a result, the compaction specification includes both maximum lift thickness and the relative compaction of approach embankment materials. Table 1 gives lift thickness and relative compaction requirements for several agencies on

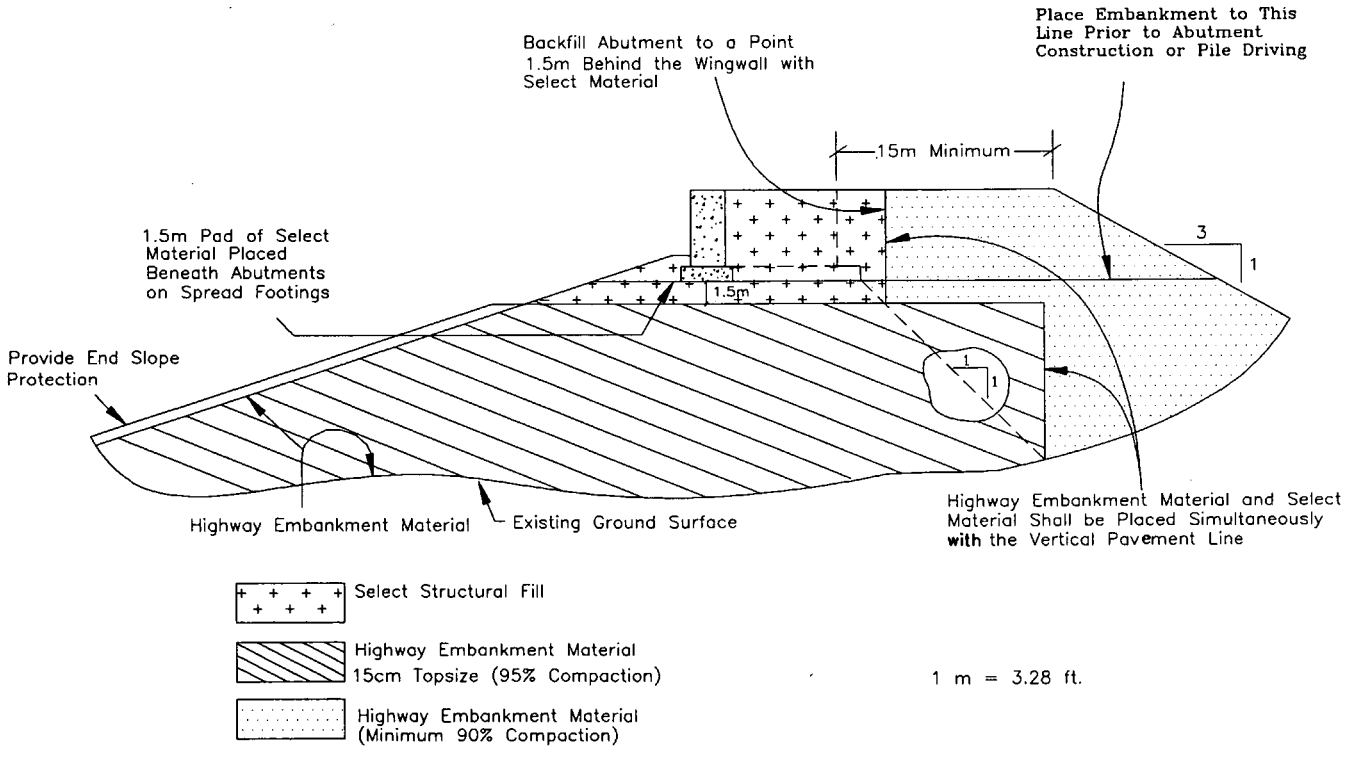

FIGURE 1 Suggested approach embankment details (*16*).

TABLE 1 Maximum Lift Thickness and Relative Compaction for Embankment Material at Abutments

State	Maximum Lift Thickness (Loose Measurements)	Relative Compaction
Arizona	20 cm	95% AASHTO T99 (Standard)
Arkansas	10 cm	95% AASHTO T99 (Standard)
California	20 cm	95%*
Colorado	15 cm	95% AASHTO T180 (modified)
Connecticut	15 cm	100% AASHTO T180 (modified) D
Delaware	20 cm	95%*
Maine	20 cm	98%*
Michigan	22 cm	95%*
Missouri	-----	95% AASHTO T99 Method C
New Hampshire	20 cm	98% AASHTO T99 Method C
Ohio	-----	98% to 102 AASHTO T99
Rhode Island	25 cm	95% AASHTO T180 Method A or D
South Carolina	15 cm	95%*

** State Test Method*

---- Not Specified

1 cm = 0.4 in.

the basis of the survey of state highway agencies conducted by Wolde-Tinsae et al. (*15*).

Most agencies recognize that compaction of the approach embankment requires special care near the structure. Even if the area is accessible, not all engineers agree to use conventional compaction equipment near the wall. In most cases, agencies require the use of small mechanical and vibration devices to perform the compaction without endangering the vertical alignment of the structure. In the case of shoulder (full-height) abutment, the usual method is to build the embankment to its final grade, construct the abutment and the first span of the bridge, and finally place and compact the backfill materials around it. This procedure tends to eliminate abutment movement during compaction of the embankments and provide enough time for the foundation to consolidate under the embankment load.

DRAINAGE SYSTEMS

The development of approach faults have often contributed to surface and subsurface erosion of the soil adjacent to the abutment and under the approach pavement. Therefore, special attention must be given to remove water from critical areas around the abutments and under the approach pavements by providing an adequate drainage system.

Surface Drainage

A good surface drainage system is important in bridge construction. The surface water should be removed quickly and completely from the bridge deck and its vicinity. Trapped or ponded water, especially in cold climates, can cause a great deal of damage to a bridge (*18*).

Deck drain is generally permitted to drain through short vertical metal pipes and spill directly into the abutment slope (Figure 2) or run down the abutment wall through joints between the bridge deck and road surface. These practices initiate erosion on the abutment slope (Figure 3) and piping from under and behind the abutment and cause cracking and settlement of the approach pavement. The removal of earth from under and behind the abutment walls by piping is a common cause of the settlement of the highway pavement.

Basic conditions essential for development of piping are (a) sufficient water to cause drainage through cracks, (b) hydraulic head sufficient to move water through a subsurface route, and (c) outlet for flow. Thus, the concentration of runoff near bridges should be prevented, and the supply of water from the overlying bridge deck and roadway pavement must be intercepted and led to a water course channel in downspout circuits.

Subsurface Drainage

The infiltrated free water must be removed from areas around the abutments and under the approach pavements by providing an adequate drainage system. Such a system includes a drainage layer behind the abutment and wingwalls that drains the free water vertically and a system of drainage pipes that carry the water to collection points outside the abutment. In

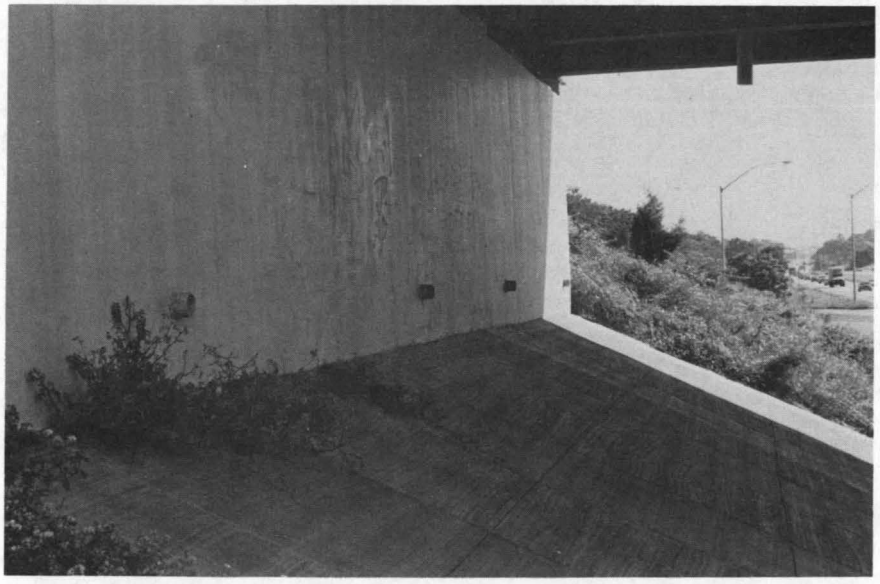

FIGURE 2 Short vertical metal pipe that spills directly onto abutment slope.

many causes the drainage system also includes a lateral drainage layer, usually but not necessarily the base that carries the infiltrated water to transverse collector drains installed at critical sections.

Drainage Layer

To remove free water from the pavement structure either vertically or laterally to the system of drainage pipes, a high-permeable drainage layer is required. Such required permeabilities can be supplied by using coarse materials surrounded by filters. Some states use asphalt-treated permeable material or cement-treated permeable material as drainage layer. California uses asphalt-treated and cement-treated permeable materials with the gradings presented in Table 2 (*19*).

Geocomposite Drainage System

New prefabricated drainage systems, called geocomposite drains, have been developed for drainage behind the abutment. The geocomposite drains are made from various types and configurations of polymeric drainage cores covered by geotextile filters that are bonded directly into the cores. The drainage system completely covers the backfilled side of the abutment with the geotextile filter attached to the side of the core facing the backfilled soil. The solid portion of the drain-

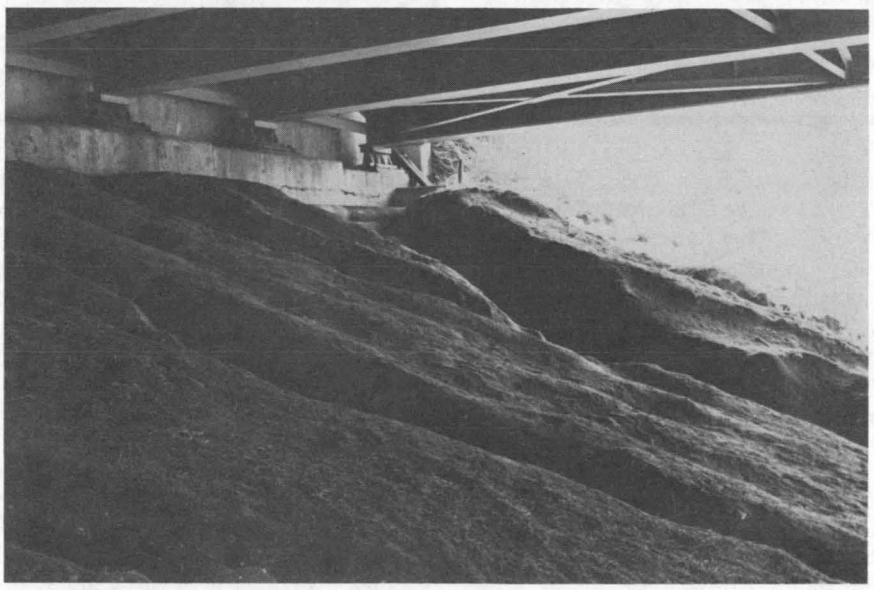

FIGURE 3 Soil erosion on abutment slope due to deck drainage.

TABLE 2 Grading of Asphalt-Treated and Cement-Treated Permeable Base (California)

ASPHALT-TREATED		CEMENT-TREATED	
Sieve Sizes	Percentage Passing	Sieve Sizes	Percentage Passing
25 mm (1)"	100	7.5 mm (1-1/2")	100
19 mm (3/4")	90-100	25 mm (1")	88-100
12.5 mm (1/2")	35-65	19 mm (3/4")	X-15
9.5 mm (3/8")	20-45	9.5 mm (3/8"	X-15
4.75 mm (No.4)	0-10	4.75 mm (No.4)	0-16
2.36 mm (No.8)	0-5	2.36 mm (No.8)	0-6
75 um (No.200)	0-2		

X = The gradation which contractor propose to furnish for the specific sieve size (for 19 mm, X=52 to 85; and for 9.5 mm, X=15 to 38)

age core supports the geotextile and maintains an open volume for free movement of water.

Subsurface Drainage Pipe

The collection system consists of a set of perforated or slotted pipes to remove water from the pavement and convey it to suitable outlets outside the roadway limits. The design of drainage pipes include (a) type of pipe used; (b) location, depth, slope, size, and outlet of pipe; and (c) provision for adequate filter protection to provide sufficient drainage capacity.

Plastic piping systems are appropriate for drainage of transportation facilities and have shown satisfactory performance (*20*). Lack of brittleness and resistance to salts and aggressive soils have made plastic piping systems more suitable than concrete and corrugated metal buried piping systems.

Filters

If the drainage layer and piping system are to remain functioning for a satisfactory period, clogging must be prevented. This can be achieved by using a filter between the drain and adjacent material.

Aggregate filters have been used for a long time and, if properly constructed, will perform well. Grain-size distribution of a graded aggregate filter creates its pore structure that, in turn, controls filtration performance. There are well-established criteria for specifying the grain size distribution of aggregate filters (*21*). These criteria based on theoretical relations among particle size, pore size, and retention ability of granular materials have proved adequate through decades of use.

The use of geotextiles in filter applications has become widespread in the past 20 years. They can be effective in protecting soil from erosion while permitting water to pass through the fabric to the drain. There are more than 600 geotextiles that consist of woven and nonwoven fabrics (*22,23*) available in the United States.

Geotextile filters have two advantages over aggregate filters: (a) they do not store a significant amount of water in the fabric layer and (b) there is more flexibility in the selection of the type and material properties desired.

The major properties of geotextile filters that should be considered in drainage application are

- Flow Rate—Permeability of the fabric filter must be greater than that of the backfill soil placed against it. This is to ensure that the fabric accept the flow coming from the backfill soil.
- Opening Size—The voids of the fabric filter must be fine enough to retain erodible soil. As the fines within backfill soil get smaller, the opening size of the fabric filter must also get smaller.
- Strength Consideration—The fabric filter must support the backfill soil without collapsing into the core thereby blocking flow. This necessitates some requirements on its mechanical properties, such as puncture strength, grab strength, and tear strength. Table 3 gives the mechanical properties of geotextile filters (*24*).

CONSTRUCTION METHODS

The construction methods used for approach embankments could considerably affect the performance of the bridge approaches (*25,26*). Careful consideration must be given to the construction of embankments placed over side-hill foundations. Benching of sloping ground is important to avoid lateral movement and provide horizontal foundation for the embankment. Granular material and perforated pipes should be used for drainage under an embankment on side hills, to collect and drain the wet-weather seepage and prevent the possible saturation of the embankment.

During construction it is essential to direct the surface water away from the abutments and retaining walls to avoid erosion of the adjacent soil. Embankments and backfill materials require careful control of the lift thickness, moisture content, and densification level. Compaction of the soil around abutments and walls should be done at the same time to prevent tilting of these structures. A good practice in approach em-

TABLE 3 Fabric Filter Survivability Requirements (*24*)

Degree of Survivability	Puncture Strength Newton		Grab Strength Newton	
	Woven	Nonwoven	Woven	Nonwoven
Medium	310	180	800	510
High	450	340	1200	800

1 Newton = 0.225 Pound Force

bankment construction is to remove any unsuitable foundation soil and replace it with well-compacted material.

It is difficult to control moisture and density of embankments that have frozen materials. Therefore, construction during cold weather should be prohibited whenever silts, clays, or sands are used for the abutment embankment. Stripping or reconstructing the top layer of an embankment is necessary if the construction process is stopped because of bad or freezing weather.

CURRENT PRACTICE IN CALIFORNIA

The survey of state highway agencies design and construction practices at approaches to bridges (*15*) revealed that a new approach slab concept developed in California provides a drainage system that minimizes the potential for water damage to the bridge approaches. This system is used on portland cement concrete pavements and on multilane asphalt concrete pavements in urban areas.

The old drainage system in California consisted of a vertical layer of permeable material 30 cm (1 ft) wide, drainage pipe near the bottom of the permeable material 20 cm (8 in.) in diameter, and weepholes through the abutment and wingwalls. Evaluation of this system (*13*) showed that

1. Simultaneous placement of the permeable layer and fill material is difficult and
2. Fines from the full tend to plug the permeable material and reduce its drainage efficiency.

It was also noted that the two other areas where water enters the fill and causes erosion and settlement problem (*13*) are (a) the joint between the slab and abutment and (b) the area along the junction of approach fill and abutment wingwall.

The new approach slab concept makes provisions for the drainage system to minimize the approach roughness due to water damage.

1. The old drainage system is replaced by a geocomposite drain system attached to the abutment backwall and wingwalls and a slotted plastic pipe drain encapsulated with treated permeable material (Figure 4). The pipe is placed along the base of the inside face of the abutment wall and carries the collected water where it will not cause erosion.
2. A treated permeable base 15 cm (6 in.) thick is placed under the approach slab and connected to the geocomposite drain along the abutment backwall (Figure 5).
3. In diaphragm-type abutments, the approach slab is placed in direct contact with the abutment and held firmly in place with reinforcing steel producing a water-tight joint.
4. The approach slab is extended laterally (cantilevered over the wingwalls) to coincide with the edge of the bridge deck and is separated from the wingwalls by a 10-cm (4-in.) gap to preclude unplanned vertical loading of the wingwalls when settlement occurs (Figure 6).

RECOMMENDATIONS

Embankment Foundation

Postconstruction consolidation of compressible foundation soils is the major cause of embankment settlement. It is suggested that

1. An adequate subsurface investigation be performed to provide information on the depth, thickness, and classification of all soils strata. Strength, compressibility, and permeability of critical strata must be determined.
2. The rate of primary consolidation and final settlement of the foundation soil be computed to estimate the amount of compression that will occur during the construction period

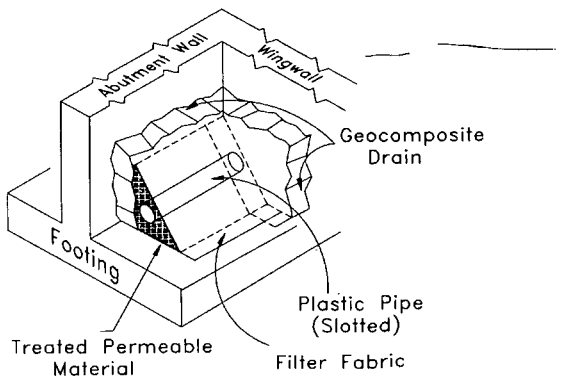

FIGURE 4 Abutment drainage details (California).

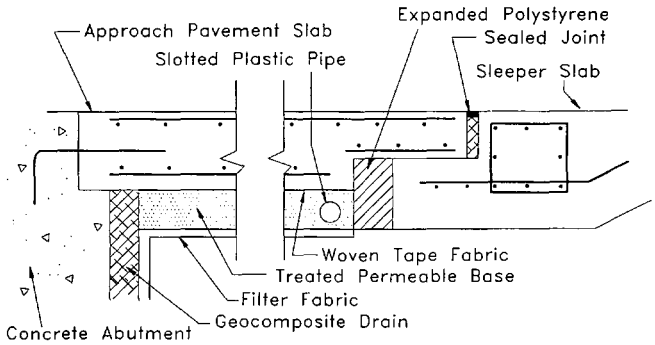

FIGURE 5 Treated permeable base under approach slab (California).

and assess the feasibility of minimizing postconstruction settlement by using special construction procedures.

3. When the behavior of a foundation soil is inadequate, the soil behavior be modified by the following methods:

- Removal of a part or all of the unsatisfactory material and replacement with suitable borrow material.
- In situ densification of foundation material when removal is uneconomical or impractical. The most commonly used methods are surcharges, vertical drains, waiting periods, and dynamic compaction.
- Reduction in approach fill weight by using lightweight embankment material such as furnace slag, expanded shale, lightweight concrete, polystyrene foam, or other materials having small unit weight.

Backfill

The use of marginal materials or inadequate compaction, or both, is the primary cause of approach problems. It is recommended that

1. Backfills be constructed with select borrow. In areas where select borrow is not available, breaker run aggregate is recommended as an alternative backfill material. The section of the approach embankment to be constructed with backfill material should be of sufficient length to accommodate standard construction equipment. The recommendation is to provide a longitudinal section projecting 1.5 m (5 ft) from the wingwall.

2. Approach embankments be constructed in 20-cm (8-in.) layers and compacted to 95 percent of standard proctor maximum dry density (AASHTO T99). The recommended tolerable range of moisture with regard to optimum moisture content is ±2 percent.

3. At a bridge approach site, project personnel be encouraged to increase inspection of materials, placement, and compaction. Furthermore, they should be alert for essential construction changes, such as the disposal of marginal materials and the need for granular backfill.

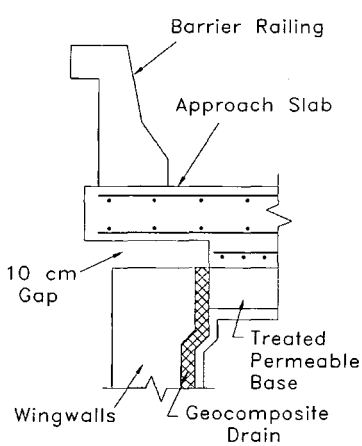

FIGURE 6 Approach slab edge detail (California).

Drainage System

Special attention must be given to removing the water from critical areas around the abutments and under the approach pavement by providing adequate drainage systems. The following points should be considered.

1. Bridge deck and adjacent roadway drainage should be collected and dropped into a channel by means of drains similar to the gutter downspouts on houses. Drains should not be discharged directly on the faces of approach slopes. When deck drain is permitted to drain through short vertical pipes over the abutment slope, splash blocks should be placed directly under the drainage pipe to dissipate the energy of the falling water and prevent erosion of the fill.

2. The face of the slopes under the bridge should be covered with a geotextile drainage fabric or sand layer to minimize the loss of soil due to erosion and seepage. Concrete revetments, if used, should also be placed on top of a geotextile drainage layer to avoid internal erosion under the revetment.

3. A preformed permeable liner with a filter fabric face should be used behind the abutment and wingwalls to remove free water from approach structure to a system of drainage pipes (see Figure 3).

4. A permeable base should be provided under the approach slab and adjoining pavement.

5. A set of perforated pipes should be installed to carry the water to collection points outside the abutment. Water from these pipes should not be allowed to drain onto unprotected slopes of the approach embankment.

ACKNOWLEDGMENTS

This paper was sponsored by the Maryland State Highway Administration in cooperation with FHWA.

REFERENCES

1. Ardani, A. *Bridge Approach Settlement.* Final Report CDOH-DTP-R-87-6. Colorado Department of Highways, Denver, April 1987.
2. McNulty, E. G. *Corrective Measures for Unstable Bridge-Approach Embankment, US 68, Licking River, Blue Licks.* Report KYP-72-38. Kentucky Bureau of Highways, Lexington, Nov. 1979.

3. Symon, I. F., and R. T. Murray. *Embankments on Soft Foundations: Settlement and Stability Study at Over Causeway By-Pass*. Report 675. U.K. Transportation and Road Research Laboratory, Crowthorne, Berkshire, United Kingdom, 1975.
4. Holroyd, J. J., et al. Design and Construction of the Approach Embankments to the River Trent Bridge on the M180 South Humberside Motorway. *Proc., Institution of Civil Engineers*. Part 1, Vol. 70, No. PT1, Aug. 1981, pp. 481–499.
5. Nicholson, D. P., and R. J. Jardine. Performance of Vertical Drains at Queenborough By-Pass. *Geotechnique*, Vol. 31, No. 1, March 1981, pp. 67–90.
6. Seim, C., et al. Wicks, Fabrics and Sawdust Overcome Thick Mud. *Civil Engineering*, ASCE, Vol. 51, No. 7, July 1981, pp. 53–56.
7. *NCHRP Synthesis of Highway Practice 2: Bridge Approach Design and Construction Practices*, TRB, National Research Council, Washington, D.C., 1969.
8. *NCHRP Synthesis of Highway Practice 159: Design and Construction of Bridge Approaches*. TRB, National Research Council, Washington, D.C., 1990.
9. Mahmood, I. U. *Evaluation of Causes of Bridge Approach Settlement and Development Prediction Models*. Ph.D. thesis. University of Oklahoma, Norman, Okla., 1990.
10. Hopkins, T. C. *Long-Term Movements of Highway Bridge Approach Embankments and Pavements*. Report LIKTRP-85-12. Kentucky Transportation Cabinet, Lexington, April 1985.
11. Allen, D. L. *A Survey of the States on Problems Related to Bridge Approaches*. Interim Report LIKTRP-85-25. Kentucky Transportation Cabinet, Lexington, Oct. 1985.
12. Timmerman, D. H. *An Evaluation of Bridge Approach Design and Construction Technqiues*. Report OHIO-DOT-03-77. Ohio Department of Transportation, Columbus, Dec. 1976.
13. Stewart, C. F. *Highway Structure Approaches*. Report FHWA/CA/SD-85-05. California Department of Transportation, Sacramento, July 1985.
14. Siriwardane, H. J., et al. Prediction of Lateral Movement of Bridge Abutments on Piles. In *Transportation Research Record 998*, TRB, National Research Council, Washington, D.C., 1984, pp. 14–24.
15. Wolde-Tinsae, A. M., M. S. Aggour, L. Moumena, and S. A. Chini. Structural and Soil Provisions for Approaches to Bridges. Final Report FHWA/MD-89/13. Maryland Department of Transportation, Annapolis, Dec. 1989.
16. *Soils and Foundations Workshop Manual*. FHWA, U.S. Department of Transportation, 1982.
17. Foster, C. R. Field Problems: Compaction. *Foundation Engineering* (G. A. Leonards, ed.), McGraw-Hill Book Company, Inc., New York, 1962.
18. *Bridge Inspector's Training Manual 70*. FHWA, U.S. Department of Transportation, 1979.
19. *Standard Specifications*. California Department of Transportation, Sacramento, July 1992.
20. *NCHRP Report 225: Plastic Pipe for Subsurface Drainage of Transportation Facilities*. TRB, National Research Council, Washington, D.C., 1980.
21. Karpoff, K. P. The Use of Laboratory Tests to Develop Design criteria for Protective Filters. In *Proc. of ASTM*, Vol. 55, 1955.
22. Van Zanten, R. V. *Geotextiles and Geomembranes in Civil Engineering*. A. A. Balkema, Rotterdam, The Netherlands, 1986.
23. Koerner, M., and B.-L. Hwu. *Geocomposite Drainage Systems; Highway Edge Drains and Retaining Wall Sheet Drains*. Final Report FHWA/PA-89-023 + 85-15. Pennsylvania Department of Transportation, Dec. 1989.
24. *Minimum Fabric Requirements*. Joint Committee of AASHTO-ABC-ARBTA, Task Force 25, July 1989.
25. Bridge Ramps Built First for Raised Freeway Grade. *Roads and Streets*, Vol. 117, No. 8, Aug. 1974, pp. 30–31.
26. Hughes, F. H. Bridge Approach Embankments. *Highway and Public Works*, Vol. 49, No. 1858, Oct. 1981, pp. 8–12.

The contents of this paper reflect the opinions of the authors and do not necessarily reflect the views of the Maryland State Highway Administration or FHWA.

Publication of this paper sponsored by Committee on Subsurface Drainage.

Determination of Free-Draining Base Materials Properties

HAIPING ZHOU, LUCINDA MOORE, JIM HUDDLESTON, AND JEFFREY GOWER

Recently, Oregon designed and constructed two types of permeable bases under both flexible and rigid pavements: an asphalt-treated permeable material (ATPM) and an open-graded aggregate material. Permeability and resilient modulus of both materials have not been determined. During pavement structural design using the *AASHTO Guide for Design of Pavement Structures*, 1986, layer and drainage coefficients had to be assumed to establish pavement thickness designs. In addition, construction with the existing open-graded aggregate revealed that the material was less stable and would ravel easily under construction traffic. In 1990, a research project was initiated to determine the desirable material properties for the two types of free-draining base materials and establish a more stable gradation for the open-graded aggregate base. This project consisted primarily of a laboratory investigation. Pavement cores of the asphalt-treated permeable base and samples of aggregate materials were tested in the laboratory for permeability and resilient modulus. The permeability was determined using both constant and falling head test procedures. The laboratory study indicated that the current Oregon ATPM has a sufficient drainage capability, and the resilient modulus of this material is typical of the findings of other states. A modified open-graded aggregate gradation resulted, which has a higher permeability and higher resilient modulus than the existing gradation. Recommendations for implementation include selection of layer and drainage coefficients for pavement structural design and use of the proposed open-graded aggregate gradation in pavement construction.

Inadequate drainage of pavement structures has been identified as one of the primary causes of pavement distress (*1–3*). For many years, researchers have theorized that improving pavement drainage might combat many pavement problems and extend the pavement service life (*4*). Subsurface drainage includes the disposal of water that has entered the pavement structure; therefore, a positive drainage layer in a pavement structure is critical for subsurface drainage. The subsurface drainage system can be designed by providing a drainage layer along with transverse and longitudinal drainage pipes to remove the water from the pavement structure.

Recently, Oregon initiated the design and construction of permeable bases under both flexible and rigid pavements. Two types of permeable bases used are an asphalt-treated permeable material (ATPM) and an open-graded aggregate material with the existing gradation designed by Oregon. Permeability and resilient modulus of both materials have not been determined. During pavement structural design, using the *AASHTO Guide for Design of Pavement Structures* (*5*), layer and drainage coefficients had to be assumed to establish pavement thickness designs. In addition, construction with the existing open-graded aggregate gradation revealed that the material was less stable and would ravel easily under construction traffic. Because of this ravelling, compaction was poor, the grade was difficult to control, and the open-graded aggregate materials did not provide a suitable surface for paving.

In 1990, a research project was initiated to better understand the characteristics of these two types of permeable base materials, develop appropriate layer and drainage coefficients for use in pavement thickness design, and improve stability and constructability of the existing open-graded aggregate material.

This project included (a) obtaining pavement cores of the ATPM and several gradations of aggregate base materials for testing permeability and resilient modulus in the laboratory (for aggregate materials, the effect of fractured faces was also examined, (b) recommending appropriate layer and drainage coefficients for use in pavement thickness design on the basis of laboratory test results, and (c) establishing an optimum gradation to improve stability and constructability of the open-graded aggregate material. For comparison, material properties of a dense-graded aggregate material were also investigated.

LITERATURE REVIEW

A literature review revealed that permeable bases can generally be grouped into two categories: (a) treated permeable base, in which aggregate material is typically mixed with 2 to 4 percent asphalt or a certain percentage of portland cement, (the asphalt treatment is more commonly used) and (b) open-graded aggregate material that is used directly in pavement base construction.

Use of Treated Permeable Base

The treated permeable base, especially the asphalt-treated permeable material (ATPM) base, has been widely used in the United States. In 1990 the National Asphalt Pavement Association distributed a questionnaire to the 50 state transportation departments. Of the 30 states indicating use or planned use of ATPM, 25 place the ATPM directly below the surfacing for interception of infiltrated surface runoff and 11 place the ATPM above the subgrade (*6*).

H. Zhou, Nichols Consulting Engineers, Chtd., 1885 South Arlington Avenue, Suite 111, Reno, Nev. 89509. L. Moore, J. Huddleston, and J. Gower, Oregon Department of Transportation, 800 Airport Road, S.E., Salem, Oreg. 97310.

The thickness required for drainage can be calculated using Darcy's law (*7–9*). Mathis (*9*) indicates that 4 in. of ATPM would provide sufficient capacity, be easily constructed, and provide for construction variability. Forsyth (*6*) indicated that the ATPM thickness ranged from 2 to 6 in., with 4 in. the most common.

The coefficient of permeability (k) of the ATPM can be affected by a number of factors, such as aggregate gradation and asphalt content used in the mixture. Although permeability of the ATPM would not be reduced significantly with the addition of 2 to 3 percent asphalt cement (*10*), it can vary from 3,000 to 15,000 ft/day (*9*), depending on the aggregate gradation.

Hicks et al. (*11*) reported ATPM resilient modulus averaging 155,000 to 270,000 psi at 75°F, depending on confining pressure. Monismith et al. (*12*) reported an average resilient modulus of 159,000 psi on samples consisting of partially crushed gravel.

Layer coefficients are used in the AASHTO guide (*5*). The value of layer coefficients used in design varied among the states that used ATPM. Forsyth (*6*) reported that of the 30 states that have or plan to use ATPM, 11 give it no structural value, 10 assign a layer coefficient corresponding to aggregate base between 0.10 and 0.14, and 6 assign layer coefficients between 0.20 and 0.30. California Department of Transportation (Caltrans) conducted a research project in 1981 with the objective of establishing a gravel factor for ATPM based on deflection attenuation resulting from the placement of a 3-in. ATPM layer. The results suggested a gravel factor corresponding to an AASHTO layer coefficient of approximately 0.20. If a resilient modulus of 140,000 psi is assumed for the ATPM, the procedure suggested by Rada et al. (*13*) results in an AASHTO layer coefficient of 0.23 (*6*).

Use of Untreated Permeable Base

Untreated permeable bases have also been used in a number of states. To provide sufficient drainage capability, the untreated permeable base is typically constructed with open-graded aggregate materials. In Oregon, this is often referred to as free draining aggregate material (FDAM).

The FDAM layer thickness required for drainage can be determined using Darcy's law (*7,8,14*). There is not much information indicating typical thickness used by other states. Oregon has been using 6 to 15 in. of FDAM in pavement construction. A minimum 6-in. FDAM appears to be necessary to have a proper compaction and minimum drainage requirement, although layer thicknesses greater than 12 in. may be difficult to compact. In 1991, the Oregon State Highway Division (OSHD) conducted a survey of OSHD project managers concerning the use of the FDAM with the current gradation (Table 1). One question was specifically related to the compaction of the FDAM. The respondents to the question indicated that the FDAM was unstable and that good compaction was difficult to achieve. Therefore, modifications to the current FDAM gradation should be made to produce a more workable and stable base material.

Gradation is the primary factor affecting the permeability of the FDAM. Mathis (*9*) indicated that the untreated permeable base materials generally had a lower coefficient of permeability than the treated permeable base materials. The estimated permeability for the untreated base materials is in the range of 200 to 3,000 ft/day.

TABLE 1 Current Aggregate Gradation for Oregon's FDAM

Sieve Passing	Percent by Weight
1-1/2"	100
1"	95-100
3/4"	55-80
1/4"	25-50
No. 10	0-15
No. 100	0-3 (Dry Sieve)

Oregon's FDAM resilient modulus has not yet been determined. However, a slightly lower modulus than typical dense-graded aggregate is expected because of the large air voids. Many studies (*15–21*) show that the resilient modulus of untreated aggregate materials is a function of material types and stress state occurring in the material. This is also to be expected for the FDAM.

Mathis (*9*) reported that test results from New Jersey and Pennsylvania indicated the untreated permeable material had similar bearing capacities to dense-graded aggregate bases. This may imply that the same layer coefficient can be assigned for both a permeable and dense-graded aggregate base in pavement design.

LABORATORY STUDY

To accomplish the research objectives, a laboratory study was conducted. The study included permeability and resilient modulus tests on both the ATPM and the FDAM used in Oregon. For permeability tests, both constant and falling head testing procedures were used. The effect of untreated aggregate fractured faces on permeability and resilient modulus was also investigated.

Permeability Tests

The purpose of the tests was to determine the coefficient of permeability (k) for the materials to be used. The apparatuses for the permeability tests were developed by the Pavements Unit of OSHD.

The constant head permeability test procedure determines the permeability of a material by maintaining a constant head (h) on the sample surface and measuring the time needed for collecting a known amount of water. The permeability can then be calculated using the equation

$$k_c = \frac{QL}{Ah} * 7200 \quad (1)$$

where

k_c = coefficient of permeability (ft/day), from constant head test;
Q = flow quantity (in.^{3}/sec);

L = flow path length or sample height (in.);
A = flow path area or sample area (in.^{2}); and
h = constant water head (in.).

The falling head permeability test determines the permeability of a material by measuring the time required for the water head to drop from a high level (h_1) to a low level (h_2). The permeability is then calculated using the equation

$$k_f = \frac{L}{T} \ln \frac{h_1}{h_2} * 7200 \quad (2)$$

where

k_f = coefficient of permeability (ft/day), from falling head test;
L = flow path length or sample height (in.);
T = time required for water head dropping from h_1 to h_2 (sec); and
h_1, h_2 = water levels (in.).

Resilient Modulus Tests

The resilient modulus is a measure of the stiffness and a dynamic test response defined as the ratio of the repeated axial deviator stress to the recoverable axial strain. For this study, resilient modulus tests were performed to develope layer coefficients of the asphalt-treated permeable base and untreated aggregate base materials and to determine a relative stability for the untreated materials.

ATPM Test Results

Sample Preparation

Asphalt-treated base core samples were obtained from two projects, both constructed in 1990. The Fir Grove Lane–Towers Road project (*22*) has a 4-in. ATPM, and the Rose Lodge–Polk County Line project (*23*) has a 3-in. ATPM. Core samples obtained from the project sites were cut and trimmed in the laboratory for permeability and resilient modulus testing. The prepared core samples were typically 1.8 to 2.5 in. thick. The diameter of the core samples was 4 in. One additional 6-in. core was also taken from each project. The 6-in. core was used in extraction tests to determine actual asphalt content and aggregate gradation. For the Fir Grove Lane–Towers Road project, 2.9 percent of PBA-2 (Performance Based Asphalt) was used. For the Rose Lodge–Polk County Line project, 2.4 percent of AC-15 asphalt was used. The aggregate gradations are in general within the specification limits, as given in Table 2.

Permeability

Permeability tests were performed following the procedures previously described. The test results (Table 3) show that for each test procedure the permeability varied substantially. For instance, the permeability for the Fir Grove Lane–Towers Road project ranges from 494 to 3,568 ft/day with the constant head test procedure and from 1,032 to 4,130 ft/day with the falling head test procedure. The variation in permeability on the same project may be due to the nonuniformity of the core material, although the variation of the permeability from two testing procedures may be due to the difference in the way water is introduced to the sample during the testing. It was difficult to maintain a constant water flow using the constant head testing procedure.

TABLE 2 Extraction Test Results

Aggregate Sieve Size	Percent Passing		Specification Limit
	Fir Grove Road	Rose Lodge Road	
1"	100	100	99 - 100
3/4"	94	(98)	85 - 95
1/2"	(68.6)	66	35 - 68
1/4"	19	19	5 - 20
#10	(6.1)	5	0 - 5
#40	4.1	3	-
#200	(2.7)	1.9	0 - 2
Asphalt Content	2.9	2.4	2 - 3

Note: Values in parenthesis exceeded specification range.

Resilient Modulus

The resilient modulus test on ATPM was conducted in accordance with ASTM D4123 standard procedure (*24*). Table 4 gives a summary of the test results. The resilient moduli from both projects are generally similar, with an average of approximately 100 ksi. The resilient modulus tests were performed at room temperature, approximately 77°F.

Bulk specific gravity test results are also given in Table 4. The average bulk specific gravity of the Fir Grove Lane–Towers Road project is about 10 percent lower than that of the Rose Lodge–Polk County Line project. The estimated air voids for the ATPM material are in the range of 20 to 25 percent.

FDAM Test Results

Gradations

Aggregate materials from a local source were obtained. Six different gradations were used to determine their permeability and resilient modulus. These gradations are existing open-graded aggregate, existing dense-graded aggregate, New Jersey open-graded aggregate, and proposed open-graded aggregate at the low end, center, and high end of the broadband limit. Table 5 gives the gradation for each aggregate. For the proposed open-graded aggregate, the samples prepared with 88 percent fractured faces aggregate were fabricated at both upper- and lower-bound specification limits, and the samples prepared with 100 percent fractured faces aggregate were fabricated at the center of the specification limit. The gradation difference is given in Figure 1. The proposed open-graded aggregate gradation is very similar to that of New Jersey (*25*).

TABLE 3 Permeability Test Results on ATPM Cores

Project Name	Sample I.D.	Permeability (ft/day)	
		Constant Head	Falling Head
Fir Grove Lane - Towers Road	1	1520	1959
	2	1618	1926
	3	2640	1920
	4	494	1032
	5	970	1299
	6	719	1086
	7	1693	2671
	8	1200	2517
	9	3568	4130
	10	628	1513
	Average	1505	2005
	Standard Deviation	965	929
	Range	494 - 3568	1032 - 4130
Rose Lodge - Polk County Line	1	Broken	
	2	3379	2273
	3	2506	1849
	4	3147	2273
	5	1518	1761
	6	1960	1678
	7	2360	2012
	8	2499	2326
	9	2348	2153
	10	Broken	
	Average	2465	2041
	Standard Deviation	595	253
	Range	1518 - 3379	1678 - 2326

TABLE 4 Summary of ATPM Resilient Modulus Test Results

Sample I.D.	Resilient Modulus (ksi)[1]	Bulk Specific Gravity
Project: Fir Grove Lane - Towers Road		
1	99	2.29
3	137	2.26
4	176	2.22
6	38	2.24
8	153	2.27
10	119	2.25
Average	120	2.26
Standard Deviation	48	0.02
Project: Rose Lodge - Polk County Line		
2	103	2.51
4	64	2.54
5	90	2.53
6	76	2.51
7	94	2.55
9	74	2.57
Average	84	2.54
Standard Deviation	15	0.02

[1]Measured at room temperature, about 77°F.

TABLE 5 FDAM Gradation

Aggregate with 88% fractured faces					
Aggregate Sieve Size	Existing open Graded[1] (A)	New Jersey[1] (B)	Proposed Upper Bound (C)	Proposed Lower Bound (D)	Existing Dense Graded[1] (H)
1-1/2"	100	100	100	100	97.5
1"	97.5	97.5	100	100	80
3/4"	67.5	86	98	80	64
1/2"	56.5	70	85	60	54
1/4"	37.5	54	60	45	42
#10	7.5	12.5	20	5	23
#40	4	3	6	0	12
#200	1	1.5	5	0	5

Aggregate with 100% fractured faces			
Aggregate Sieve Size	New Jersey[1] (E)	Proposed Open Graded[1] (F)	Existing Dense Graded[1] (G)
1-1/2"	100	100	97.5
1"	97.5	100	80
3/4"	86	89	64
1/2"	70	68	54
1/4"	54	53	42
#10	12.5	13	23
#40	3	3	12
#200	1.5	2.5	5

Note: All values are percent passing by weight
[1] Center value of the specification limit.

To evaluate the effect of fractured faces of aggregates on permeability and resilient modulus, aggregates with 88 and 100 percent fractured faces were tested. The percentage of fractured faces was determined following the OSHD TM-213 test procedure (*26*). The OSHD TM-213 is a visual inspection procedure for determining the percent, by weight, of the rock retained on the ¼-in. sieve having at least two fractured faces. For comparison, both open- and dense-graded aggregates were evaluated.

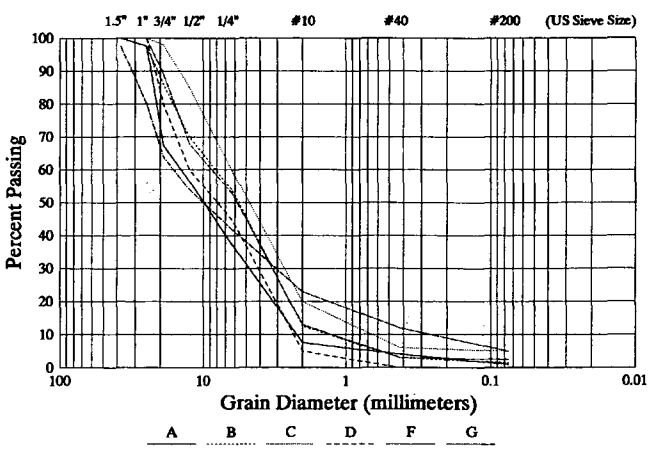

FIGURE 1 Aggregate gradations.

Sample Preparation

Ten samples at each gradation were made. Five were tested for permeability and five for resilient modulus. Eighty samples were prepared for the laboratory study. All samples were to be made on the basis of their water-density relationships, which were determined before sample preparation. The maximum dry density and the optimum moisture content for each gradation is shown in Table 6.

Samples for the permeability test were 4 in. in diameter and 6 in. high. For the resilient modulus test, samples were 6 in. in diameter and 12 in. high. All samples were to be prepared at the optimum moisture contents.

Permeability

The permeability test results (Table 7 and Figure 2) indicate that for open-graded aggregates, the percent of fractured faces have a substantial influence on the permeability. For the same gradation, as shown by Gradations E and B, the aggregate with 100 percent fractured faces is more permeable than aggregate with 88 percent fractured faces. The bound limit also influences the permeability significantly. As can be seen for the proposed aggregate gradation, the lower-bound Gradation D has a much higher permeability than the upper-bound Gradation C. This is to be expected because Gradation D is much coarser than Gradation C. Gradation F is the centerline of the proposed gradation band. With 100 percent fractured

TABLE 6 Maximum Dry Density for Each Gradation

Gradation	Maximum Dry Density (pcf)	Optimum Water Content (%)
A	115.5	6.5
B	112.2	4.0
C	108.6	8.0
D	105.0	6.0
H	120.3	5.3
E	117.6	3.5
F	115.9	3.2
G	123.6	3.3

TABLE 7 Summary of Permeability Test Results for Untreated Base Materials

Sample I.D.	Constant Head (ft/day)		Falling Head (ft/day)	
	Average	Standard Deviation	Average	Standard Deviation
A	971	322	1031	223
B	770	138	723	145
C	226	42	316	77
D	3018	370	3694	143
H	140	64	76	30
E	2376	338	1962	181
F	2489	309	1876	169
G	475	150	153	31

faces, Gradation F is expected to have a higher permeability than with 88 percent fractured faces, as shown by Gradations E and B. The results also show that the permeability of Gradation F is closer to that of Gradation D, which is the lower bound of the proposed gradation limit. This appears to indicate that as the percentage of aggregate fractured faces increases, the permeability of the aggregate material would also increase. For dense-graded aggregate, the difference in permeability due to fractured faces is not substantial.

The permeability test results from both constant and falling head test procedures appear in general to be similar for each type of aggregate gradation. The permeability results from the falling head test appear to have a smaller standard deviation than those from the constant head test.

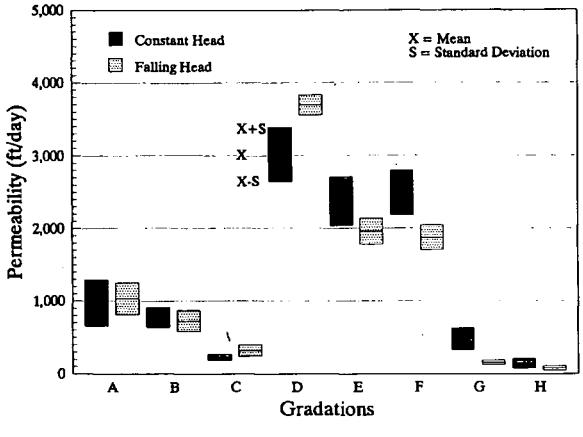

FIGURE 2 Comparison of permeability from different gradations.

Resilient Modulus

The resilient modulus test on untreated aggregate base materials was conducted in general accordance with AASHTO T-274 procedure (*27*), which was the standard testing method available for unbound materials. The test results are given in Table 8. The resilient modulus results are

$$M_R = k_1 \theta^{k2} \quad (3)$$

where

M_R = resilient modulus (psi),
k_1, k_2 = regression coefficients of material, and
θ = bulk stresses (psi).

This expression shows that the resilient modulus of untreated aggregate is a function of both bulk stress and material properties.

The resilient modulus test results indicate that for open-graded aggregates the percent of fractured faces has a significant influence on the resilient modulus. For the same type of gradation, the aggregates with 100 percent fractured faces have a much higher resilient modulus than aggregates with 88 percent fractured faces, as shown in Figure 3 (*top*). For dense-graded aggregate, the difference in resilient modulus due to fractured faces is not obvious, as shown in Figure 3 (*bottom*).

Figure 4 (*top*) shows the test results for the proposed aggregate gradation versus the existing aggregate gradation. The figure clearly shows that the proposed FDAM Gradation F had a higher resilient modulus than the existing FDAM Gra-

TABLE 8 Summary of Resilient Modulus Test Results for Untreated Aggregate Materials

Gradation	Modulus = $k_1\theta^{k_2}$	R^2	Actual Dry Density (pcf)[a]	Actual Water Content (%)[a]
A	$2{,}557\theta^{0.592}$	0.92	107.6	3.4
B	$1{,}943\theta^{0.619}$	0.96	104.1	3.9
C	$1{,}786\theta^{0.615}$	0.87	102.6	5.8
D	$3{,}240\theta^{0.568}$	0.94	105.4	3.4
H	$4{,}144\theta^{0.525}$	0.95	120.2	4.5
E	$4{,}054\theta^{0.574}$	0.74	119.1	2.9
F	$3{,}475\theta^{0.569}$	0.81	116.3	2.6
G	$4{,}355\theta^{0.511}$	0.94	124.1	2.9

[a] Average of test results from five samples for each gradation.

dation A. For comparison, resilient moduli for each gradation are plotted in Figure 4 (*bottom*).

Table 8 also gives actual dry density and water content data measured immediately after the resilient modulus test. Some of the actual dry densities measured during resilient modulus test are slightly higher than the maximum dry densities determined during the development of water-density relationship for the aggregate materials, and the actual moisture content of the samples is slightly lower than optimum water content. The exact cause of inconsistency in dry densities is not known. It may have been caused by variation in sample fabrication, which was conducted by two different laboratories. The slightly lower actual water content of the samples may have been caused by water loss during the modulus testing process.

USE OF RESEARCH RESULTS

The laboratory test results have been analyzed for the development of design inputs and specification for use in Oregon. The design inputs include resilient modulus and layer coefficients. The specification includes recommendation for modification of the current FDAM gradation of OSHD.

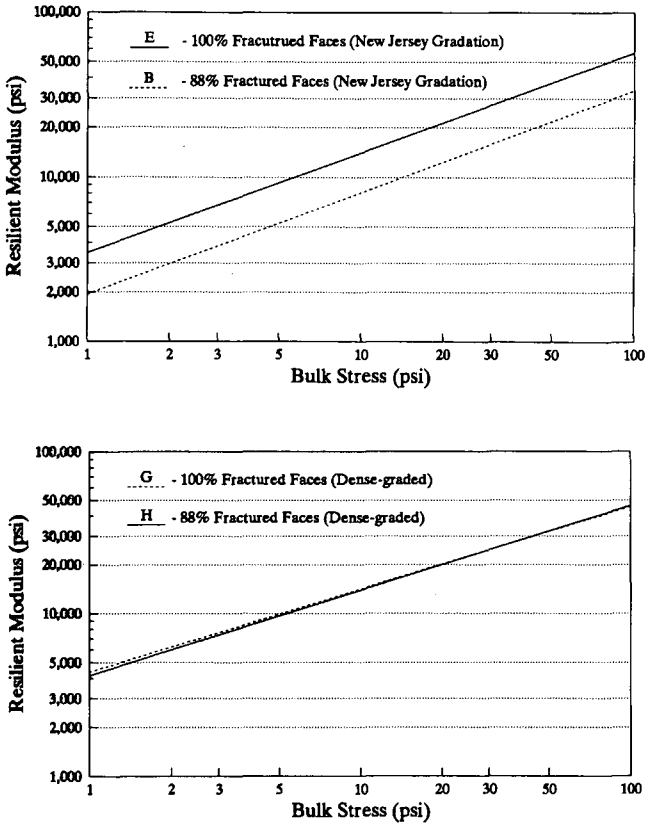

FIGURE 3 Effect of fractured faces on resilient modulus: *top*, open-graded aggregate; *bottom*, dense-graded aggregate.

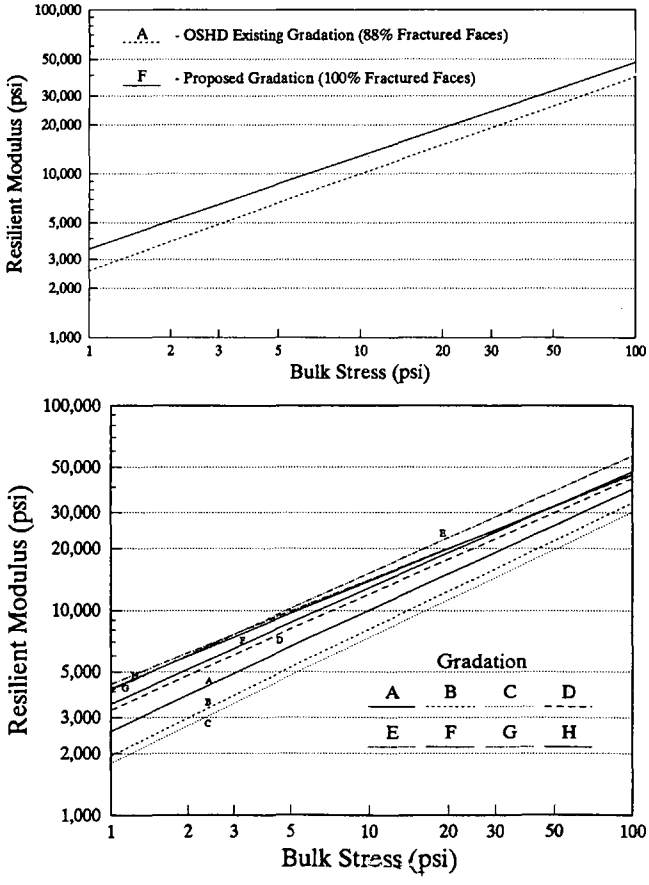

FIGURE 4 Comparison of resilient moduli: *top*, proposed gradation versus existing gradation; *bottom*, all aggregate gradations investigated.

ATPM Resilient Modulus and Layer Coefficient

For the Fir Grove Lane–Towers Road project, the average resilient modulus measured in the laboratory is 102 ksi with a standard deviation of 48 ksi. For the Rose Lodge–Polk County Line project, the average resilient modulus is 84 ksi with a standard deviation of 15 ksi. The resilient modulus of the ATPM was measured at 77°F without confinement, and the stiffness of ATPM would vary with the change of temperature. Although a modulus-temperature relationship for Oregon's ATPM is not known, it is expected that the modulus will increase when temperature decreases. In Oregon the ATPM base layer may experience a much lower temperature than 77°F because of its position in the pavement structure. Therefore, the actual modulus may be much higher than those measured in the laboratory.

Considering the temperature effect on the resilient modulus and using a modulus-layer coefficient conversion chart recommended by AASHTO (*5*), a corresponding layer coefficient can be determined. For Oregon's ATPM, the average resilient moduli are adjusted to 68°F using a procedure in the AASHTO guide (*5*). The temperature-adjusted resilient moduli are then used to determine the layer coefficient. This would result in a layer coefficient between 0.14 and 0.19.

The drainage coefficient should be included in the pavement structural design. For pavements to provide a positive drainage, a minimum permeability of 1,000 ft/day should be achieved (*2,28*). Oregon's current ATPM appears to have a sufficient drainage capability, as can be seen from the laboratory test results in Table 3. With this drainage capability, a drainage coefficient between 1.15 to 1.25 is recommended for use in Oregon. This recommendation is based on an assumption that the pavements would have a good quality of drainage and 1 to 5 percent of the time during the year the pavement structure would be exposed to moisture levels approaching saturation (*5*).

FDAM Resilient Modulus and Layer Coefficient

The layer coefficient for the FDAM may be determined knowing the resilient modulus, which can be calculated from Equation 3. For a specific aggregate material, a corresponding equation or relationship should be used to calculate the modulus. The resilient modulus for untreated aggregate is a function of stress state in a pavement structure; therefore, an anticipated stress level should be used to determine the resilient modulus. Guidelines for determining stress state may be found in the AASHTO guide (*5*). For pavement design in Oregon, a layer coefficient between 0.08 to 0.14 is recommended for both base and subbase layers. These correspond to a resilient modulus between 16 to 30 ksi for the base and 11 to 20 ksi for the subbase materials.

A drainage coefficient between 1.00 to 1.15 is recommended for use in Oregon. This recommendation is based on an assumption that the pavements would have a good quality of drainage, and 5 to 25 percent of the time during the year pavement structure would be exposed to moisture levels approaching saturation. The percent of time FDAM moisture levels approach saturation is higher than that of the ATPM; this is because of concerns about contamination of the FDAM. Also, most FDAM designs have not provided longitudinal edge drains. Consequently, water is outlet on the shoulder; therefore, the shoulders may become contaminated over time. If edge drains are provided, a higher drainage coefficient may be appropriate.

Gradation Specification Changes

One objective of this paper is to evaluate the existing FDAM gradation and its performance during construction. The OSHD project manager questionnaire survey indicated that the existing gradation was unstable and difficult to compact during construction. An appropriate modification of this gradation has been made in using as much of the existing aggregate stockpile as possible. This modification (newly proposed) is represented by Gradation F with 100 percent fractured faces. The broadband of the proposed gradation is shown in Table 9.

Laboratory tests on Gradation F showed a substantial increase in resilient modulus as well as in density, compared with the existing gradation. This improvement in material property, due to gradation changes and increased fractured faces percentage, may also improve its constructability and stability. Another major improvement due to gradation change is a considerable increase in permeability. Compared with the

TABLE 9 Proposed Gradation Specification

Sieve Size	Percent Passing % (Centerline)	Broadband Limit
1-1/2"	100	100
1"	100	100
3/4"	89	80-98
1/2"	68	60-85
1/4"	53	45-60
#10	13	5-20
#40	3	0-6
#200	2.5	0-5
Measured permeability (ft/day)	Constant Head	Falling Head
Average Standard deviation	2,489 309	1,876 169

existing gradation, the permeability of the modified gradation is almost double.

CONCLUSIONS

1. Many states are paying great attention to subsurface drainage. The design and construction of a positive drainage system in pavement structures is becoming more common.
2. Typical ATPM layer thickness ranges from 3 to 4 in. The typical asphalt content used in ATPM is 2 to 3 percent. Within this range, the amount of asphalt appears to have a minor influence on permeability.
3. The current ATPM of OSHD has sufficient drainage capability. The resilient modulus of this material is typical of the findings of other states.
4. The proposed gradation for open-graded aggregate with 100 percent fractured faces has a considerably higher permeability than the existing gradation. The aggregate with the proposed gradation also has a higher resilient modulus.
5. The percent of fractured faces has a substantial influence on the permeability of open-graded aggregate. For the same type of gradation, the aggregate with 100 percent fractured faces is more permeable than the aggregate with 88 percent fractured faces. For dense-graded aggregate, the difference in permeability due to fractured faces is not significant.
6. The percent of fractured faces has a significant influence on the resilient modulus of open-graded aggregate. For the same type of gradation, the aggregates with 100 percent fractured faces have a much higher resilient modulus than aggregates with 88 percent fractured faces. For dense-graded aggregates, the difference in the resilient modulus due to fractured faces is not obvious.

RECOMMENDATIONS

1. For pavement structural design with ATPM, a layer coefficient of 0.14 to 0.19 is recommended. A drainage coefficient of 1.15 to 1.25 is recommended.
2. The proposed gradation for FDAM is recommended for use. To ensure sufficient drainage and strength, 100 percent of the material retained above the ¼-in. sieve should be fractured on at least two faces. In locations in which this is not obtainable, 90 percent fracture on at least two faces should be specified. Where 100 percent fracture can be specified, a layer coefficient between 0.11 and 0.14 is recommended. Where 90 percent fracture is specified, a layer coefficient between 0.08 and 0.11 is recommended. The specific value may be determined knowing the anticipated stress in the aggregate.
3. A drainage coefficient of 1.05 to 1.15 is recommended for the FDAM with 100 percent of the material retained above the ¼-in. sieve fractured on two faces and 1.00 to 1.05 for 90 percent fractured on at least two faces.
4. A prime coat may be used on top of FDAM. This will make the FDAM material easier to run construction equipment on and more stable. However, it may reduce the permeability of FDAM. To reduce aggregate segregation, plant mix is recommended.

ACKNOWLEDGMENTS

The work in this paper was conducted as a part of a Highway Planning and Research project funded through FHWA, U.S. Department of Transportation, and Oregon Department of Transportation (ODOT). The authors are grateful for the support of the ODOT Pavements Unit and Pavement Services, Inc. The authors thank the ODOT Soils and Bituminous crews of the Materials Unit and Roger Miles, ODOT Pavements Unit; Amy Edwards, Pavements Unit; Gary Hicks, Oregon State University; and Scott Nodes, ODOT Research Unit.

REFERENCES

1. Cedergren, H. R. Why All Important Pavements Should Be Well Drained. Presented at 67th Annual Meeting of the Transportation Research Board, Washington, D.C., 1988.
2. Cook, M., and S. Dykins. Treated Permeable Base Offers Drainage, Stability. *Roads and Bridges*, May 1991, pp. 46–49.
3. Mathis, D. M. Permeable Bases Prolong Pavements, Studies Show. *Roads and Bridges*, Vol. 28, No. 5, May 1990, pp. 33–35.
4. Flynn, L. Open-Graded Base May Lengthen Pavement Life. *Roads and Bridges*, Sept. 1991, pp. 33–42.
5. *AASHTO Guide for Design of Pavement Structures*. AASHTO, Washington, D.C., 1986.
6. Forsyth, R. A. *Asphalt Treated Permeable Materials—Its Evolution and Application*. Quality Improvement Series QIP 117. National Asphalt Pavement Association, Lanham, Md. 1991.
7. *Drainage of Asphalt Pavement Structures*. Manual Series 15 (MS-15). The Asphalt Institute, College Park, Md., Sept. 1984.
8. Wells, G. K. *Determine Permeabilities of ATPB and CTPB Materials*. Report of Minor Research Project 631140-30019. California Department of Transportation, Sacramento, May 1986.
9. Mathis, D. M. *Design and Construction of Permeable Base Pavements*. FHWA, U.S. Department of Transportation, 1989.
10. Lovering, W. R., and H. R. Cedergren. Structural Section Drainage. *Proc., International Conference on the Structural Design of Asphalt Pavements*, Ann Arbor, Mich. 1962.
11. Hicks, R. G., L. E. Santucci, D. G. Fink, and R. Williamson. Effect of Laboratory Curing and Compaction Methods on the Stress Strain Behavior of Open-Graded Emulsion Mixes. Presented at the 58th Annual Meeting of the Transportation Research Board, Washington, D.C., Jan. 1979.
12. Monismith, C. L., K. Wallac, E. Harm, and B. Unban. *Pavement Design Considerations for Two Layer Pavements Containing Open-Graded Asphalt Mixtures, Final Report*. University of California, Berkeley, 1982.
13. Rada, G. R., M. W. Witczak, and S. D. Rabinow. Comparison of AASHTO Structural Evaluation Techniques Using Non-Destructive Deflection Testing. In *Transportation Research Record 1207*, TRB, National Research Council, Washington, D.C., 1988.
14. Cedergren, H. R., K. H. O'Brien, and J. A. Arman. *Guidelines for the Design of Subsurface Drainage Systems for Highway Structural Sections*. Final Report (summary), Report FHWA-RD-72-30. FHWA, U.S. Department of Transportation, June 1972.
15. Hicks, R. G. *Factors Influencing the Resilient Properties of Granular Materials*. Ph.D. dissertation. University of California, Berkeley, 1970.
16. Hicks, R. G., and F. N. Finn. Analysis of Results from the Dynamic Measurements Program on the San Diego Test Road. *Proc., The Association of Asphalt Paving Technologists*, Vol. 39, 1970, pp. 153–185.
17. Allen, J. J. *The Effects of Non-Constant Lateral Pressures on the Resilient Response of Granular Materials*. Ph.D. dissertation. University of Illinois at Urbana-Champaign, 1973.
18. Kalcheff, I.V., and R. G. Hicks. A Test Procedure for Determining the Resilient Properties of Granular Materials. *Journal of Testing and Evaluation*, ASTM, Vol. 1, No. 6, 1973.

19. Boyce, J. R., S. F. Brown, and P. S. Pell. The Resilient Behavior of a Granular Materials Under Repeated Loading. *Proc., Australian Road Research Board*, 1976.
20. Monismith, C. L., J. A. Epps, D. A. Kasianchuk, and D. B. McLean. *Asphalt Mixture Behavior in Repeated Flexure*. Report TE 70-5. University of California, Berkeley, Jan. 1972.
21. Albright, S. *Evaluation of Crushed Aggregate Specifications Used by the Alaska Department of Transportation and Public Facilities.* M.S. thesis. Department of Civil Engineering, Oregon State University, Corvallis, 1986.
22. Zhou, H., and I. J. Huddleston. *Final Pavement Design Report: Fir Grove Lane–Towers Road Section Project.* Oregon State Highway Division, Salem, 1990.
23. Gower, J. L., and I. J. Huddleston. *Final Pavement Design Report: Rose Lodge–Polk County Line Project.* Oregon State Highway Division, Salem, 1989.
24. *Annual Book of ASTM Standards.* ASTM, Philadelphia, Pa., 1989.
25. Kozlov, G. S. *Improved Drainage and Frost Action Criteria for New Jersey Pavement Design, Volume III.* Report FHWA-NJ-84-015. FHWA, U.S. Department of Transportation, 1984.
26. *Laboratory Manual of Test Procedures.* Materials Section, Highway Division, Oregon Department of Transportation, Salem, 1986.
27. *Standard Specifications for Transportation Materials and Methods of Sampling and Testing.* AASHTO, Washington, D.C., 1986.
28. Yoder, E. J., and M. W. Witczak. *Principles of Pavement Design*, 2nd ed. John Wiley and Sons, Inc., New York, 1975.

Publication of this paper sponsored by Committee on Subsurface Drainage.